Sexual Dimorphism of the Cerebral Cortex

Thesis
presented to the Faculty of Arts
of the University of Zürich

for the degree of Doctor of Philosophy

by

Eileen Lüders

of Germany

Accepted on the recommendation of
Professor Dr. Lutz Jäncke, Ph.D.
Professor Dr. Ulrike Ehlert, Ph.D.

Los Angeles
2006

List of Figures

List of Tables

List of Abbreviations

A
AC = Anterior Commissure
ANOVA = Analysis Of Variance

B
BA = Brodmann Area
BSE = Brain Surface Extraction

C
CAM = Cell-Adhesion Molecule
CC = Corpus Callosum
CNS = Central Nervous System
CSF = Cerebrospinal fluid

D
DBM = Deformation-based Morphometry

E
EEG = Electro-Encephalography
EQ = Encephalization Quotient

F
FDR = False Discovery Rate
FID = Free Induction Decay
fMRI = Functional MRI
FWHM = Full Width at Half Maximum

G
GM = Gray Matter

I
ICBM = International Consortium of Human Brain Mapping

L
LONI = Laboratory of Neuro Imaging

M
MEG = Magneto-Encephalography
MNI = Montreal Neurological Institute
MRI = Magnetic Resonance Imaging

N
NMR = Nuclear Magnetic Resonance

P
PC = Posterior Commissure
PET = Positron Emission Tomography

R
RF = Radio Frequency
ROI = Region of Interest

S
SEM = Standard Error of Mean
SD = Standard Deviations
SF = Scaling Factor
SpFr = Spatial Frequency
SPM = Statistical Parametric Mapping

T
TE = Time of Echo
TBM = Tensor-based Morphometry
TBV = Total Brain Volume
TMS = Transcranial Magnetic Stimulation
TR = Time of Repetition

U
UCLA = University of California, Los Angeles

V
VBM = Voxel-based Morphometry

W
WM = White Matter

Z
ZENIT = Center for Neuroscientific Innovation and Technology

2, 3
2D = Two-Dimensional
3D = Three-Dimensional

Acknowledgments

First of all, I want to express my gratitude to my supervisor Dr. Lutz Jäncke at the University of Zurich. He was the one who introduced me into the fascinating world of neuroscience. He set up my first brain research project and he provided me with subsequent outstanding opportunities to collect valuable research experiences. He gave me the world.

I would also like to sincerely thank the members of the Laboratory of Neuro Imaging at UCLA who not only provided me with exceptional professional advice and support but also created an environment that made me feel home away from home. I want to express my gratitude especially to Dr. Katherine Narr, Dr. Arthur Toga, Dr. Paul Thompson, as well as to Andrew Lee and Yungping Wang.

In addition, I wish to thank Dr. Christian Gaser at the University of Jena. Significant parts of this thesis are product of an inspiring collaboration and unique friendship. Similarly, I would like to thank Derrick Rostagno. His inputs certainly served as an extremely valued source for finalizing this body of work. Furthermore, I also highly appreciate the time and effort of Dr. Ulrike Ehlert at the University of Zurich, who kindly agreed to review this thesis.

Finally, I want to say thank you to all people who contributed to this thesis in their own wonderful way by being part of my life. Although their names are too numerous to be listed here, they are and will be remembered.

Summary

The work summarized in this thesis addresses the presence and direction of cerebral gender differences in a large and well-matched sample of young and healthy adults. Several brain-anatomical characteristics were studied for the first time by employing high-resolution magnetic resonance imaging (MRI) data and sophisticated image analysis tools. Moreover, it was systematically investigated how image preprocessing and analysis can influence the magnitude and direction of structural differences in brain morphology between genders. Altogether, four main studies were designed to examine gender differences in brain structure were variables included total brain volume (TBV), global tissue volumes [gray matter (GM), white matter (WM), cerebrospinal fluid (CSF)], regional GM concentration, cortical thickness and convolution of the cortical surface.

Results from these studies showed larger global GM volumes, greater regional GM concentration and cortical thickness, as well as a larger degree of cortical convolution in females compared to males, after correcting for individual brain sizes. Interestingly, even when brain volumes were analyzed in their native dimensions, regional thickness of the cortex was larger in females than in males. In contrast, when individual brain volumes were not taken into account, we detected larger global tissue volumes (GM, WM, CSF) in males corroborating widely-documented prior observations of larger brain volumes in men.

The findings revealed from the above investigations support the assumption of a dimorphic organization in male and female brains that appears to involve the cortical architecture. This cerebral sexual dimorphism may have functional significance and possibly account for gender-specific abilities and behavioral differences between men and women.

Zusammenfassung

Die in der vorliegenden Arbeit zusammengefaßten Studien verdeutlichen das Vorhandensein zerebraler Geschlechtsunterschiede in einer großen und sorgfältig zusammengestellten Stichprobe von jungen und gesunden Erwachsenen. Unter Zuhilfenahme hochauflösender Kernspintomographie und fortschrittlicher Auswertungsmethoden wurden mehrere hirnanatomische Komponenten erstmalig analysiert. Darüberhinaus wurde systematisch erforscht, wie Vorverarbeitung and Analyse-Ansatz die strukturellen Ergebnisse beeinflussen können. Insgesamt wurden vier Hauptstudien konzipiert, um Gesamtgehirnvolumen, globale Gewebevolumina (graue Substanz, weisse Substanz, Cerebrospinalflüssigkeit), regionale Konzentration der grauen Substanz, kortikale Dicke, sowie Faltung der kortikalen Oberfläche zu untersuchen.

Wir ermittelten größere globale Volumina und regionale Konzentrationen der grauen Substanz in weiblichen Gehirnen, sowie auch dickere und stärker gefaltete kortikalen Oberflächen, wenn die Ergebnisse anhand der individuellen Gehirngrössen korrigiert wurden. Interessanterweise übertraf sogar in unkorrigierten Daten die kortikale Dicke der Frauen die der Männer. Im Gegensatz dazu waren die unkorrigierten globalen Gewebevolumina in männlichen Gehirnen signifikant grösser, was mit dem Befund über ein durchschnittlich größeres männliches Gesamtgehirnvolumen einhergeht.

Unsere Ergebisse unterstützen die Annahme einer geschlechtsspezifischen Hirnorganisation, die sich in der Architektur des Kortex zu widerspiegeln scheint. Dieser zerebrale Geschlechtsdimorphismus könnte funktionell bedeutsam sein und geschlechtsspezifische Fähigkeiten und Verhaltensunterschiede zwischen Männern und Frauen erklären.

I. THEORETICAL SECTION

1. Introduction and Overview

1.1. The Fascination about Gender and the Brain

Although equality between men and women constitutes a politically and socially motivated goal, we will never stop wondering why men and women are so obviously different. In most cases, these inquisitive thoughts are stimulated by seemingly innate behavioural discrepancies that evoke mysterious intrigue over and over again. Why is it that on so many occasions, the opposite sex does not appear to think, feel or act the same way we do? And of course, even when these occasions have exceptions, gender-specific behaviour remains a puzzling issue, leading inevitably to the question for the cause. Likewise we could ask which factors trigger the remarkable differences in some aspects of gender-specific cognitive abilities. Women are known to outperform men in fields of memory and language, while men excel in tasks that require spatial abilities. Over the centuries countless explanations from various fields have been introduced, modified, sometimes smiled at, and frequently discarded. We actually do not really know how men relate to Mars and women to Venus, as vividly brought up in the popular scientific literature, and possibly we will never find the complete answer. However, we can make assumption that gender-specific behaviour exists because male and female brains function differently.

As early as a few millenniums ago, we recognized that the brain has something to do with how we act and who we are. Already the ancient Greeks debated whether the heart or the brain was the essence of the mind. The study of the human brain is still in its infancy, but today we know that the brain is divided into functional networks or systems that play different roles in our daily functioning. Thus, it is reasonable to assume that

certain parts of the brain might be different in men and women, while others are not. The cerebral cortex – the large surface layer of the brain, which is only a few millimeters thick but holds two thirds of the brain's neurons – appears to be a promising candidate in the endeavour to find some morphological substrates for gender-specific behaviour. The cerebral cortex is essential for many higher-order functions like information processing, problem solving, and language. It is often referred to as 'the origin of thinking' and appears to be the determining component for consciousness. Cognition and/or behaviour in men and women might be altered due to different wiring patterns between single neurons or cortical processing units, different amounts of available brain tissue in cortical regions, or different ratios between input-output components. The source for potential contributors appears to be vast, and it is very likely that a conglomerate of all those factors modulate behavioural and functional outcomes. However, the captivating question addressed in the present thesis is whether gender effects exist on a macroscopic level for relevant cortical features such as cortical thickness, tissue concentration, and surface convolution.

1.2. Organization of this Thesis

Following the introduction and overview, the present thesis is divided into three main sections, encompassing a theoretical part (Chapters 2-4), where I provide a broad background for the empirical studies, an empirical part (Chapters 5-10), where the actual studies are presented, and a general discussion (Chapters 11-13).

In **Chapter 2**, I introduce the topic of the cerebral cortex with its structural and organizational characteristics. I elaborate on micro- and macro structure, as well as on the

link between anatomy and function. Subsequently, I highlight developmental aspects related to morphogenesis and phylogenesis.

In **Chapter 3**, I provide relevant information related to MRI-based *in vivo* morphometry, starting with basic principles of MRI, followed by analysis approaches including classical region-of-interest (ROI) analyses and more recent whole-brain analyses. I also review some potential drawbacks in MRI-based measurements addressing artifacts related to image acquisition and the vague link between actual structure and measurement.

In **Chapter 4**, I focus on reviewing the literature in order to provide a comprehensive overview with respect to the sexual dimorphism in the brain. Although I will also discuss gender effects on correlates of brain function, I place predominant emphasis on structural findings. Moreover, against the background of the thesis' content, I will focus on macro-structural gender differences.

In **Chapter 5**, I transition into the empirical part of the thesis by summarizing general aims, followed by describing subject selection and data acquisition in **Chapter 6**. In the subsequent chapters, I present background, methods, and empirical data from specific studies.

In **Chapter 7**, I describe the first study, designed to complement analyses of global tissue volumes (GM, WM, and CSF) with examinations of regional GM in the same set of data. The effect of gender on tissue components is investigated employing statistical mapping techniques. In addition, spatially detailed maps of average GM distribution and variability

are generated, given that these descriptors are not well characterized in the normative literature.

In **Chapter 8**, I describe the second study, designed to analyze the regional specificity of gender effects on cortical thickness, where the influences of brain size correction on structural outcomes are established. Similar as in the first study, spatially detailed maps of average thickness distribution are generated. However, in contrast, not only scaled brains and lateral surfaces are presented, but also unscaled brains and medial surfaces.

In **Chapter 9** and **10**, I describe the third and fourth studies, which are designed to compare cortical convolution between men and women. While the third study reflects cortical convolution as a measurement based on the *fractal dimension* for five functionally relevant cortical regions, the fourth study captures very local measures of *mean curvature* across the cortex. In addition, the effect of affine transformations on the latter measurement is established.

In **Chapter 11** and **12**, I provide a general discussion for the empirical studies presented in this thesis. I elaborate on factors that possibly determine profound differences in the brains of men and women, as observed in the studies. Furthermore, I highlight how alterations in gross cerebral structure may result in gender-specific behavioural outcomes even though these relationships will not be a focus of this thesis.

In the **Appendix**, I provide details and references for the image analysis methods used in the studies presented throughout this thesis.

2. The Cerebral Cortex

2.1. Structure and Organization of the Cerebral Cortex

The cerebral cortex is a folded sheet of neural tissues that covers the cerebral hemispheres. It contains approximately 80 % of the neurons of the central nervous system (CNS). The cerebral cortex measures only 1.5-4.5 mm, but its extent reaches 4000 cm^3 (Kruggel & von Cramon, 2000). It is typically divided into the *neocortex* of relatively recent evolution and the evolutionarily older *allocortex,* comprising of the *archicortex* (hippocampus) and *paleocortex* (olfactory cortex). While the allocortex exhibits only limited lamination, the neocortex – which is only present in mammals – has 6 layers of neurons. Of note, all subsequent descriptions will predominantly refer to the latter mentioned neocortex, hereafter referred to as *cerebral cortex* to simplify matters.

2.1.1 Neuronal Organization

The cerebral cortex contains 50-100 billion neurons with two major groups: (a) spiny neurons and (b) smooth or sparsely spiny neurons. Spiny neurons include the population of pyramidal cells (large, pyramid-shaped, apical dendrite, very long axon) and spiny stellate cells (small, star-shaped, short axons) that form excitatory synapses. In contrast, smooth or sparsely spiny neurons (e.g., smooth stellate cells, basket cells, chandelier cells and double bouquet cells) form predominantly inhibitory synapses. Approximately 75-85 % of the neurons in the neocortex are pyramidal cells, which are also called *projecting cells*. Conversely, non-pyramidal neurons in the neocortex are referred to collectively as *interneurons*.

In general, cortical neurons are thought to be organized into multiple, small repeating microcircuits, where the basic microcircuit is formed by a pyramidal cell and its input-output connections. Excitatory inputs only arrive at the dendritic arbor of the pyramidal neurons and originate from extrinsic afferent systems and spiny neurons. In contrast, inhibitory inputs from interneurons (other than spiny stellate cells), terminate on the dendrites, soma and axon initial segment of the pyramidal neuron. Interneurons are also interconnected between themselves with the exception of chandelier cells, which only form synapses with the axon initial segment of pyramidal neurons (DeFelipe et al., 2002).

2.1.2 Laminar Organization

One fundamental aspect of cortical organization is that each layer of the cortex has particular cell types that predominate. By convention, the layers of the neocortex are numbered I through VI, starting at the cortical surface. Communication between cortical areas originates predominantly above layer IV in the *supra-granular* layers II and III, but also in layer I. Layer I mainly consists of apical dendrites from pyramidal neurons from lower layers and axons synapsing on those dendrites. In contrast, layer II contains many small densely-packed stellate cells and a few small pyramidal neurons, while layer III contains loosely packed stellate cells and medium-sized pyramidal neurons. Layer IV – also called the *granular layer* – contains bands of densely packed stellate cells (but no pyramidal neurons) and receives input from outside the cortex (e.g., thalamus). Outputs leading outside the cortex (e.g., thalamus, basal ganglia, brain stem, and spinal cord) originate below layer IV in the *infra-granular* layers V and VI. Layer V contains the

largest pyramidal neurons, while layer VI consists of pyramidal neurons of various sizes. Both layers contain also loosely packed stellate cells (Pinel, 2002).

Although all neocortex is six-layered, cortical areas differ with respect to laminar thickness, consistent with their functional differences. Layer IV, for example, with its densely packed stellate cells tends to be thickest in sensory cortices (that even split into three sub-layers in the primary visual cortex). Conversely, primary motor cortices have a virtually non-existent layer IV but a particularly well-developed layer V with its large pyramidal neurons (Thompson and Toga, 2003). Moreover, there seem to exist considerable differences between the cytoarchitectures of gyri and sulci, with thicker inner cortical layers and thinner outer layers in gyri compared to sulci (Welker, 1990 according to White et al., 2003).

2.1.3 Columnar Organization

In addition to the laminar pattern of the cortex, neurons appear to be organized in vertical columns that are about 0.5-1.0 mm in diameter. According to Thompson and Toga (2003), there are over a million of these columns in the human cortex, particularly prominent in the temporal cortex and more prominent in gyri than in sulci (Welker, 1990 according to White et al., 2003). These so-called *micro-columns* form a series of repeating units running orthogonally to the horizontal laminae (Hubel and Wiesel, 1962; Jones, 2000). The columns were proposed to be the fundamental processing units of the cortex based on the assumption that neurons in middle layers of the cortex (in which, for example, thalamic afferents terminate), should be joined by narrow vertical connections to other neurons in

layers located above and underneath to them. Consequently, all cells in the column would be excited by incoming stimuli with only small latency differences (Mountcastle, 1957; Jones, 2000). That is, neurons in a given vertical column often form a mini-circuit that performs a single function (Pinel, 2002). It was suggested that the columnar organization is strongly related to the migration of neurons from the ventricular and sub-ventricular zones into radial columns during development (Rakic, 1988). For further details on neuron migration and development of the cortex, see section 2.2.

2.1.4 Topological Organization

Cortical sensory areas contain so called *topological maps* reflecting the layout of corresponding sensory organs. For example, neurons in the primary visual cortex represent a *retinotopic* map in which positioning mirrors locality on the retina (e.g., moving an electrode tangentially through layer IVc corresponds systematically to locations moving from the fovea to the periphery of the eye). In the same way, the primary auditory cortex contains *tonotopic* maps. Here, the maps reflect the layout of a sheet of receptors in the cochlea, which respond to different frequencies of sound (Thompson et al., 2001a). Similarly, topological maps exist in the motor and somatosensory cortex. In these two areas, topological maps of the body surface reveal an orderly layout of neurons that project or receive signals to or from different parts of the body. However, bizarre distortions in terms of representation appear in which vastly greater amounts of neurons are devoted to body regions with substantial motor innervations (e.g., fingers and mouth) or high sensitivity (e.g., lower lip and tongue) – the so called motor and sensory *homunculus*.

2.1.5 Macro Structure

Sub-divisions of the cortex can not only be distinguished on the micro-anatomical level by their histological and neuro-chemical characteristics or their afferent and efferent fiber systems, but also by their macro-anatomy. The following description will provide a general orientation. For an exhaustive overview about cortical structures refer to Duvernoy (1999), Ono et al. (1991) and Hanaway et al. (1998).

The two cerebral hemispheres possess both lateral and medial surfaces, which are deeply convoluted. These convolutions increase the amount of cerebral cortex without increasing the overall volume of the brain. Ridges in the cortex are called *gyri* (*gyrus*) and furrows lying between two gyri are called *sulci* (*sulcus*). Approximately two thirds of the cerebral cortex is buried within the cortical sulci (Kuperberg et al., 2003). Particularly deep sulci are called *fissures*. Both hemispheres are almost completely separated by the largest of the fissures: the *Longitudinal fissure*. The principal sulci on the lateral surface of the hemisphere are the central fissure or *Rolandic fissure* (Figure 1, left) and the lateral fissure or *Sylvian fissure* (Figure 1, left). The course and pattern of the sulci and gyri differ not only in individuals but even between hemispheres of the same brain, with greatest variability in frontal and parieto-occipital regions (Ono et al., 1991).

The lateral surface of each cerebral hemisphere is divided into four lobes: Frontal, temporal, parietal and occipital lobe (Figure 1, left). The medial surface is made up of the medial extensions of the frontal, parietal, temporal and occipital lobes in addition to the cingulate gyrus which is located right above the corpus callosum (Figure 1, right).

Interestingly, macroscopical landmarks are not always reliably associated with cyto-architectonically defined borders of cortical areas (Zilles et al., 2004).

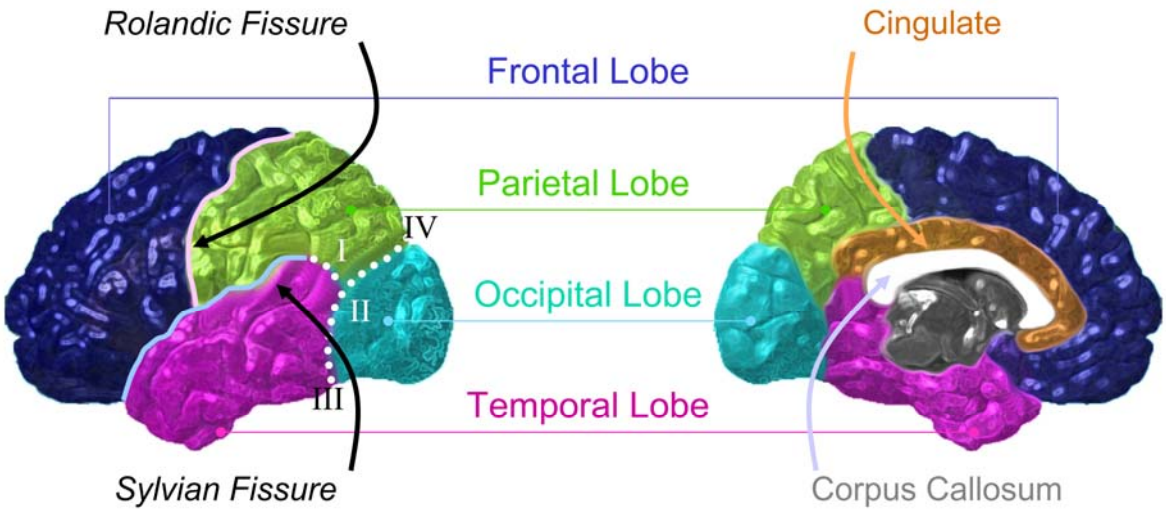

Figure 1. The lateral and medial surface of the cortex
Demonstrated are some of the characteristic landmarks on a cortical surface model of the left hemisphere of a random brain from the sample analyzed in the present thesis. The boundaries for the lobes are formed by natural structures or by artificial lines. The Rolandic fissure divides the frontal lobes from the parietal lobes. The temporal lobe is separated from the frontal and parietal lobes by the Sylvian fissure and the temporo-occipital line (I) – an artificial line drawn from the posterior end of the Sylvian fissure to the middle of the parieto-occipital line (II). The occipital lobe is separated from the temporal and parietal lobes by the parieto-temporal line (II) – another imaginary line running from the pre-occipital notch (III) on the basal surface of the hemisphere to the superior part of the parieto-occipital sulcus (IV) on the medial wall of the hemisphere.

2.1.6 Link between Structure and Function

At the beginning of the twentieth century, the German anatomist Korbinian Brodmann divided the human cortex into 52 cytoarchitectural areas (some being further subdivided) primarily on the basis of the size, shape, packing density and lamination of neurons in Nissl-stained preparations. Further studies revealed that neurons with similar electrophysiological properties are located within the same area (Vogt and Vogt, 1919 according to Geyer et al., 2001). The finding that architectonic areas are functional entities gave strong support to the concept of cortical specialization (Geyer et al., 2001), as

confirmed by classic lesion studies and modern functional imaging. For example, Brodmann area (BA) 17 is considered the primary visual cortex, which is surrounded by BA-18 and BA-19 both representing secondary visual areas that perform higher-order computations on visual features. BA-1, BA-2, and BA-3 – the first areas Brodmann investigated – include the primary somatosensory cortex, which processes sensations from the body surface. BA-6 and BA-8 contain the motor and premotor cortex, which control voluntary movements. Other key areas include the primary auditory cortices (BA-41 and BA-42), Broca's speech area (BA-44 and BA-45), and Wernicke's language comprehension area (BA-22).

Although Brodmann's map had a tremendous impact for our understanding of the functional organization of the brain, the classic architectonic maps of the human cerebral cortex do not seem to match the high degree of cortical segregation as shown by functional imaging (Zilles et al., 2004). Thus, the regional and laminar distribution of various transmitter receptors, rather than cell bodies or myelin, was suggested to be a functionally more relevant indicator for the regional organization of the cortex (Zilles et al., 2004). Interestingly, analyzing the regional distribution of transmitter receptors not only reflected well-established cyto- and myelo-architectonically defined borders of cortical areas, but also revealed more cortical areas than previously demonstrated (Zilles et al., 2004). The worldwide expansion of brain mapping efforts has produced large databases of maps of cortical function and structure. These provide new insights into how the cortex is organized and describe anatomical and functional variations due to age, gender, disease, genetics and other factors [for further reading please refer to (Toga and Mazziotta, 2000)].

2.2. Development of the Cerebral Cortex

Brain development and maturation occur as a consequence of orderly processes that begin in utero. In very early stages of the development of the embryo, the tissue that eventually develops into the CSF is a fluid-filled tube evolving from the neural plate during the 3rd and 4th week of gestation. First indications of the developing brain are three swellings that occur around the 6th week of gestation at the anterior end of this tube (Pinel, 2002). They will develop into the *Prosencephalon* (forebrain), the *Mesencephalon* (midbrain), and *Rhombencephalon* (hindbrain) each attached to the other, atop the spinal cord. Later, the initial three swellings in the neural tube become five through growth of the Prosencephalon into the *Telencephalon* and *Diencephalon*, and the Rhombencephalon into the *Metencephalon* and *Myelencephalon*. Each of these vesicles contains a primitive ventricle, which will eventually give rise to the future ventricles and their systems of the brain: the telencephalic paired lateral ventricles, the diencephalic third ventricle, the mesencephalic cerebral aqueduct, and the rhombencephalic fourth ventricle.

2.2.1 Cell Migration

One remarkable feature in the embryonic development of the cortex is that neurons, later constituting the cerebral cortex, are not generated in the cortex itself but in the so-called *ventricular zone*. The ventricular zone is the region adjacent to the fluid-filled center of the telencephalic vesicle, although newer analysis also revealed that a sub-population of neocortical interneurons originates from the primordia of the basal ganglia (Anderson et al., 1997). Neuronal precursor cells must migrate from the site of their origin to proper

laminar and areal positions in the expanding cerebral hemisphere (Rakic, 1998). According to the *radial unit hypothesis* (Rakic, 1972; Rakic, 1988), the migration takes place based on a temporary construction of a radial scaffolding which is made up of extremely elongated glial cells in the neuronal tube. The glia cells are attached to the ventricular surface by their end feet and have radial processes that protrude toward the pial surface, spanning the cortical width (Rakic, 1998). This scaffolding guides neuronal precursor cells to their destinations in the cortex, where they come into contact with *reelin* – a protein which signals them to detach from the glial surface and stop their migration.

Of note, each successively generated neuron must bypass predecessors that migrated along the same glial fiber, before ultimately settling at its final destination (Rakic, 1998). That is, when the cerebral cortex is built below the cerebral surface, inner layers of the cerebral cortex are made up of older neurons, creating an "inside-out" pattern of cortical layering (Ganeshwaran et al., 2004). The migration of neurons into the cerebral cortex appears to peak between the 11th and 15th week of gestation in humans (Sidman and Rakic, 1973), where the majority of the neurons seems to have reached the cortex by the 24th week of gestation (Marin-Padilla, 1990). There are many complex and necessary processes related to the initiation of migration, path finding, locomotion itself, and selection of the final neuronal position within the cortex (Rakic, 1998). For example, both migration and final alignment with other developing neurons that have migrated to the same area are thought to be mediated by cell-adhesion molecules (CAMs). These extra cellular and cell surface proteins have the ability to recognize molecules on other cells and adhere to them – the reason why they are also called “the glue of life”.

2.2.2 Axon Growth, Synapse Formation, and Neuron Death

Each time a neuron has stopped migrating and arrived at its final destination in the cortex, it extends its axons and dendrites to build synaptic connections. For this purpose, specialized amoeba-like structures located at the growing tips of axons or dendrites (so-called *growth cones*) extend and retract fingerlike cytoplasmic extensions (so-called *filopodia*). It was hypothesized that growth cones found their synaptic targets by chemical labels released by each post-synaptic surface (chemoaffinity hypothesis) and by specific mechanical trails through the extra cellular matrix blazed by pioneer growth cones that found their correct trail by interacting with the CAMs of cells along the route (blueprint hypothesis). For a good overview with regard to potential weaknesses and strengths of these theories, as well as for supplementary explanations, refer to Pinel, 2002 (pp 226).

Many cortical neurons initially project axons and dendrites to a much wider set of targets than are eventually found in the adult brain. For example, the number of synapses in the primary visual cortex peaks around the 8th postnatal month in humans; the maximum synapse density in the prefrontal cortex is reached in the 2nd postnatal year (Pinel, 2002). Similarly, periods of synaptic loss occur at different times in different parts of the brain. For example, synaptic density in the primary visual cortex declines to adult level at around the 3rd postnatal year, whereas declines in prefrontal regions do not manifest until adolescence (Pinel, 2002).

Synaptic elimination and rearrangement is also closely related to neuron death. In fact, about 50 percent more neurons are produced than required (Pinel, 2002), and consequently the number of neurons reaching a target field in the developing nervous

system exceeds the number found in the mature innervated target. Major reductions of cortical neurons occur during the last 10 weeks of human gestation (Rabinowicz et al., 1996). The population of neurons becomes much smaller through a programmed neuronal death, an active process called *apoptosis* (in contrast to *necrosis* – the passive cell death). However, life-preserving chemicals (so-called *neurotrophins*), that are secreted by cells in the target field, can protect the neurons from apoptosis by preventing the genetic suicide program inside the neurons to be triggered. Consequently, if neurons fail to compete successfully for neurotrophins, they will die. In addition, inhibitory effect of steroids, like estrogens and androgens, were reported to reduce the incidences of apoptosis (Davis et al., 1996; Wise et al., 2001; Wise, 2002). Notwithstanding, complementary growth-inhibiting effects of estrogens were also proposed (Sandhu et al., 1986; Diamond, 1987; Diamond, 1991). Although those hormonal effects are proposed to constitute lifelong influences on aspects of brain architecture and function (Forget and Cohen, 1994), the majority of neurons that compose the adult human brain seem to have developed and migrated to their appropriate location already by the 7th month of prenatal development (Pinel, 2002).

Later in life, most likely candidates for cell death are neurons and synapses not activated by experience (Pinel, 2002). The activation of neural systems appears to be crucial in determining which connections are retained and which are lost (Thompson et al., 2000a). For a good overview and further references with respect to mechanism by which experience might influence neurodevelopment see Pinel (2002, pp. 231) and refer to section 11.1. Paralleling the process of cell death, *neurogenesis* (the birth of new neuronal cells) appears to continue into and throughout adult human life (Gross, 2000; Hastings et

al., 2000; Kaplan, 2001; Eriksson, 2003; Mackowiak et al., 2004). Contrasting traditional views that the generation of neurons is restricted to a discrete developmental period, studies observed new neurons in the primate brain in the olfactory bulb (Altman, 1969) and hippocampus (Eriksson et al., 1998), as well as in some neocortical association areas (Gould et al., 1999).

2.2.3 Changes in the External Appearance of the Brain

The human brain grows substantially before and after birth, which is predominantly a result of the formation of new synapses, myelination of axons (starting in the first few months after birth and continuing into adolescence), and increased branching of dendrites, with the latter following the same inside-out pattern as the neuronal establishment of the cortex. The rate of brain expansion during embryonic development is not uniform, which leads to changes in shape as the brain grows. For example, the so-called *insula* on the lateral surface of the developing brain sustains relatively slow growth during this time. It forms an almost stationary point around which the growing hemisphere turns as it expands, so that later, in the adult brain, it is hidden in the *Sylvian* fissure (Castellano, 1999).

Between the 8th and 10th week, so-called transitory furrows appear. They achieve their maximal development in the 3rd to 4th month but disappear completely and are, thus, not precursors of the definitive furrows (Ono et al., 1992). The surface of the brain is essentially smooth during the 5th and 6th months of gestation (Magnotta et al., 1999), albeit for example, the central sulcus can be observed as early as the 20th week of gestation (Sidman et al., 1982 according to Vogeley et al., 2000). Also starting in the 20th week of

gestation, the four different lobes in the two hemispheres become obvious (Castellano, 1999). Around the 26th week of development, most of the primary sulci have appeared, while tertiary and secondary sulci continue to develop while the brain grows.

It is not entirely clear when gyrification and fissurization of the brain is finally completed. Gyrification, which becomes progressively more complex during gestation, seems to reach a stable plateau shortly after birth (Haug, 1987; Armstrong et al., 1995; Zilles et al., 1997). Nevertheless, contrasting reports of significant positive correlations between age and frontal brain regions in a sample of children and adolescents (ages 6 to 16) also exist, which indicate that gyrification also occurs later in the course of human development (Blanton et al., 2001). Other studies, examining subjects between 18 and 82, revealed a flattening and opening up of the sulci with increasing age starting with the late teens, while gyral crowns become narrower and sharper. However, as pointed out by the authors, it is unresolved exactly when the ongoing developmental modeling (e.g., pruning or activity-dependent changes) transforms into a degenerative process (Magnotta et al., 1999). Moreover, although the human brain seems to undergo changes in gyral and sulcal shape as a consequence of the aging process, gyrification pattern per se might not be altered. Several mechanisms associated with the genesis of gyrification patterns of the human brain have been suggested, and a detailed discussion is provided in section 11.1.2.

2.3. Evolution of the Cerebral Cortex

With respect to the evolution of the brain, or more specifically, the primate brain, there are only two sources of evidence: paleontological data from fossil skulls and endocasts, and

data from extant vertebrates. The former reveals how TBV has changed during evolution. Nevertheless, the study of endocasts constitutes only a rough estimate of brain surface anatomy without access to deep structures (Rilling and Insel, 1999a). Therefore, most investigations rely on the latter, more indirect form of phylogenetic evidence.

All vertebrate brains are constructed of neurons and also display the same gross structures (e.g., forebrain, midbrain and hindbrain). However, as the following paragraphs show, considerable neurological differences between species have developed during the course of evolution. Although numerous investigations (Rilling and Insel, 1998; Rilling and Insel, 1999b; Weaver, 2005; Sherwood et al., 2005) revealed large differences in various aspects of the brain (including cerebellar proportions, cytoarchitecture of the brainstem, interhemispheric connectivity), this thesis will limit its focus to deviations regarding cerebral size, tissue components, cortical dimensions and gyrification among and within mammalian orders.

2.3.1 Size of the Brain

Many research efforts have been made to test whether (non)allometric rules based on data from nonhuman primates hold true for the human brain. For example, a so-called *Encephalization Quotient* (EQ) is often used to represent the level of encephalization. EQ is a measure of observed brain size relative to expected brain size derived from a regression of brain weight on body weight for a sample of species. EQ values are essentially residuals from the regression line with values standardized as one, less than one, and greater than one for relative brain sizes that are average, below average, and above

average, respectively (Marino, 2004). The EQ of modern humans was reported as 7.0, followed by several delphinid species with EQs above 4.0 (Marino, 2004). Additional sources indicate similar non-allometric trends with human brains being three to four times bigger than expected for a primate of the same body size. Those data suggest that brain expansion throughout hominid evolution did not follow a predictable allometric trend (Rilling and Insel, 1999a).

Nevertheless, several analyses focused on the inter-species comparison of brain size stimulated by the notion that brain size and intellectual capacity might be closely related. In fact, when the brain's evolution is traced from fish to amphibians to reptiles to mammals and finally to humans, brain size has increased considerably in humans. Moreover, in the process of hominization, the hominid species with smaller brains were gradually replaced by species with larger ones, where brain volume approximately tripled (Rilling and Insel, 1999a). However, research also revealed that humans have smaller brains (ca. 1,350 grams) than whales or elephants (5000 or 8000 grams). Thus, a related measurement was established by expressing brain size or weight as a percentage of total body weight. Surprisingly, it was revealed that human brains (albeit now outranging elephants and whales) rank behind the shrew brain with 2.33 % versus 3.33 % (Pinel, 2002). That is, the neuro-anatomical substrate for intelligence can not be solely reflected in absolute or relative brain size. It is more likely that brain evolution was accompanied by a tremendous reorganization of structures or redistribution of functions. Consequently, in addition to global comparisons of (relative) brain size and weight, more specific analyses were conducted with regard to cerebral constituents (e.g., the cerebral cortex), cerebral sub-

components (e.g., GM and WM), cortical regions (e.g., the prefrontal cortex), or specific cortical features (e.g. convolution). Their outcomes will be summarized in the next paragraphs, although little is known about the functioning within brains of non-human species.

2.3.2 Size of the Cerebral Cortex and Cerebral Tissue Components

One of the most notable trends in mammalian evolution is the massive increase in size of the cerebral cortex, especially in primates. For example, in fish and amphibian brains, there is no neocortex, whereas in primates it accounts for 38 % to 51 % of the brain (Rilling and Insel, 1999a). Comparing earlier evolved primates (so-called *prosimians*) with later evolved primates (so-called *anthropoids*) revealed a relatively larger neocortex in the more recently evolved group (Radinsky, 1975; Barton, 1996). Moreover, using allometric regression analyses in order to relate neocortical volume to body weight, it was discovered that the human neocortex is between 18 % and 24 % larger than predicted by nonhuman primate allometric trends, which suggests extra-allometric expansion (Rilling and Insel, 1999a).

Similarly, WM was 22 % larger and the sum of GM and WM was even 61 % larger in humans than expected for an anthropoid primate of the same size (Rilling and Insel, 1999a). It has also been observed that cerebral WM seems to outpace increases in neocortical GM during evolution (Rilling and Insel, 1999a). Since WM is composed of axons while GM is largely composed of neuronal cell bodies, these data might imply that increases in the number of connections between neocortical neurons outpaces increases in

the number of neocortical neurons (Rilling and Insel, 1999a). Nevertheless, as discussed by Rilling and Insel (1999a), the increase in WM is probably not sufficient to maintain the same amount of connectivity among neocortical neurons as the number of neurons increases. It was estimated that the number of WM connections would need to increase at the square of the number of neurons in order to preserve maximum connectivity, where each neuron is connected to every other one (Frahm et al., 1982). Most likely, long-distance connections between the two hemispheres, which become slower with increasing brain size, are preferentially eliminated. This might have had the effect of confining certain functions to a single hemisphere. For further discussions, also with respect to alterations of structural laterality in the course of evolution, refer to (Ringo et al., 1994; Rilling and Insel, 1999a; Hopkins and Rilling, 2000; Hopkins et al., 2000). Evolutionary changes in gross tissue properties are accompanied on a cellular level by alterations in neuronal size and number of connections during primate evolution as body weight and brain weight increases. For further details refer to Sherwood et al. (2003).

2.3.3 Surface Area of the Cerebral Cortex and Gyrification

The larger cortex in humans does not only contain a larger number of neurons or neuronal fiber connections. Over the course of evolution, the cerebral cortex has grown considerably in surface area. The cortex in humans is only 15 % thicker than in macaque monkeys, but has at least 10 times more surface area. Similarly, but with an even larger discrepancy, the human cortex is only twice as thick as the cortex of the mouse, but has about 1,000 times the surface area. This enormous enlargement in surface area seems to be the result of a

larger brain and, perhaps more important, an increased folding of the brain's surface (probably in order to accommodate an expanding neocortical surface that must fit within the confines of a spherically shaped skull). For example, several studies revealed that larger anthropoid primate brains are more convoluted than smaller ones (Elias & Schwartz, 1971; Jerison, 1982; Zilles et al.,1989, Rilling and Insel, 1999a according to Rilling and Insel, 1999a). In addition, cortical folding was reported to increase more rapidly with brain size among later evolved anthropoid primates compared with earlier evolved prosimians (Zilles et al., 1988; Zilles et al., 1989). Only the high degree of cortical gyrification in many cetacean brains (e.g. dolphins, whales etc.) and resulting neocortical surface area is supreme to that of humans cortices (3745 cm^2 versus 2275 cm^2), which, however, are considerably thicker than cetacean neocortices (3.0 mm versus 1.3-1.8 mm) (Haug, 1987; Marino, 2004).

Supplementary findings exist with respect to the regional pattern of gyrification suggesting that hominid evolution also involved the specific expansion of certain neocortical regions (rather than an expansion that acted uniformly across the whole cortex). For example, the prefrontal cortex in humans has been reported to account for 29 % of the entire neocortex, whereas in chimpanzees it accounts for only 17 %. This discrepancy is also clearly reflected in the degree of gyrification: as revealed by Rilling and Insel (1999a), the human prefrontal cortex is significantly more convoluted than expected for an anthropoid primate of the same size, corroborating earlier *post mortem* reports (Zilles et al., 1988). Furthermore the gyrification in parietal and posterior temporal cortices was reported to be larger than expected in the human brain (Rilling and Insel, 1999a).

Deviations from nonhuman allometric trends in global and regional gyrification as well as cerebral and cortical dimensions have been discussed as morphological substrate that supports some of our species' most distinctive cognitive abilities. For example, a unique evolutionary modification of the appearance of the human prefrontal cortex is intriguing given its involvement in working memory, symbolic thinking, decision making, planning, and goal achievement, while in species other than primates it is dedicated to voluntary motor control (Rilling and Insel, 1999a). Nevertheless, brain evolution involved more than just alterations in the gross anatomy of the brain and its subcomponents. It also involved a large degree of reorganization to support specific, uniquely human, cognitive tasks, including those involved in linguistic processing, social intelligence and a highly developed facility for manufacturing and manipulating tools. However, despite more than a century of effort, there is little consensus about how and when such reorganization occurred (Weaver, 2005).

3. MRI-based In Vivo Morphometry

3.1. Magnetic Resonance Imaging (MRI)

This thesis analyzes and discusses data from high-resolution MRI scans obtained on 60 subjects on a 1.5 Tesla scanner. The following chapter provides a comprehensive picture of the basic principles of MRI, where most of the information is taken from web publications and web tutorials[1]. For further information, also with respect to more advanced mathematics and imaging physics, please refer to Mansfield and Morris (1982).

3.1.1 General Facts and Historic Milestones

MRI is an imaging technique used primarily in medical and research settings to produce high quality images with high spatial resolution of the inside of the human body. MRI is based on the principles of nuclear magnetic resonance (NMR). Notwithstanding, the technique was called magnetic resonance imaging rather than nuclear magnetic resonance imaging because of the negative connotations associated with the word nuclear in the late 1970's.

In 1946, Felix Bloch and Edward Purcell discovered the magnetic resonance phenomenon independently. In the period between 1950 and 1970, NMR was developed and used for chemical and physical molecular analysis. In 1971, Raymond Damadian discovered that the structure and abundance of water in the human body was the key to

[1] See http://www.erads.com/mrimod.htm;
http://www.cis.rit.edu/htbooks/mri/mri-main.htm;
http://airto.bmap.ucla.edu/BMCweb/CourseWork/M285/MRI;
http://smuc.siemens.se/applikation/mrtutorial/mrtutor/index.html.

MRI, and that hydrogen emitted a signal that was both detectable and recordable. In 1973, MRI was first demonstrated on small test tube samples by Paul Lauterbur. In 1975, Richard Ernst proposed magnetic resonance imaging using phase and frequency encoding, and the Fourier Transform. In 1980, Edelstein and co-workers demonstrated imaging of the body using Ernst's technique, where a single image could be acquired in approximately five minutes. By 1986 the imaging time was reduced to about five seconds, without sacrificing too much image quality.

Magnetic resonance started out as a tomographic imaging modality for producing NMR images of a slice through the human body, but has now advanced to a volume imaging technique. Clearly, MRI is a young, but growing science. Already in 2003, there were approximately 10,000 MRI units worldwide and approximately 75 million MRI scans per year performed with numbers increasing.

3.1.2 Spin Physics

Spin is a fundamental property of nature and describes the tendency of an object to keep rotating at the same speed about the same axis of rotation. Spin comes in multiples of 1/2 and can be plus (+) or minus (-). Protons, electrons, and neutrons possess spin. Individual unpaired electrons, protons, and neutrons each possess a spin of 1/2. Two or more particles with spins having opposite signs can pair up to eliminate the observable manifestations of spin. Unpaired nuclear spins (e.g. in the hydrogen atom) have the largest resulting overall spin and are exceptionally sensitive to MRI for this reason. Consequently, but also due to

its abundance in the human body, MRI is almost exclusively limited to the study of hydrogen.

The spin of the hydrogen proton behaves like a tiny magnet with a north and south pole. When the proton is placed in an external magnetic field, the spin vector of the particle aligns itself with the external field, just like a magnet would. There is a low energy configuration (where the poles are aligned parallel to the external magnetic field: N-N; S-S) and a high energy state (anti-parallel to the external magnetic field: S-N; N-S). At any instant in time, the magnetic field due to all the spins in the so-called *spin ensemble* can be represented by a magnetization vector revealing the so-called *net magnetization*. Given that the parallel oriented spins are more numerous than the anti-parallel oriented ones, the resulting net magnetization is oriented parallel to the external magnetic field.

However, protons do not only align themselves; they also move around with a periodic wobble in the axis of the rotation. This movement is called *precession*. The stronger the magnetic field, the stronger the precession frequency (e.g. the frequency is twice as high in a 1.0 Tesla magnetic field as in a 0.5 Tesla magnetic field).

3.1.3 Signal Generation

A Radio Frequency (RF) pulse is designed to disturb the protons that peacefully and quietly precess in the parallel alignment of the external magnetic field. When the RF pulse is switched on, some protons will undergo a transition from the parallel alignment (low energy state) to the anti-parallel alignment (high energy state) by absorbing a photon from the RF pulse. The essence is that the energy of the photon must exactly match the energy

difference between the two states (RF impulse and protons must have the same frequency). This principle of energy transfer occurring at a specific frequency is called *resonance*. When the RF pulse is switched off, the whole system goes back to its original random state. This phenomenon is called *relaxation.*

Adapting the conventional NMR coordinate system, the external magnetic field and the net magnetization before the RF pulse are both along the z-axis. Magnetization along the z-axis is called *longitudinal magnetization*. In contrast, magnetization along the x- or y-axis is called *transversal magnetization.* Before turning on the RF pulse, protons randomly point left, right, back and forth, and the transversal magnetization is zero. After the RF pulse, however, the protons point in the same direction at the same time (they are in phase). The magnetic vectors add up in the transverse direction, so that the transversal magnetization increases, while the longitudinal magnetization decreases. After the RF pulse is turned off, the new transverse magnetization starts to disappear while the longitudinal magnetization returns to its original magnitude.

3.1.4 T_1- and T_2-Processes

Protons gain energy from the RF pulse but start to lose it as soon as the RF pulse is switched off. They return from the higher level of energy to the lower level. The time constant which describes how the longitudinal magnetization returns to equilibrium is called "T_1" or *longitudinal relaxation time*. In other words, T_1 is the time it takes for 63 % of the longitudinal magnetization to recover. T_1-relaxation is the result of thermal motion of the molecules, which excites the dipoles to give up energy to the molecular lattice (T_1 is

also called *spin-lattice relaxation time*). Different types of tissue have different relaxation times. For example, pure water and CSF have a very long T_1 because a small water molecule can move quickly and randomly through its molecular environment. It does not have much of a chance to emit energy by interacting with its neighboring molecules during a specific unit of time. In contrast, fat has a large, slow-moving molecule in a dense atomic lattice with a very short T_1.

The time constant which describes when the transversal magnetization has decreased to 37 % of its initial value, is called "T_2" or *transversal relaxation time*. That is, the transverse magnetization precesses freely, induces a signal (called "FID" or *free induction decay)* and decays immediately after the end of the RF pulse. T_2-relaxation describes the process where proton's precessions begin to diphase (some precess faster and some precess slower), so that energy is transferred from one proton to another or "spin to spin". (T_2 is also called *spin-spin relaxation time*). In addition to such molecular interaction, T_2 is also influenced by magnetic field inhomogeneities. The combination of these two factors is what actually results in the decay of transverse magnetization. The combined time constant is called "T_2*". Similar like T_1, T_2 is tissue-specific but in contrast to T_1, T_2 is very short for fluids or CSF and longer for fat.

3.1.5 Contrast Generation

The stronger the energy of the stimulating RF pulse, the greater the angle of deflection for the magnetization. A 90° pulse flips the magnetization directly into the xy-plane. Right after submitting the 90° pulse, the longitudinal magnetization is zero and can not be flipped

anymore. This phenomenon is known as *spin saturation*. However, we could send a 90° pulse, wait a certain amount of time, called TR (time of repetition), and then emit a second 90° pulse. If we choose a TR long enough to allow all of the protons to relax, the MR signal after the second pulse, will be identical to the MR signal after the first pulse. However, if we choose a shorter TR, protons from one tissue "A" might have completely relaxed before emitting the second pulse, while protons from another tissue "B" have not. Thus, the longitudinal magnetization is higher for tissue "A" before applying the second pulse. Consequently, the resulting signal will be also stronger for "A" than for "B", because more longitudinal magnetization can be converted into transversal magnetization to induce the MR signal.

A 180° pulse inverts the magnetization vector and flips it into the opposite direction. If we sent a 180° pulse (after sending the first 90° pulse) we would cause the dephasing protons to turn around, so that they precess in the opposite direction (i.e. the faster-precessing protons are now behind the slower ones). When the protons finally rephrase, a new MR signal is generated: the so-called *spin echo*. The time between the initial 90° RF pulse and the echo is called echo time (TE). If we apply a succession of 180° pulse (a so-called *pulse sequence*), the echo amplitude and, thus, our measurable MRI signal gets progressively smaller because of the random interaction between the spins. Again, the degree of decrease in echo amplitude is tissue-dependent.

By varying the time interval between the two 90° pulses (varying TR) and between the 180° pulses (varying TE), we get different types of tissue contrast: If we combine a long TR with a long TE, the differences in T_2 become pronounced, and the images are T_2-

weighted. In contrast, by combining a short TR with a short TE, differences in T_1 will show up and we get T_1-weighted images. Examples for T_1-weighted images (as analyzed in the present thesis) are provided in figure 2.

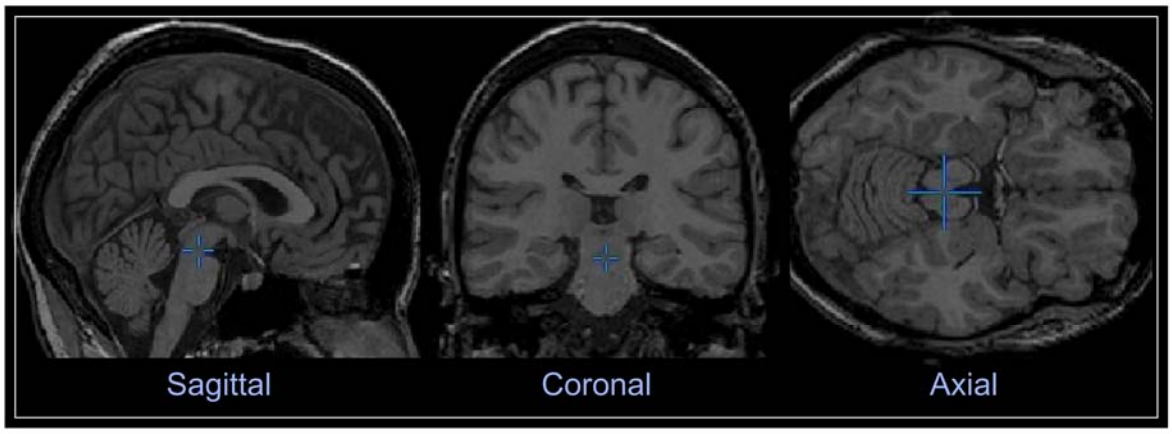

Figure 2. Sagittal, coronal, and axial view of a T1-weighted image
CSF appears dark in T_1-weighted images because lower MR signals (as a result of a long T_1) are translated into smaller intensity values. In contrast, WM appears lighter because higher MR signals (as a result of a short T_1) are translated into larger intensity values.

3.1.6 Spatial Coding

In order to determine the location of the signal, we first have to code the slice of interest. Slice selection in MRI is the selection of spins in a plane through the object. Slice selection is achieved by applying a one-dimensional, linear magnetic field gradient during the period that the RF pulse is applied. That is, a second magnetic field is superimposed on the external field. This additional field is a gradient field and is produced by the gradient coils during the RF pulse. This gradient field modifies the strength of the original magnetic field which now has different strengths in varying locations. Consequently, the protons have different precessional frequencies, too. In order to visualize only a particular area of the brain, we can send in an RF pulse that contains only the frequencies that excite the protons

in the slice of interest. This gradient field is called a *slice-selecting gradient*. Importantly, slice-selecting gradients can be superimposed in any direction. In order to determine the slice's thickness, we send in an RF pulse that not only has a specific frequency, but a certain range of frequency (bandwidth). The wider the range of frequencies, the thicker is the slice in which protons will be excited. However, we can further influence the slice thickness by modifying the slope of the gradient. In a steeper gradient field, the precessional frequencies will also vary to a larger degree. The data of the present thesis are based on a slice thickness of 1.5 mm.

In order to determine the location of the signal in a particular slice (i.e. from left to right; columns in a 256 x 256 matrix), we apply a so-called *frequency encoding gradient*. The frequency-encoding gradient decreases from left to right. The result is that the protons in the different columns emit their signals with different frequencies. Finally, in order to discriminate between the signals from protons in the same column in a particular slice (i.e. from top to bottom; rows in a 256 x 256 matrix), we apply a *phase-encoding gradient*, which causes the spins in top rows to accelerate more than spins in bottom rows. Consequently, protons in the different rows emit their signals with different phases.

That is, after applying all these gradients we get a mixture of different signals. They have different frequencies, and signals with the same frequency have different phases, all according to their location. In order to obtain an image of the location, the free induction decays are analyzed through a so-called *Fourier transformation* on a computer. For this purpose, the signals are first transformed in the X direction to extract the frequency domain information and then in the Y direction to extract information about the locations in the

phase encoding gradient direction. Since these signals can be assigned to a certain location in the slice, the image can be reconstructed. The acquisition of MR data from a volume rather than an only tomographic slice is called *volume imaging*. It can be thought of as collecting several contiguous slices through an imaged object, where the number of contiguous slices will always be a multiple of 2.

3.1.7 Safety

Although MRI does not use ionizing radiation, there are still important safety considerations. For example, caution must be taken to keep all ferromagnetic items away in order to prevent injury or even death of the individual in the magnet. Furthermore, there are additional concerns regarding the effect of magnetic field on ferromagnetic metal implants and electronic circuitry in those being imaged. Thus, individuals with pace makers or foreign metal objects such as shrapnel or older ferromagnetic implants are usually not imaged. The RF energy from an imaging sequence can cause heating of the tissues of the body, so exposure to RF energy should be limited. Any pulse sequence must not raise the temperature by more than 1^{o} C and under no circumstance reach greater than 38^{o} C in the head. Similar restrictions exist with respect to acoustic noise produced by the imaging gradients. An excellent resource for MRI safety is provided by the Institute for Magnetic Resonance Safety, Education, and Research at http://www.mrisafety.com/.

3.2. Analysis of MRI-based Images

The increasing sophistication of MRI allows neuroanatomical structures to be visualized *in vivo* with exquisite detail. This imaging detail combined with advanced image analysis algorithms significantly contributes to our ability to identify cerebral structures and detect group-specific patterns (Ashburner et al., 2003; Thompson et al., 2003). In the following paragraphs, I will give a brief overview about potential approaches to assess structural peculiarities of the brain that are significantly related to the effects under study. For further readings refer to Jancke (2003), Ashburner et al. (2003) and Thompson (2003).

3.2.1 Regions of Interest Analyses

Traditionally, many brain studies were based on the analysis of ROIs. Here, certain areas of the brain are manually (or semi-automatically) outlined using a set of contiguous brain slices or only a single brain slice, followed by assessing tissue compartments or shape, area, and volumes of those regions. However, using ROIs defined *a priori* limits the identification of changes elsewhere in the cortex, may introduce user bias and makes it impractical to study large populations given that manual delineations are labor intensive and extremely time-consuming. Notwithstanding, manually-derived measures also continue to provide extremely valuable information for certain structures of interest, for example as done in our group for the CC (Luders et al., 2003; Luders et al., 2005). ROI-studies have the additional advantage of being theoretically motivated (Kuperberg et al., 2003). Moreover, they serve as a standard to validate newer, more automated techniques, such as Voxel-Based Morphometry [VBM] (Tisserand et al., 2002; Luders et al., 2004).

Finally, often significant information is gained by combining manual approaches with more automated ones (Thompson et al., 2003). For example, sulci may be traced manually on a cortical model extracted automatically, or automatically generated brain masks may be manually corrected for greater accuracy, as done, for example, in the analyses of the current thesis.

3.2.2 Whole-Brain Analyses

Fully-automated whole-brain analysis techniques are considerable faster than traditional ROI-approaches; they allow the examination across the entire brain or cortex while avoiding the need for *a priori* defined ROIs. Moreover, user-introduced bias is diminished or absent, which in turn, ensures a high level of reliability. Automated approaches do not only avoid error-prone and labor-intensive manual measurements, but also provide an exceptional precision, where brain-volume differences of 0.5 % between images from the same individual can bet detected (Ashburner et al., 2003). A variety of tools and approaches have been developed to analyze MR images automatically, where underlying principles and assed domain can differ considerably. While not an exhaustive list, the following describes some key methods for analyzing MRI data with respect to group differences in brain structure. Before addressing major approaches, the concept and rationale of spatial normalization, as a fundamental step of many automated methods, is explained.

3.2.2.1 Spatial Normalization

The success of brain mapping has been promoted by the international adoption of a coordinate-based three-dimensional (3D) reference system for brain data (Thompson et al., 2003). That is, images are aligned with a standard brain template, typically one based on the Talairach stereotaxic atlas (Talairach and Tournoux, 1988). Transformations into the Talairach space require the re-positioning of the anterior commissure (AC) at the origin of the 3D coordinate space, followed by vertically aligning the interhemispheric plane, and horizontally orienting the line connecting the two commissures. Each point in the transformed brain is labeled by an (x-, y-, and z-) co-ordinate referable to the atlas brain. Of note, the Talairach stereotaxic system was originally developed for surgery in order to accurately position surgical apparatus within a patient's brain. However, given that the Talairach template was based on inconsistent, orthogonal sections acquired *post mortem* from one 60-year-old female subject, alternative composite T1-weighted MRI datasets were constructed.

The *MNI-305* template is the original template of the Montreal Neurological Institute (MNI) that was approximately matched to the Talairach brain in a two-stage procedure. First, various landmarks were manually defined in 241 normal MRI scans in order to identify a line very similar to the Anterior Commisure-Posterior Commisure (AC-PC) line. Each brain was scaled to match the landmarks to equivalent positions on the Talairach atlas. Using 9-parameter affine transforms (followed by intensity normalizations and averaging on a voxel-by-voxel basis), a different set of 305 normal MRI scans was matched to the average of the 241 brains that had been matched to the Talairach atlas

(Evan al., 1994). The *ICBM-152* template is the standard template of the International Consortium for Brain Mapping (ICBM). It represents the average of 152 normal MRI scans that have been matched to the MNI-305 template using 9-parameter affine transforms (Mazziotta et al., 1995). The ICBM-152 is implemented in several approaches and thus widely used in a number of labs and also for normalization in the present thesis[2].

Spatial normalization ensures that homologous regions between and within subject groups can be compared. It also facilitates the comparisons of data across experiments, data modalities, and over time. Moreover, the analysis of brain data in a stereotaxic space makes it easier to define spatial masks to restrict the analysis to a particular anatomical region or gather priors in order to guide the behavior of an image analysis algorithm (Thompson et al., 2003).

3.2.2.2 Voxel-based Approaches

In the statistical comparisons of different groups the variable of interest can be derived from the grey-scale values of voxels (voxel-based approaches). The classic VBM (as implemented in the software package SPM) uses linear and non-linear warping algorithms to globally align individual MR scans to a template in standard 3D coordinate space. This registration is followed by a tissue classification (e.g. into GM, WM, CSF and non-brain). Tissue classified compartments (e.g. GM) are smoothed before statistical tests are conducted at each voxel of the smoothed (GM) compartments throughout the entire brain[3].

[2] Although the ICBM-152 atlas constitutes the template for normalization, findings will be described as in ICBM-305 space (given that the ICBM-152 atlas had been originally matched to the MNI-305 template).

[3] Essential steps in most automated approaches (e.g., brain extraction, tissue segmentation, etc.) are explained in great detail in the appendix.

3.2.2.3 Deformation-based Approaches

In contrast to VBM, which compares normalized images, *Deformation-based morphometry* (DBM) and *Tensor-based morphometry* (TBM) compare so-called *deformation fields*. Deformation fields are obtained by non-linear registration of brain images; they store information on the extent of warping and intensity increase or decrease (or a combination of both) for each voxel to obtain the precise match between images (Ashburner et al., 2003). Utilizing features of the Jacobian Matrix (morphometric measures derived from the deformation field), those methods reveal global shape differences by analyzing the relative positions of cerebral structures (DBM), or local shape differences by analyzing local compressions or dilations (TBM).

3.2.2.4 Cortical Pattern Matching

Cortical pattern matching techniques are hybrids between voxel-based methods that assess tissue distribution, and deformation-based methods that map shape differences using high-dimensional warping transforms (Thompson et al., 2003). These cortical analyses tease apart the effects of gyral shape variation and differences in the effect of interest (e.g. GM concentration). An exhaustive description of this modeling technique is provided in the Appendix. Briefly, MR scans are first globally aligned to a standard 3D coordinate space using linear transformations only. This registration is followed by skull-stripping and tissue classification. In addition, from each individual's MR scan, 3D cortical surface models are extracted. On the cortical surfaces, sulcal features are manually outlined and automatically aligned across individuals with a warping technique. Measures of interest (e.g. GM from

the tissue classified images) are convected along with these warps and smoothed before statistical tests are conducted at approximately 65,536 surface points, throughout the entire cortex.

3.2.3 Potential Drawbacks in MRI-based Studies

Several factors complicate the interpretation of research findings that are based on MR imaging. The following paragraphs will outline two main categories of problems, occurring at the very beginning of a study's cycle when images are acquired, and at the very end, when a meaning has to be assigned to the study's findings. As they become relevant, further confounds associated with image preprocessing and analysis are introduced and discussed in the respective sections of the studies A-D.

3.2.3.1 Potential Artifacts through Image Acquisition

In the course of the image acquisition procedure, several factors might lead to the generation of images with features that are not present in the original imaged object, so-called *image artifacts*. An image artifact can be the result of improper operation of the imager, but also a concomitant of the imaging technique and apparatus, or a consequence of natural processes or properties of the human body. Below is a selection of frequent problems that accompany image acquisition, as well as their sources and potential corrections and/or avoidance. For more details on further artifacts (e.g., RF quadrature artifacts, gradient artifacts, chemical shift artifacts, flow artifacts, wrap around artifacts, and Gibbs ringing) refer to http://www.cis.rit.edu/htbooks/mri/inside.htm.

Partial Volume Artifacts: A partial volume artifact is any image artifact which is caused by the size of the image voxel. For example, if a small voxel contains only the CSF or WM signal, a larger voxel might contain a combination of the two (CSF + WM), consequently altering the outcome of tissue classifying procedures. For example, partial volume effects can cause some periventricular WM to be classified as GM, given that the intensity of GM in T1-weighted images lies between CSF and WM. Another manifestation of this type of artifact is a loss of resolution often reflected in fuzzy boundaries between GM and its neighboring compartments. The solution to partial volume artifacts are smaller voxels, which, however, may result in poorer signal-to-noise ratios in the image.

Inhomogeneity Artifacts: On the one hand, an inhomogeneous external magnetic field will cause (1) distortions in intensity (if the field homogeneity in a certain location is larger or less than that in the rest of the imaged object) or (2) spatial distortions (if long-range field gradients cause spins to resonate at Larmor frequencies other than that prescribed by an imaging sequence). On the other hand, RF inhomogeneities are a variation in intensity across an image, resulting from (a) non-uniform magnetic fields created by the RF coil, (b) non-uniform sensitivities in a receiving coil, or (c) the presence of non-ferromagnetic material in the imaged object. In order to obtain values which are comparable across brain regions and between individuals, spatial variations of image intensity are corrected, to some extent, by intensity inhomogeneity corrections that are often implemented in tissue classifying procedures (e.g., Shattuck et al., 2001).

Motion Artifacts: Motion artifacts are caused by motion of the imaged object or a part of the imaged object during the imaging sequence. The motion of the entire object

during the imaging sequence generally results in a blurring of the entire image, while movement of a small portion of the imaged object results in a blurring of that small portion of the object across the image, also called *ghosting*. Motion artifacts due to head movements, for example, can be diminished or even avoided by immobilizing the head. Other sources of motion artifacts (e.g., heart beat, breathing) are addressed by gating the imaging sequence to the cardiac or respiratory cycle of the imaged subject.

3.2.3.2 Potential Misinterpretations of Analysis Results

At this point, it is unclear how exactly the cellular and fiber structure is reflected in high-resolution MRI scans (also see the General Discussion section). Qualitative differences, such as related to the micro-topography of synaptic relations among neurons or in the metabolism of neurotransmitters, are not reflected in MRI scans. That is, intuitive inferences about the association between the quantity of micro- and macrostructure are problematic, such as drawn with respect to cortical convolution, cortical thickness or GM concentration. Greater folding complexities of the cortex, for example, were proposed to accompany higher intracortical connectivities and smaller descending projections. Similarly, increased GM concentration and cortical thickness were interpreted as an indicator of increased neuronal numbers and density. However, some studies reported negative relationships between cell density and layer thickness in deep cortical layers in some regions (Chance et al., 2004; Gittins and Harrison, 2004), clearly challenging the assumption of a direct link between detectable cortical macro-structure and actual neuronal characteristics. Furthermore, less detectable cortical thickness or GM might also result

from myelin deposition in the cortical neuropil, smaller neuronal sizes and/or densities, decreased number and length of dendrites, dendritic spines, and length of postsynaptic thickening (Diamond, 2001; Sowell et al., 2003; Sowell et al., 2004), and, thus, not necessarily reflect smaller neuronal numbers. Moreover, some *post mortem* analyses revealed an increased rather than a decreased number and density of cortical neurons in men and significantly more interstitial space in female brains (Pakkenberg and Gundersen, 1997; Rabinowicz et al., 1999), contrasting with findings of increased GM in women (Gur et al., 1999; Luders et al., 2002). Finally, different macroscopic parameters might reflect micro-architecture differently. For example, correlating GM concentration and cortical thickness in the same sample of subjects led to moderate and high correlations in general, but also revealed some discrepancy in the temporal poles (Narr et al., 2005).

Although, a recent analysis by Kruggel and colleagues (2003) revealed a high correspondence between MRI-based intensity profiles and cytometry-based descriptions of the local layer structure and cytoarchitectonic fields, technological limitations in brain image acquisition do not allow for a resolution needed to detect cellular characteristics. At this point, only by integrating findings from the *post mortem* and *in vivo* literatures can we approximate the cellular meaning of our anatomical findings. Clearly, based on macro-anatomical findings alone we cannot draw inerrant conclusions with respect to micro-anatomical characteristics, or even functional consequences, albeit speculations will serve to generate hypotheses which can be tested in future studies.

4. Sexual Dimorphism in the Brain

Human brains are structurally and functionally different from those of other mammals. But even within the human species, there is a large inter-individual variance. Notwithstanding, over the past years it has been demonstrated that, in spite of such an enormous diversity, there are certain features more common in some people than in others. For example, brain structures in older people differ in some aspects from brain structures in younger people. Similarly, healthy subjects are neurologically different from patients with certain diseases or disorders. Likewise, brains of people with certain abilities deviate from those of people lacking these abilities. Over the past decades, many research endeavors have been conducted to shed light on group-specific peculiarities (with respect to many more populations of interest than merely the aforementioned). The anatomical difference between male and female brains is both a classic and continuing topic of major interest, likely a result of subtle but prominent differences in perception, feeling, thinking, and behavior of men and women noticeable in our daily experiences. Nevertheless, commenting on those cognitive and behavioral gender differences is beyond the scope of this thesis. For a very informative and exhaustive overview with regard to "sex and cognition", please refer to Kimura (1999).

In the following paragraphs I will summarize important research findings regarding the sexual dimorphism in the brain, putting predominant emphasis on macro-structural findings and the cerebral cortex, in particular. Of note, the following list of gender-specific cerebral aspects is not exhaustive but rather composed to demonstrate the large variety of research findings. Clearly, the presence and direction of gender effects strongly depends on

the measurement of interest, brain region and/or cortical layer assessed. Furthermore, I aimed to provide sufficient evidences to support the notion that many questions are still unresolved, mainly due to conflicting results across studies or sparseness of research findings.

4.1 Gender Differences in Functional Correlates

Gender differences have been demonstrated in brain-related physiological findings. Using a large variety of approaches [e.g., functional MRI (fMRI), Positron Emission Tomography (PET), Transcranial Magnetic Stimulation (TMS), Electro-Encephalography (EEG), and Magneto-Encephalography (MEG)], men and women were reported to be different with respect to the rate of cerebral blood flow and blood oxygen levels, glucose metabolism, cortical excitability, electric currents and magnetic fields (Andreason et al., 1994; Shaywitz et al., 1995; Gur et al., 1995; Esposito et al., 1996; Ragland et al., 2000; Walla et al., 2001; Pitcher et al., 2003; Pravitha et al., 2005). Gender-effects were established for rest and activation states, with different strengths and locations of the functional correlate. Given that gender-specific activational patterns could be related to well-known gender-specific performances or behaviour, they seem to be a matter of course rather than a puzzling result. Nevertheless, gender has also been suggested to modulate the relationship between brain and behaviour (Ragland et al., 2000). Moreover, gender-specific activations have been observed when male and female subjects were perfectly matched according to prior performances in tasks of interest (Jordan et al., 2002).

In addition to differences in functional correlates, several studies revealed gender-specific effects of aging on the brain (Cowell et al., 1994b; Murphy et al., 1996; Giedd et al., 1996; Xu et al., 2000; De Bellis et al., 2001; Good et al., 2001b). Other studies provided evidence for differences between men and women with respect to risks for mental disorders, learning abilities, cerebral diseases and lesions, as well as their progression, recovery and consequences (e.g., cognitive impairments) [for a good overview and further references, please refer to de Court (1999)].

4.2 Gender Differences in Structural Design

4.2.1 Micro Anatomy

Important insights with respect to gender differences in (a) the micro-topography of synaptic relations among neurons, (b) the metabolism of neurotransmitters, and (c) steroid receptor mechanisms in neurons, mostly come from animal studies. For an exhaustive overview, please refer to Arnold and Gorski (1984). Some studies that were conducted directly on human samples also revealed pronounced gender effects associated with the distribution of androgen receptors or the levels of certain neurotransmitters (Konradi et al., 1992; Fernandez-Guasti et al., 2000). In addition, some nuclei or specific cell groups of the hypothalamus and stria terminals were demonstrated to be larger in men than in women (Swaab and Fliers, 1985; Allen et al., 1989; Zhou et al., 1995). Moreover, several studies revealed increased neuronal densities in a number of cortical loci in male brains (Pakkenberg and Gundersen, 1997; Rabinowicz et al., 1999; de Court, 1999; Rabinowicz et al., 2002). In contrast, regional neuropil or dendritic arborization, as well as neuronal

densities (e.g., in language regions, such as the planum temporale, Wernicke's area), were reported to be larger in females compared to males (Jacobs et al., 1993; Witelson et al., 1995; Rabinowicz et al., 1999; Rabinowicz et al., 2002).

4.2.2 Macro Anatomy

Gender-specific findings on a microscopic level are supplemented by findings revealed through macro-anatomical *post mortem* and *in vivo* analyses. The most consistent observation is a larger volume and weight of the brain in men compared to women, a cerebral peculiarity that is only partly accounted for by males' larger body dimensions (Peters, 1991; Ankney, 1992). Other gender-related morphometric analyses concerned the dimensions of cortical and sub-cortical regions. For example, the left planum temporale and Sylvian fissure were found to be larger or longer in males compared to females (Witelson and Kigar, 1992; Kulynych et al., 1994; Harasty et al., 1997). Even the bifurcation patterns with respect to the ascending and descending ramus of the Sylvian fissure were reported to be different between men and women (Ide et al., 1996). Furthermore, the volumes of the superior temporal cortex, Broca's area, hippocampus and caudate (expressed as a proportion of total cerebral volume), were significantly larger in females (Filipek et al., 1994; Harasty et al., 1997). Such volumetric differences are complemented by gender-specific effects on the shape of cerebral structures. Swaap and Fliers (1985), for example, reported the supra-chiasmatic nucleus to be elongated in women and more spherical in men. Similar shape-related findings exist for the splenium of the CC (for details see below) or the whole brain, with female brains being shorter but

wider than male brains in Caucasians (Zilles et al., 2001). The following paragraphs will provide a detailed overview with respect to further structures of interest, which repeatedly attracted the interest of researchers over the past decades and until today.

4.2.2.1 Corpus Callosum

The corpus callosum (CC) is the largest fiber tract in the human brain, connecting the two hemispheres through more than 200 million fibers and allowing for an inter-hemispheric transfer of information (Aboitiz et al., 1992). Sexual dimorphisms related to the CC include (but are not limited to) larger total or forebrain volume-adjusted size of the CC in females (Holloway and de Lacoste, 1986; Johnson et al., 1994; Steinmetz et al., 1995), larger raw or proportional isthmus areas in females (Witelson, 1989; Steinmetz et al., 1992; Clarke and Zaidel, 1994), larger raw or proportional splenial areas in females (DeLacoste-Utamsing and Holloway, 1982; de Lacoste et al., 1986; Holloway and de Lacoste, 1986; Clarke et al., 1989; Davatzikos and Resnick, 1998), and larger posterior callosal regions in males (Denenberg et al., 1991). Furthermore, shape differences were reported indicating a more bulbous splenium in females compared to males (DeLacoste-Utamsing and Holloway, 1982; Holloway and de Lacoste, 1986; Allen et al., 1991; Clarke and Zaidel, 1994). In addition, when comparing angles determined by lines connecting particular points of the CC and other brain regions, gender differences have been observed in the callosal orientation (Oka *et al.*, 1999). Although these findings suggest that sexual dimorphisms exist in callosal morphology, replications have not been consistent across laboratories [for review see Bishop and Wahlstein (1997)].

A number of explanations may account for discrepancies in results between laboratories, including the composition of brains examined (e.g., *post mortem* versus *in vivo*). For example, it is possible that *post mortem* measurements may be compromised by a non-uniform shrinkage of the CC. Furthermore, differences in the methods employed for measuring callosal sub-regions might lead to different results. A widely used method to subdivide the midsagittal section of the CC into macroscopic sub-regions is the partition method proposed by Witelson (1989) and Clarke and Zaidel (1994). Here the CC is arbitrarily divided into several regions according to maximal length, e.g. thirds. Others have used a different approach by subjecting midsagittal callosal width measurements to factor analytic techniques that have generated 6 or 7 regional clusters on average (Kertesz et al., 1987; Denenberg et al., 1989; Allen et al., 1991; Denenberg et al., 1991; Cowell et al., 1994a; Peters et al., 2002). However, parcellation schemes based on geometrical solutions (e.g., the Witelson scheme) could be biased by local variability in callosal shape while measures based on statistically defined internal cohesiveness (factor analysis) could produce factors that do not necessarily correspond to any functional boundaries. Finally, the largest source of discrepancy appears to be the failure of most studies to take total brain weight or volume into account.

Albeit less numerous, more consistent gender differences were observed with respect to other fiber tracts connecting (a) both temporal lobes through the AC, and (b) both thalami through the massa intermedia: fiber numbers and midsagittal area of the AC as well as the massa intermedia are larger in women than men, and the latter structure is more often absent in males than in females (Allen and Gorski, 1991; Highley et al., 1999).

4.2.2.2 Cerebral Tissue Compartments

There is extensive literature on sexual dimorphism of the major cranial tissue compartments, such as GM (predominantly consisting of cell bodies and dendrites) and WM (neuronal axons that connect cells). It is well documented that larger volumes of GM and WM exist in male brains if tissue measurements are not related to individual brain size (Blatter et al., 1995; Gur et al., 1999; Good et al., 2001a; Luders et al., 2002). If, however, brain size is taken into consideration, some studies revealed higher percentages of GM in females (Gur et al., 1999), while others failed to detect any gender differences (Schlaepfer et al., 1995; Nopoulos et al., 2000), or observed higher GM (Good et al., 2001a) and WM proportions in males (Filipek et al., 1994; Passe et al., 1997; Gur et al., 1999; Goldstein et al., 2001). Another interesting aspect was pointed out by Allen et al (2003): overall, the sexual dimorphism appears to be greater for WM than GM, resulting into GM-WM ratios that are higher across structures in women. That is, while both absolute GM and WM volumes are smaller in women than men, the WM difference is more pronounced, with the result that women have a higher overall proportion of GM than men. Related to the measurement of GM, different studies examined global cortical thickness, which is defined as the 3D distance between inner WM/GM border and outer GM/CSF border. Those analyses revealed a trend toward larger global thickness in males (Salat et al., 2004) or no gender differences (Nopoulos et al., 2000).

In addition to global analyses, various findings reflect also locally a sexual dimorphic tissue composition. For example, higher GM percentages in the dorsolateral prefrontal cortex, superior temporal gyrus (Schlaepfer et al., 1995), and right parietal lobe

(Nopoulos et al., 2000), were reported in women compared to men. Additional gender differences in the volume of intrasulcal GM were found in the cingulate sulcus with larger volumes in females and in the para-cingulate sulcus with larger volumes in males (Paus et al., 1996). In contrast to those ROI-analyses, automatic voxel-based morphometric whole-brain analyses exposed numerous additional brain regions with significantly increased GM volumes in both females (inferior frontal, inferior parietal, lateral orbital, cingulate, para-hippocampal, middle temporal, transverse temporal gyri, planum temporale, superior temporal and central sulci) and males (amygdala, hippocampi, entorhinal and perirhinal cortex, anterior superior temporal gyrus, anterior lobes of cerebellum) (Good et al., 2001a). Interestingly, analyses of regional GM *concentration* reflecting regional differences in the relative volume of GM, revealed different results than comparing the absolute amounts, as outlined above. That is, GM concentration was increased extensively and relatively symmetrically in several (sub)cortical regions in females (frontal, posterior temporal, parietal cortex, para-hippocampal gyri, adjacent to the caudate heads, cingulate and calcarine sulci), while no increased GM concentration was detected in males (Good et al., 2001a).

To some extent, this variety of findings in regional GM is likely attributable to different approaches of analyzing GM (e.g., ROI versus whole-brain analyses), GM measures used for assessment (e.g., volume, percent, concentration etc.), and composition of brains examined (e.g., old versus young, *post mortem* versus *in vivo*). Furthermore, the fact that some analyses took total brain weight or volume into account, while others did

not, seems to be a major source of discrepancy in results between laboratories. Similar factors seem to be partly responsible for conflicting results in global tissues volumes.

4.2.2.3 Structural Asymmetry and Functional Lateralization

Gender differences in structural hemispheric asymmetry, with larger inter-hemispheric differences in males compared to females, have been reported widely and are complemented by behavioral and neuro-activational measurements. For detailed summaries with respect to behavioral and functional lateralizations, as well as intra- and inter-hemispheric interactions please refer to (Hiscock et al., 1994; Shaywitz et al., 1995; Hiscock et al., 1995; Azari et al., 1995; Hiscock et al., 1999; Sadato et al., 2000; Kansaku et al., 2000; Gur et al., 2000; Hiscock et al., 2001; Medland et al., 2002).

With respect to structural asymmetry, Amunts et al. (2000) reported that male right-handers have a significantly deeper central sulcus on the left hemisphere than on the right, whereas no inter-hemispheric asymmetry was found in female right-handers. Similarly, in our own analyses we observed a larger leftward GM asymmetry in males compared to females in a region posterior to the central sulcus (Luders et al., 2004). Possibly related to those findings, our group further detected significant asymmetries in the anterior callosal midbody in men (and much less in women)– a region known to connect the motor cortices situated near the central sulcus (Luders et al., 2005). Other analyses revealed a more pronounced rightward asymmetry of the planum parietale in right-handed men compared to right-handed women, while left-handed subjects demonstrated the opposite pattern (Jancke et al., 1994). Further studies revealed gender-dependent asymmetries of the inferior

parietal lobe and planum temporale, with males having significantly larger leftward asymmetries, and females showing either reversed, diminished or no asymmetries (Kulynych et al., 1994; Frederikse et al., 1999; Good et al., 2001a). Another study revealed a stronger lateralization of right frontal petalia (in right-handers and left-handers) and occipital petalia (in left-handers only) in men compared to women (Zilles et al., 1996), confirming previous findings of greater frontal and occipital asymmetries in men and reversals of the typical asymmetries in women (Bear et al., 1986). Notwithstanding, although the majority of studies seemed to have revealed indicators for diminished asymmetries in female brains, a number of studies also exist that either failed to detect significant gender effects with respect to hemispheric differences (Foundas et al., 1999; Watkins et al., 2001) or revealed even more pronounced asymmetries in females (Rabinowicz et al., 2002).

II. EMPIRICAL SECTION

5. General Aims

Our goal was to use high-resolution T1-weighted MR data and advanced image analysis techniques to investigate gender differences in cortical anatomy. We set out to examine several morphological characteristics for the first time in young and healthy men and women, such as cortical thickness and complexity (Study B, C, and D). Furthermore, we wished to apply newly developed state-of-the-art methods in pilot measurements, such as the measurement of local mean curvature (Study D). A related goal was to combine measurements of interest in an intelligent fashion in order to verify the correspondence between different measurements in the same set of data, such as with respect to global GM volume and regional GM concentration (Study A). In addition, we developed follow-up methods to verify and extend our original findings with more advanced techniques (Study C and D). Moreover, some of the projects were designed to supply significant insight as to how image pre-processing and analysis can influence the structural outcomes, and thus alter the detected sexual dimorphism (Study B and D). Finally, independent from the analysis of gender effects, we set out to generate spatially detailed maps for some measurements of interest given that these descriptors are not well characterized in the normative literature (Study A, B, and D). The primary aims of our studies addressing the characterization of gender differences in particular are listed below. Specific hypotheses for each experiment are described separately in each chapter where empirical data are presented.

Aim A. To establish the presence and direction of gender differences with respect to (a) global volumes of the brain and its tissue compartments (a_1) on scaled and (a_2) unscaled brains in ICBM-305 space, as well as (b) regional concentration of GM across the cortex on scaled brains in ICBM-305 space.

Aim B. To establish the presence and direction of gender differences with respect to regional cortical thickness across the cortex (a) on scaled and (b) unscaled brains in ICBM-305 space.

Aim C. To establish the presence and direction of gender differences with respect to cortical complexity on scaled brains in ICBM-305 space (expressed as lobar fractal dimension).

Aim D. To establish the presence and direction of gender differences with respect to cortical complexity on scaled brains in ICBM-305 space (expressed as local mean curvature).

6. Subject Selection and Data Acquisition

6.1. The Study Group

We analyzed the brains of 60 healthy subjects selected from a database of high-resolution anatomical MR images acquired at the Center for Neuroscientific Innovation and Technology (ZENIT) in Magdeburg, Germany. Male and female subjects were matched in terms of numbers (30 women, 30 men) and age (women: 24.32 ± 4.35 years; men: 25.45 ± 4.72 years). Young adults with a relatively narrow age range were recruited so as to minimize the influences of age and possible interactions of age with gender, which have been demonstrated to influence cortical measurements of GM concentration, thickness, asymmetry and variability (Magnotta et al., 1999; Courchesne et al., 2000; De Bellis et al., 2001; Jernigan et al., 2001; Good et al., 2001b; Sowell et al., 2003). Given that previous reports also revealed structural differences in the brains of left and right handers (Steinmetz et al., 1991; Witelson and Kigar, 1992; Jancke et al., 1994; Zilles et al., 1996; Amunts et al., 2000), only right-handed subjects were included in the analyses, where handedness was determined by referring to self-reports of hand preference. Subjects were volunteers and included university students from different fields who were recruited via notice board and/or Internet advertisements. All subjects gave informed consent according to institutional guidelines (Ethics Committee of the University of Magdeburg).

6.2. The Scanning Protocol and Image Preprocessing

All images were obtained on a 1.5-T MRI system (General Electric, Waukesha, WI, USA) using a T1-weighted spoiled gradient echo pulse sequence with the following parameters:

TR = 24 ms, TE = 8 ms, 30° flip angle, FOV = 250 x 250 mm^2, matrix size = 256 x 256 x 124, voxel size = 0.975 x 0.975 x 1.5 mm.

Of note, because the first part of the image preprocessing was conducted in a similar way for each sub-study, a detailed description of each early preprocessing step is given in the Appendix. In contrast, each Methods section of the sub-studies delivers only an overview of the image analysis methods used. Additional sub-study-specific modules are explained as they become applicable. For summary, illustration, and orientation regarding imaging preprocessing throughout this thesis please also refer to figure 14.

7. Study A: Gray Matter – Part I: Regional GM Concentration

7.1. Background

Although numerous sexually dimorphic characteristics have been identified in the human brain, observations of larger brains in men compared to women are most replicated. *Post mortem* data further suggests that neuronal number and density are modulated by gender (Witelson et al., 1995; Pakkenberg and Gundersen, 1997; Rabinowicz et al., 1999). Similarly, neuroimaging studies show sexual dimorphisms in the major cranial tissue compartments, although results lack consistency. For example, global GM and WM volumes are reported as larger in males (Blatter et al., 1995; Luders et al., 2002), but when GM is computed as a percentage of TBV, females show larger GM ratios irrespective of TBV corrections (Gur et al., 1999). Other studies show larger GM percentages in males (Good et al., 2001a), or fail to detect significant gender effects in GM and WM percentages (Schlaepfer et al., 1995; Nopoulos et al., 2000).

Gender differences in regional (as opposed to global) GM distributions have also been examined where traditional ROI-studies are complemented by voxel-wise comparisons using methods like VBM. For example, ROI-analyses have revealed increased GM percentages in the dorsolateral prefrontal cortex and superior temporal gyrus in females (Schlaepfer et al., 1995). Furthermore, increased GM volumes in cingulate cortices in females and para-cingulate cortices in males were observed after transforming images into standardized stereotaxic space to control for TBV (Paus et al., 1996). Studies employing VBM have revealed GM volume increases in females in parietal, temporal, inferior frontal and cingulate cortices and GM concentration increases across the cortex

and surrounding the para-hippocampal, cingulate and calcarine sulci. In contrast, males showed GM volume increases in mesial/lateral temporal and cerebellar regions, but no significant increases in GM concentration (Good et al., 2001a).

Taken together, previous analyses of global and regional tissue volumes clearly indicate gender differences, albeit findings lack consistency. These inconsistencies may stem from differences in measurement methods (e.g., measurement of GM volume versus GM concentration; whole-brain versus ROI-analyses using either contiguous brain slices or a single brain slice only). Another major contributor to discrepancies in findings is the failure of some studies to take brain size differences between men and women into account. Moreover, even when brain size is taken into account, the different strategies used to correct for individual brain volumes may lead to different results.

The present study was designed to address these issues. We set out to complement analyses of global tissue volumes (GM, WM, and CSF) with examinations of regional GM in the same set of data. Furthermore, identical procedures to correct for individual brain volumes were applied for global and regional analyses, and achieved through a 12-parameter linear transformation into the standard co-ordinate system of the ICBM-152 template (Mazziotta et al., 1995). Analyses in a scaled standard space – a method frequently used in VBM studies – might be a better approach to control for individual brain size than including TBV as covariate in (log)linear statistical models if the relationship between TBV and tissue compartment lacks linearity. In order to compare our findings with others in the literature, gender effects on global GM, WM, and CSF volumes were additionally examined in raw scanner space without controlling for individual differences

in TBV. Finally, we set out to generate spatially detailed maps of (a) average GM distributions and (b) GM variability across the entire cortex in ICBM-305 space given that these descriptors are not well characterized in the normative literature.

7.2. Methods

7.2.1. Preprocessing

T1-weighted anatomical image volumes passed through a number of preprocessing steps described in the Appendix and visualized in figure 14: Creating a brain mask based on the anatomical raw image (Module I); Normalization of brain mask and anatomical images into ICBM-305 space using 12 parameter (Module II); RF corrections in anatomical images (Module III); 3D cortical surface extraction based on normalized RF corrected anatomical images (Module IV); Skull stripping in RF corrected anatomical images (Module V); Segmentation into GM, WM, and CSF in RF corrected and skull stripped anatomical images (Module VI); Manual delineation of sulcal anatomy in extracted 3D cortical surfaces (Module VII); cortical pattern matching (Module VIII).

7.2.2. Global Analyses of TBV and Tissue Volumes

To examine whether males and females differed with respect to overall brain tissue volumes, we compared the volumes of the three different types as estimated by counting the number of voxels classified as GM, WM, or CSF from scalp-edited image volumes in ICBM-305 space. However, gender effects on global GM, WM, and CSF volumes were additionally examined in raw scanner space without controlling for individual differences

in brain volume in order to compare our findings with others in the literature. TBV was determined in liters and estimated from the brain masks (created during Module I). Both cerebellum and brainstem, as located above the last slice of the cerebellum, were included in our measurements of tissue volumes and TBV. The statistical analyses were performed on a PC workstation using SPSS 10.0 (http://www.spss.com) and SYSTAT 9.0 (http://www.systat.com/). Bonferroni corrected, repeated measures analyses of variance (ANOVAs) were used to compare volume differences of TBV, GM, WM, and CSF in ICBM-305 and raw scanner space between males and females (which were followed by univariate analyses when appropriate). Prior to these analyses, we inspected the distribution of the data to ensure the dependent measures did not deviate from normality.

7.2.3. Regional Analyses of Cortical GM Concentration

The deformation fields obtained from the cortical pattern matching methods (Module VIII) provide a spatial correspondence between equivalent cortical surface locations in each subject that also correspond to point locations in the images that contain the GM information. Local measurements of GM may thus be obtained from homologous cortical locations in each individual. To quantify the concentration of cortical GM, a sphere with a radius of 15mm was centered at each of the 65,536 cortical surface points that were matched in each subject. Local GM concentration was defined as the number of GM voxels relative to the total number of voxels within the sphere. GM concentration measures thus represent values ranging from 0.0 (no GM voxels within the sphere) to 1.0 (all GM voxels) and provide a local estimate of GM volume within the cortical mantle in each individual.

Although GM concentration is often also referred to as density, to avoid confusion with the cell packing density measured cytoarchitectonically, in this study we use the term "concentration" (Ashburner and Friston, 2000).

The means and standard deviations for GM concentration values obtained from each cortical surface point were calculated to provide maps of average GM concentration and inter-subject variability across the entire cortical surface in standard ICBM-305 space for the whole sample and within groups defined by gender. Independent sample Student's t-tests were then performed at each cortical surface location to asses the effect of gender on cortical GM. Uncorrected two-tailed probability values from these t-tests were mapped directly onto the average cortical surface model of the entire sample. That is, we generated detailed and spatially accurate statistical maps of local GM differences between men and women in standard ICBM-305 space indicating significant differences of $p<0.05$.

However, given that t-tests were made at thousands of cortical surface points and adjacent data points are highly correlated, permutation testing was employed to serve as a safeguard against Type I error (rejecting the null hypothesis when it is true). For permutation testing, subjects were randomly assigned to either male or female groups 100,000 times, and a new statistical test was performed at each cortical surface point for each random assignment. The number of significant results from these randomizations was then compared to the number of significant results in the true assignment[4] to produce a corrected overall significance value for the uncorrected statistical maps.

[4] The number of significant results in the true assignment was determined by calculating the surface area (number of surface points) of significant effects in the real statistical maps. In contrast to calculating the surface area by applying a threshold of $p<0.05$ (which is the threshold chosen to color-code the significance maps), we ran the permutation with a stricter threshold of $p<0.01$.

7.3. Results

7.3.1 Effects of Gender on TBV and Global Tissue Volumes

Table 1 shows the means and standard deviations (SD) of TBV and tissue volumes obtained in raw scanner space (unscaled) and ICBM-305 space[5] (scaled). The repeated measurement ANOVAs resulted in a significant omnibus effect: $F(1, 58)=40.945$, $p<0.0001$. Follow-up tests revealed larger unscaled volumes in males compared to females: TBV ($F(1,58)=47.195$, $p<0.0001$), GM volume ($F(1,58)=36.019$, $p<0.0001$), WM volume ($F(1,58)=39.062$, $p<0.0001$), and CSF volume ($F(1,58)=9.522$, $p<0.003$).

In contrast, comparing scaled volumes in ICBM-305 space, we revealed larger GM values in females ($F(1,58)= 12.444$, $p<0.001$) and larger WM values in males ($F(1,58)= 10.231$, $p<0.002$), while TBV and CSF did not show any significant gender effects ($F(1,58)= 2.246$, $p<0.139$ and $F(1,58)=0.053$, $p<0.819$, respectively).

Table 1. Statistical descriptors for tissue volume measurements (in liters)

	Unscaled Volumes: Mean (SD)		Scaled Volumes: Mean (SD)	
	Males	Females	Males	Females
TBV	1.40 (0.11)*	1.22 (0.09)	1.79 (0.01)	1.79 (0.02)
GM	0.72 (0.05)*	0.64 (0.05)	0.92 (0.04)	0.95 (0.03)*
WM	0.55 (0.06)*	0.47 (0.05)	0.71 (0.03)*	0.68 (0.03)
CSF	0.13 (0.02)*	0.11 (0.02)	0.16 (0.03)	0.16 (0.02)

* indicates the significantly larger volume

[5] Brain volumes in MNI-305 space and normalized to the ICBM-152 template are somewhat larger in comparison to other *post mortem* and *in vivo* measures as found in the literature because the ICBM-152 template is an average of 152 individual brains, resulting in blurred edges and therefore slightly increased template dimensions.

7.3.2 Average Regional GM Concentration

Figure 3 shows the average GM concentration in standard ICBM-305 space for the whole sample. The lowest concentrations bilaterally are in superior regions of the pre- and post-central gyrus as well as surrounding the occipital poles. The highest GM concentrations are located at the apex where the temporal lobes separate from frontal lobes and on the inferior surface of the temporal lobes. For temporal and superior-frontal regions, the concentration of cortical GM appears to be higher in the left hemisphere compared to the right. The local distributions of average GM concentration were similar in males and females (not shown).

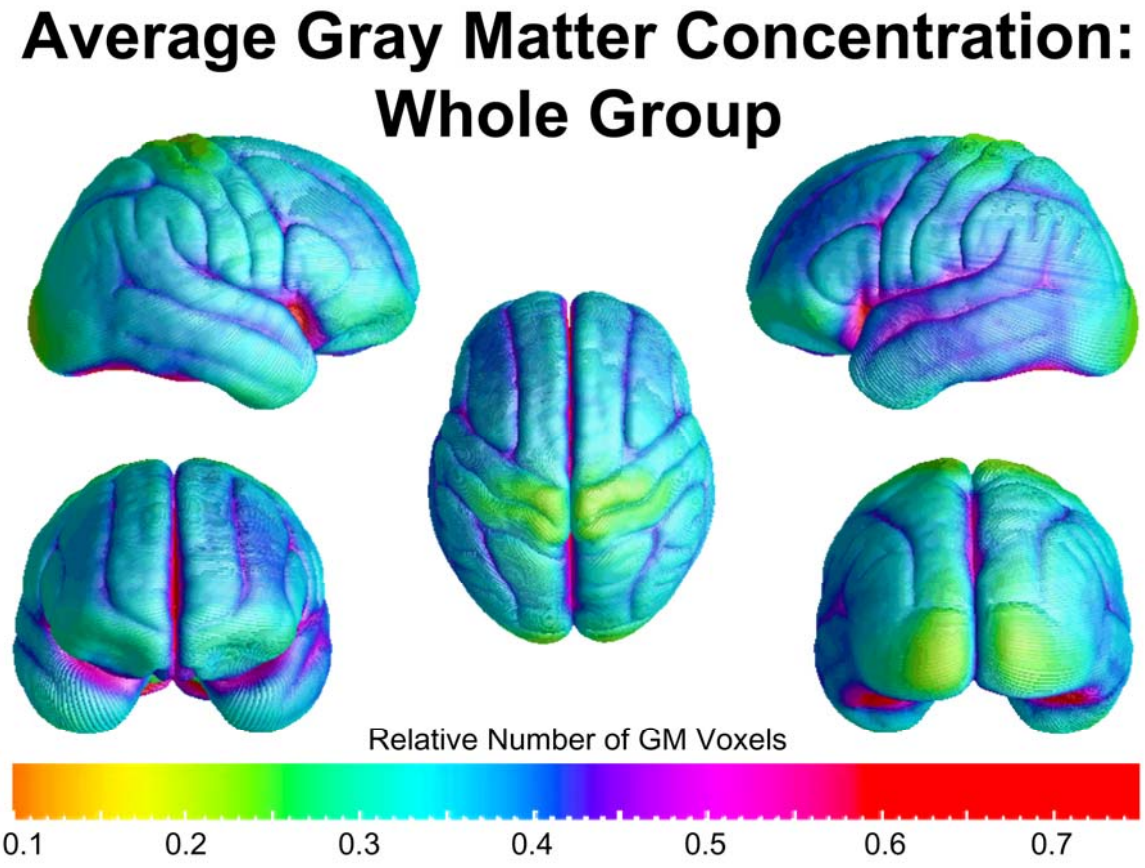

Figure 3. Average maps of regional GM concentration
Average GM concentration was mapped for the whole sample in ICBM-305 space after using 12-parameter transformations. The color bar encodes the proportion of GM voxels relative to the total number of voxels within a sphere using a radius of 15 mm obtained from homologous surface points in each individual. Smaller values indicate lower GM concentrations, while larger values indicate higher GM concentrations.

7.3.3 Variability of Regional GM Concentration

Mapping the variability of GM concentration revealed similar results in males and females. Figure 4 shows the variability of GM concentration in standard ICBM-305 stereotaxic space for the whole sample. The largest standard deviations, and thus the highest variability of cortical GM, are evident bilaterally in inferior regions near the occipital pole extending into the inferior surface of the posterior temporal lobe. Variability is also more pronounced in the inferior frontal gyrus (left and right *pars orbitalis*, *triangularis*, and right *pars opercularis*), in anterior-superior surfaces of both temporal lobes as well as in areas around pre- and post-central sulcus, proximal to the midline.

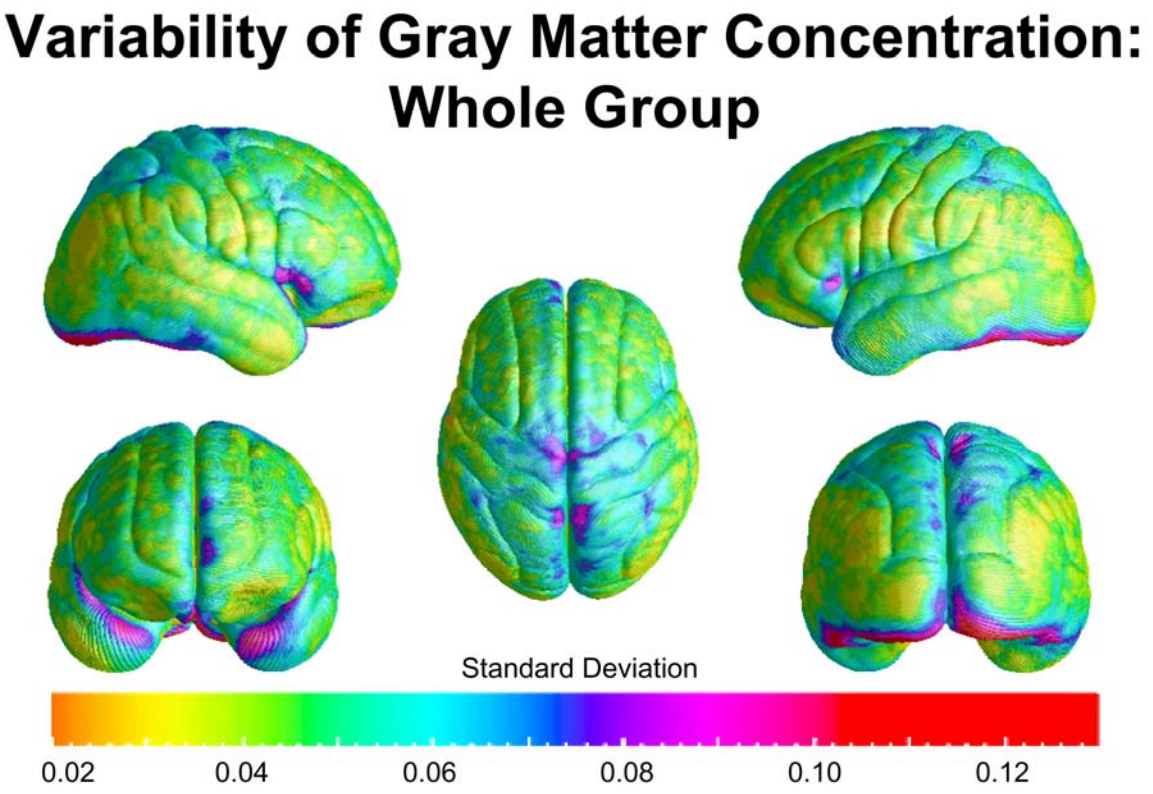

Figure 4. Variability maps of regional GM concentration
GM variability was mapped for the whole sample in ICBM-305 space after using 12-parameter transformations. The color bar encodes the standard deviation of GM concentration values. Smaller values indicate less variation of cortical GM (yellow, green and light blue regions), while larger values indicate more variability (dark blue regions) or the highest variability (pink and red regions).

7.3.4 Effects of Gender on Regional GM Concentration

Statistical analyses of differences in cortical GM concentration revealed several regions of significantly increased GM in women compared to men, after inter-individual differences in brain size had been removed by transforming images into standard ICBM-305 stereotaxic space (Figure 5). No significant increases in GM concentration were observed in males. Brain regions demonstrating significant GM concentration increases in females are spread over the whole brain surface and can be detected in all four lobes in each hemisphere. Permutation tests were significant for the comparison of GM between males and females ($p<0.002$) indicating that the observed gender effects do not occur by chance.

The most significant and largest clusters of GM increases can be seen bilaterally in the pre- and post-central gyrus on the superior brain surface proximal to the midline, but also further inferior along the pre-central gyri and post-central sulci extending into the supramarginal gyri. Significant increases in GM concentration can also be identified surrounding the temporal and occipital poles, bilaterally expanding into posterior regions of the inferior temporal gyrus in the right temporal lobe. While increased GM in the right hemisphere is also represented in the angular gyrus surrounding the ascending branch of the superior temporal sulcus, GM differences in the left hemisphere are highly significant (a) in a distinct region situated posteriorly in the superior temporal gyrus, (b) in the inferior frontal gyrus comprising the *pars orbitalis*, *triangularis* and *opercularis*, and (c) along the border between temporal and occipital lobe. Additional smaller regions of higher GM concentration in women are spread over the whole cortex (most prominently in anterior areas of the left and right frontal lobes).

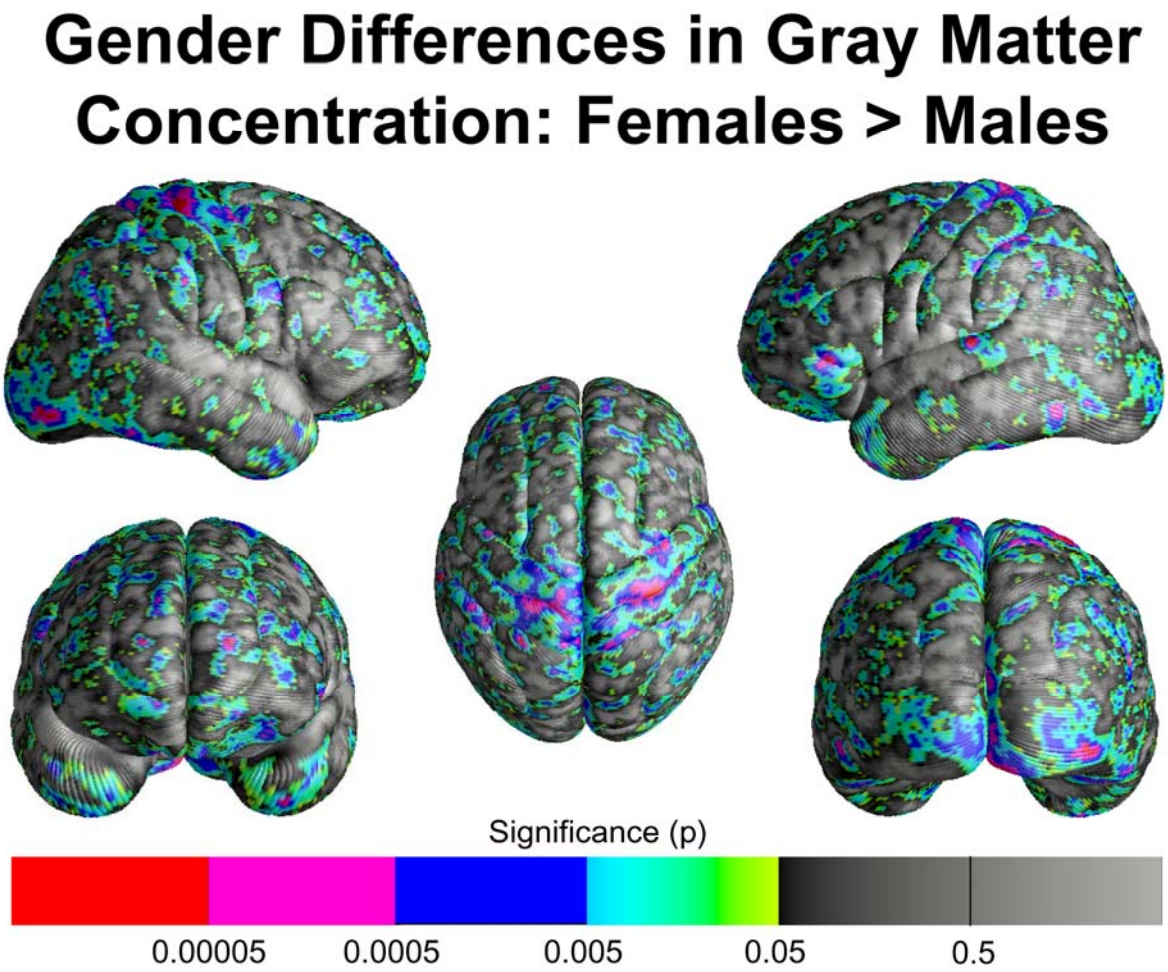

Figure 5. Uncorrected maps of gender differences in regional GM concentration
Gender differences in GM concentration were established in ICBM-305 space after using 12-parameter transformations. The color bar encodes the p-value associated with the t-tests of GM concentration performed at each cortical surface point. All colored cortical regions indicate statistically significant differences. All gray-shaded regions are not significantly different between males and females (the lighter the gray the more similar the GM concentration).

7.4. Discussion

7.4.1. Global Tissue Volumes

Statistical analyses of major cranial tissue component measures in raw scanner space (unscaled volumes) yielded significant gender differences with males having larger volumes of GM, WM, and CSF than females which agrees with earlier findings (Blatter et al., 1995; Good et al., 2001a; Luders et al., 2002). Furthermore, consistent with previous findings, we detected significantly larger TBVs in males than in females. Notably, sex is genotype, and genes influence brain size, accounting for larger male and smaller female brains on average. Thus the question occurs whether brain size corrections are really necessary to accurately establish the effects of gender on cranial compartments. Interestingly, in the present study, approximately 63 percent of individual brain volumes (male and female) fell between the minimum TBV of males and the maximum TBV of females. That is, even though men have larger brains than women on average, there exist small male brains and large female brains that approach or exceed the average brain dimensions of the opposite sex. Given that brain size overlaps substantially between the sexes, it appears to be necessary to control for individual brain volumes in order to study sex influences on tissue volume measures.

Comparing tissue volumes in scaled brains revealed larger GM in females and larger WM in males, contrasting with previous analyses that detected higher GM percentages in males (Good et al., 2001a) or failed to detect significant gender effects on percentages of overall tissue volumes (Schlaepfer et al., 1995; Nopoulos et al., 2000). These conflicting results may be due to different methods for obtaining tissue measurements and/or

controlling for TBV. That notwithstanding, other MRI studies support our results and show that women have a higher percentage of GM, whereas men have a higher percentage or proportion of WM (Gur et al., 1999; Goldstein et al., 2001).

7.4.2. Regional GM Concentration

7.4.2.1 Distribution and Variability

The distribution of GM appears to be rather heterogeneous, with different cortical regions reflecting different proportions of GM. Similar reports exist from classic *post mortem* studies showing that cortical thickness varies across the cortex (von Economo, 1929). Average GM concentrations might reflect the underlying cyto-architecture related to the organization of pyramidal and granular layers. However, given that the post-central gyrus and occipital pole contain granular cortices while the pre-central gyrus contains agranular cortex, cytoarchitectural boundaries may not map exactly with the patterns of average cortical GM concentration. Thus, it is possible that other factors, such as the density of cortical neurons, may influence the signal intensity values associated with cortical GM in imaging data. Patterns of GM concentration and variability appear to be similar in each hemisphere (although higher cortical GM concentrations may exist in the left temporal and superior frontal lobe compared to the right).

7.4.2.2 Gender Effects and Correspondence with Previous Findings

While the spatial distribution and variability profiles of cortical GM concentration do not appear to differ between men and women, we observed pronounced gender differences in

local GM concentrations. After inter-individual differences in brain size had been removed by transforming images into ICBM-305 stereotaxic space, numerous cortical regions showed increased GM concentration in females compared to males. We did not detect any region showing significantly increased GM concentration in males. Of note, the determining factors for our gender-specific observations in each sub-study and their possible association with gender-specific behavior will be expatiated in the closing General Discussion section, rather than at the end of studies A-D.

Our results of locally increased concentration of cortical GM in females corroborate our findings of larger global GM volumes in scaled brains in females and are consistent with previous findings of larger overall cortical volumes relative to cerebrum size in women compared to men (Goldstein et al., 2001). Cerebral regions reflecting increased GM in females also agree with reports of higher GM percentages or proportions in the dorsolateral prefrontal cortex, superior temporal gyrus, and right parietal lobe (Schlaepfer et al., 1995; Nopoulos et al., 2000) even though these previous findings were generated from ROI-analyses of cerebral lobes or selected brain slices. Our results are also consistent with the VBM findings of Good et al., (2001a), perhaps because our methodological approach has many similarities to VBM. Specifically, spatial registration, tissue classification, and smoothing of MR data are included in both image analysis preprocessing streams, although the present method compares the proportion of GM between groups in spheres of 15 mm on the cortical surface rather than in voxelwise contrasting of image intensities throughout the whole brain. Furthermore, the term GM concentration in VBM reflects the proportion of GM to other tissue types within a region

after spatial normalization similar to the present approach. While earlier VBM results reflected local increases of GM *volumes* (in terms of true volumetric differences) in both females and males, local GM *concentration* was increased only in females as consistent with our findings. In further agreement with Good et al., (2001a) we detected increased GM concentration in females in parietal, posterior temporal, and frontal brain regions, although some deviations occurred in hemisphere and cluster size. For example, unlike Good et al. (2001a) who detected increased GM in the *left* angular gyrus, in the *right* orbital gyrus, and inferior frontal gyri *bilaterally*, we observed GM increases predominantly in the *right* angular gyrus, *left* orbital gyrus, and *left* inferior frontal gyrus, although small clusters of higher GM concentration were also detected in the opposite hemisphere. Increases in GM concentration in subcortical regions (Paus et al., 1996; Good et al., 2001a) would have remained undetected in our investigation, given that GM concentration measurements were restricted to the cortex.

7.4.2.3 Potential Confounds

We detected the most significant and largest clusters of GM increases in females in the pre- and post-central gyrus on the superior brain surface proximal to midline and surrounding temporal and occipital poles. Similarly, previous studies reported increased relative volumes in pre-central and superior frontal gyri (Goldstein et al., 2001) and spatially diffuse increases in GM concentration within frontal and parietal regions in females (Good et al., 2001a). One might argue that some of the highly distinct and significant gender differences in cortical GM concentration in some of the most extreme parts of the brains

(pre- and post-central gyrus, occipital pole) could present a potential confound: as men tend to have larger heads and brains than women, the outer limits of their brains are farther away from the center of the coil and, therefore, might be located in less homogenous parts of the field. As a result, the intensity of the signal might be less in these locations leading to regionally decreased GM measurements in male brains. Although our findings of lower GM concentration in the pre- and post-central gyrus as well as in the occipital pole might seem to stand in agreement with this assumption, the frontal pole, for example, does not show such an extremely low GM concentration (as can be clearly seen in figure 3). Furthermore, our average maps of GM concentration are similar to *post mortem* estimations of cortical thickness (von Economo, 1929), which cannot be influenced by intensity inhomogeneities. Finally, a 1.5 T whole body scanner was used for the acquisition of the data. Therefore, field inhomogeneities are minor and would be restored by the explicit correction for RF inhomogeneity, so that is extremely unlikely that inhomogeneities account for the observed gender differences. The finding that some regional gender differences appear to correspond to cortical areas with lower average GM concentration, however, may warrant further examination in future studies.

Another potential confound might result from the possibility that GM proportion measures could be influenced if the sulcal space is widened. That is, group differences may represent characteristics intrinsic to the sulci rather than differences associated with cortical GM. However, since a sphere with a fixed radius of 15 mm was used to measure GM proportions at each cortical surface location, proportion measures were smoothed to increase signal to noise ratios. Moreover, male and female groups were matched for age

and represent a young and healthy cohort. There does not appear to be any evidence to suggest that sulcal widening is different between males and females. Gender differences in sulcal depth, if present, were normalized through the transformation into the ICBM-305 stereotaxic space. More precisely, because the curvature penalty during the surface extraction is applied in a standard space, it yields sulcal fissures at a depth which is the same regardless of the original geometry and scale of the cortex.

8. Study B: Gray Matter – Part II: Regional Cortical Thickness

8.1. Background

The thickness of the cortex reflects the underlying cyto and myeloarchitecture of the brain (the organization of cortical layers, the size, number, and density of neuronal cell bodies and/or synaptic connections, and the myelination of fibers). The analysis of cortical thickness, although related to regional measures of cortical GM volume and concentration, may provide new insight into gender-related differences in brain morphology. With novel computational image analysis algorithms (Fischl and Dale, 2000; Jones et al., 2000; Kabani et al., 2001; Memoli et al., 2004; Lerch and Evans, 2005), cortical thickness can be measured over the entire cortex, but few MRI studies have analyzed gender differences in cortical thickness specifically. Some studies, however, have examined gender effects while assessing neurodevelopmental or disease-related hypotheses (Kuperberg et al., 2003; Sowell et al., 2004; Salat et al., 2004; Narr et al., 2005). Specifically, Narr et al., (2005) examined sex differences collapsed across groups of schizophrenia patients and healthy controls, showing thicker parietal cortices in women, and thicker medial frontal regions in men. Cortical thickness differences were not measured in healthy subjects separately, and patients with schizophrenia showed decreased cortical thickness in several cortical regions while gender interactions were present. A different study conducted to investigate the influence of aging revealed a trend toward larger global thickness in males in the left and right hemispheres (Salat et al., 2004), while another study revealed no significant differences between men and women (Nopoulos et al., 2000).

In the context of sparse and inconsistent results concerning gender differences in cortical thickness, our goal was to examine regional thickness across the cortex in a large and well-matched sample. In contrast to our former GM approach, where regional analyses were restricted to the lateral cortex, we now set out to investigate thickness across the lateral and medial cortices. We further aimed to establish the presence and direction of gender differences in cortical thickness using both *scaled* (after transforming images into standard ICBM-305 space applying 12-parameter transformations) and *unscaled* imaging data (after applying 6-parameter rigid-body transformations). Many previous studies assessing gender differences in GM concentration using VBM (Ashburner and Friston, 2000) and sulcal pattern matching approaches (Thompson et al., 2004) have conducted analyses on data scaled to a template using linear or non-linear registrations. These normalization procedures are performed to control for global shape and brain size differences. The optimized VBM procedure (Ashburner and Friston, 2000; Good et al., 2001b) contains a volume preserving step: modulating the intensity values in the segmented images by the Jacobian determinants, or volume expansion factors, derived from the spatial normalization. Even so, the issue of how spatial normalizations alter gender differences in morphological features has been largely neglected. We hypothesized that gender effects would parallel previous findings of larger global GM percentages / proportions and larger cortical GM volume / concentration in females (Gur et al., 1999; Goldstein et al., 2001; Good et al., 2001a; Luders et al., 2002). We expected regionally increased cortical thickness in women after brain size normalizations (with scaling) and less pronounced gender differences when examining brains in their original dimensions (without scaling).

8.2. Methods

8.2.1 Preprocessing

T1-weighted anatomical image volumes passed through a number of preprocessing steps described in the Appendix and visualized in figure 14: Creating a brain mask based on the anatomical raw image (Module I); Normalization of brain mask and anatomical images into ICBM-305 space using 12 parameter (Module II); RF bias field corrections in anatomical images (Module III); 3D cortical surface extraction based on normalized RF corrected anatomical images (Module IV); Skull stripping in RF corrected anatomical images (Module V); Segmentation into GM, WM, and CSF in RF corrected and skull stripped anatomical images (Module VI); Manual delineation of sulcal anatomy in extracted 3D cortical surfaces (Module VII); cortical pattern matching (Module VIII).

8.2.2 Regional Analyses of Cortical Thickness

Cortical pattern matching methods (Module VIII) were used to spatially relate homologous regions of cortex between subjects in order to permit the inter-individual comparison of cortical thickness in equivalent surface locations. Cortical thickness was defined as the 3D distance (in mm) between inner GM-WM border and the closest point on the outer surface (CSF-GM border) using an implementation of the 3D Eikonal equation (Memoli et al., 2004; Thompson et al., 2004). More specifically, we identified the GM-WM interface as the set of voxels classified as GM that have at least one neighboring WM voxel, setting the distance values for this layer of voxels to zero [similar to the methods used by (Miller et al., 2000; Ratnanather et al., 2001; Lohmann et al., 2003)]. In order to estimate cortical

thickness, we coded successive layers of voxels by assigning them a value equal to the closest 3D distance to the GM-WM interface. That is, in a series of subsequent passes over the image (from inside to outside), layers that are adjacent to the voxel layer coded in the last step will be processed and assigned a distance value. The primary reason for this wavefront propagation is to prevent distances from propagating across CSF by setting the rules for serial propagation in such a way that this is forbidden. Essentially, the process computes the shortest distance from a given GM voxel to the nearest WM voxel, avoiding solutions where this line would pass through CSF. Avoidance of WM voxels is not necessary since the existence of a shortcut across WM automatically implies that the shortest path has not yet been found (Thompson et al., 2005).

Our approach circumvents the need to find an accurate surface representation of the GM-CSF interface, which can be difficult or impossible if no CSF appears to separate gyri across the walls of a deep sulcus. The current method will code GM voxels on either side of the sulcus with increasing distance values in a series of passes over the data, until they meet in the middle. This method suffers from ambiguity when two GM surfaces meet without being separated by a CSF intensity voxel due to partial voluming. In this case, the method must effectively assume that the boundary lies at the point that produces equal thickness for both of the opposing GM surfaces. However, this has virtually no impact on the results; for example, assigning both surfaces 4 mm is effectively indistinguishable from assigning 3 mm and the other 5 mm (which might be the true values) due to the subsequent smoothing (Thompson et al., 2005).

Finally, a local smoothing kernel of radius 15 mm was defined at each vertex on the cortical surface model. The mean distance code was computed for all voxels in the local maxima field that lie under the 15 mm kernel, disregarding voxels that are not in the local maxima field. This is equivalent to applying a uniform spatial filter of radius 15 mm to the local maxima field, only retaining voxels with non-zero values, and reading off the resulting values at each surface vertex.

8.2.3 Statistical Approach

The mean values for cortical thickness obtained from each cortical surface point were calculated to provide maps of average cortical thickness across the lateral and medial surfaces. In addition to our analyses on *scaled* brains (average ICBM-305 space using 12-parameter transformations), we examined cortical thickness in unscaled brains (average ICBM-305 space using 6-parameter transformations) to preserve the actual brain size of men and women while correcting for head alignment and tilt. For this purpose, we applied a specific set of inverted transformation files (generated through the prior linear normalization procedure) in order to convert our sulcal pattern matching outcomes and images that contain the thickness information from ICBM-305 12-parameter space back into ICBM-305 6-parameter space. Independent sample Student's t-tests were then performed on *scaled* and *unscaled* data at each 3D cortical surface location to assess the effect of gender on cortical thickness. Uncorrected two-tailed probability values ($p<0.05$) from these tests were mapped directly onto the average cortical surface model of the entire sample providing detailed and spatially accurate maps of local thickness differences

between groups. Finally, given that statistical tests were made at thousands of cortical surface points and adjacent data points are highly correlated, permutation testing was employed using a threshold of p=0.01, as described in section 7.2.3.

8.3. Results

8.3.1 Average Cortical Thickness

Figure 6 shows the average distribution of *scaled* and *unscaled* cortical thickness in standard ICBM-305 stereotaxic space for the whole sample. Average cortical thickness ranges from 1.5 to 3.4 mm on the lateral and medial brain surfaces (with slightly lower peaks on the upper end of thickness values in *unscaled* data). In both *scaled* and *unscaled* data, the lowest cortical thickness on the lateral and medial surfaces appears to be located in superior portions of the post-central gyrus and surrounding the occipital poles. The highest cortical thickness on the lateral surface seems to be located in the temporal lobes, mainly in anterior parts of the superior temporal gyrus and posterior parts of the medial and inferior temporal gyri. Higher thickness was also detected on the medial surface in the frontal lobe and covering anterior portions of the cingulate gyrus as well as partly extending into the parietal lobe in *scaled* data. The distributional pattern of *scaled* and *unscaled* average cortical thickness seems to be similar in males and females (figures not shown).

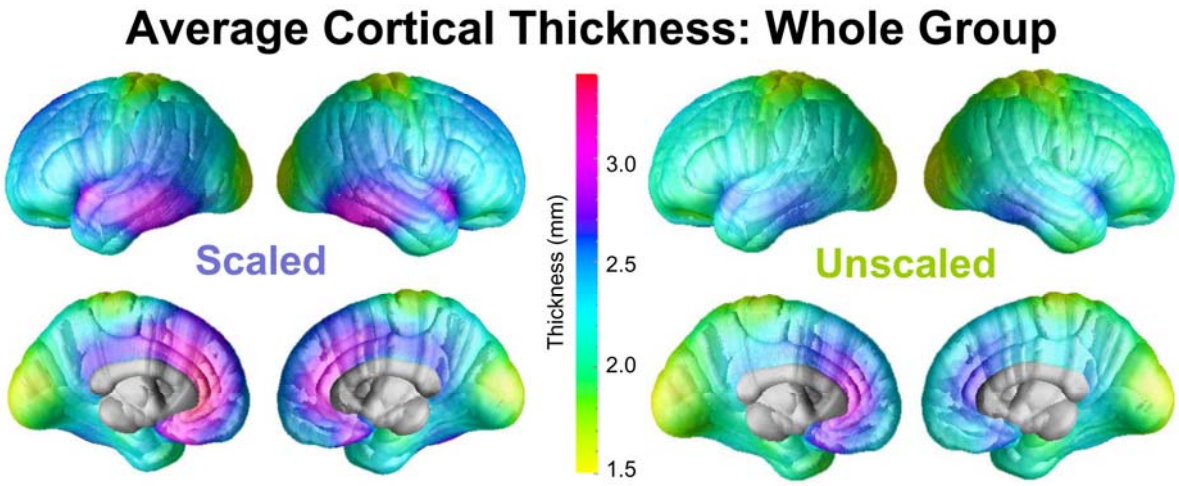

Figure 6. Average maps of regional cortical thickness
Average cortical thickness was mapped for the whole sample in ICBM-305 space after using 12-parameter transformations (left) and after using 6-parameter transformations (right). The brain surface is color coded according to the color bar, where thickness is shown in millimeters. Callosal, subcallosal, and midbrain regions have been excluded on the medial aspect of the surface.

8.3.2 Effects of Gender on Cortical Thickness

Statistical analyses revealed significantly increased cortical thickness in women compared to men, after inter-individual differences in brain size had been removed by transforming images into standard ICBM-305 stereotaxic space using 12-parameter transformations (Figure 7, left panel). No regions with significantly increased cortical thickness were observed in males. Similarly, when the actual brain sizes of men and women were preserved (using only 6-parameter (rigid-body) transformations into ICBM-305 space), we revealed the same pattern and general direction of gender differences in cortical thickness, albeit significance was much less pronounced. A small cortical region in the left lateral temporal lobes showed increased thickness in males (Figure 7, right panel). Permutation tests were highly significant for the comparison of thickness between males and females for *scaled* (left hemisphere: $p<0.00001$; right: $p<0.00002$) and *unscaled* data (left

hemisphere: $p<0.00268$; right: $p<0.01389$), indicating that the observed gender effects do not occur by chance and that thickness is greater in women than men, regardless of scaling.

Brain regions demonstrating significantly higher cortical thickness in women in *scaled* data appear to be spread over the whole lateral brain surface and can be detected in all four lobes in each hemisphere, with temporal regions being least different. While increased female thickness in occipital and parietal lobes appears to be equally pronounced in the left and right hemisphere, gender differences are more prominent in the left frontal lobe than in the right. The gender effect is also stronger in the left hemisphere on the superior surface of the brain close to midline. In contrast, anterior portions of the temporal lobe demonstrate a stronger effect in the right hemisphere. Gender differences on the medial surfaces are less pronounced, but are evident. The most spatially extended and significant areas were identified in the cingulate gyrus, para-central and medial frontal lobe. Here, differences in the left hemisphere were more pronounced than in the right.

In *unscaled* data, increased female thickness on the lateral surface was restricted bilaterally to superior pre- and post-central regions, the occipital lobe, the most anterior tip of the temporal lobe, and in the vicinity of the left inferior and superior frontal gyrus. A small region in the left posterior temporal lobe (surrounding the border between medial and inferior temporal gyrus) showed significantly increased thickness in males. Again, gender effects on the medial surfaces seem to be more concentrated in the left hemisphere with the largest regions of increased female thickness in the para-central lobe. Increased thickness in females in the right hemisphere was distributed more diffusely and especially pronounced in occipital regions as well as between pre-cuneus and para-central lobe.

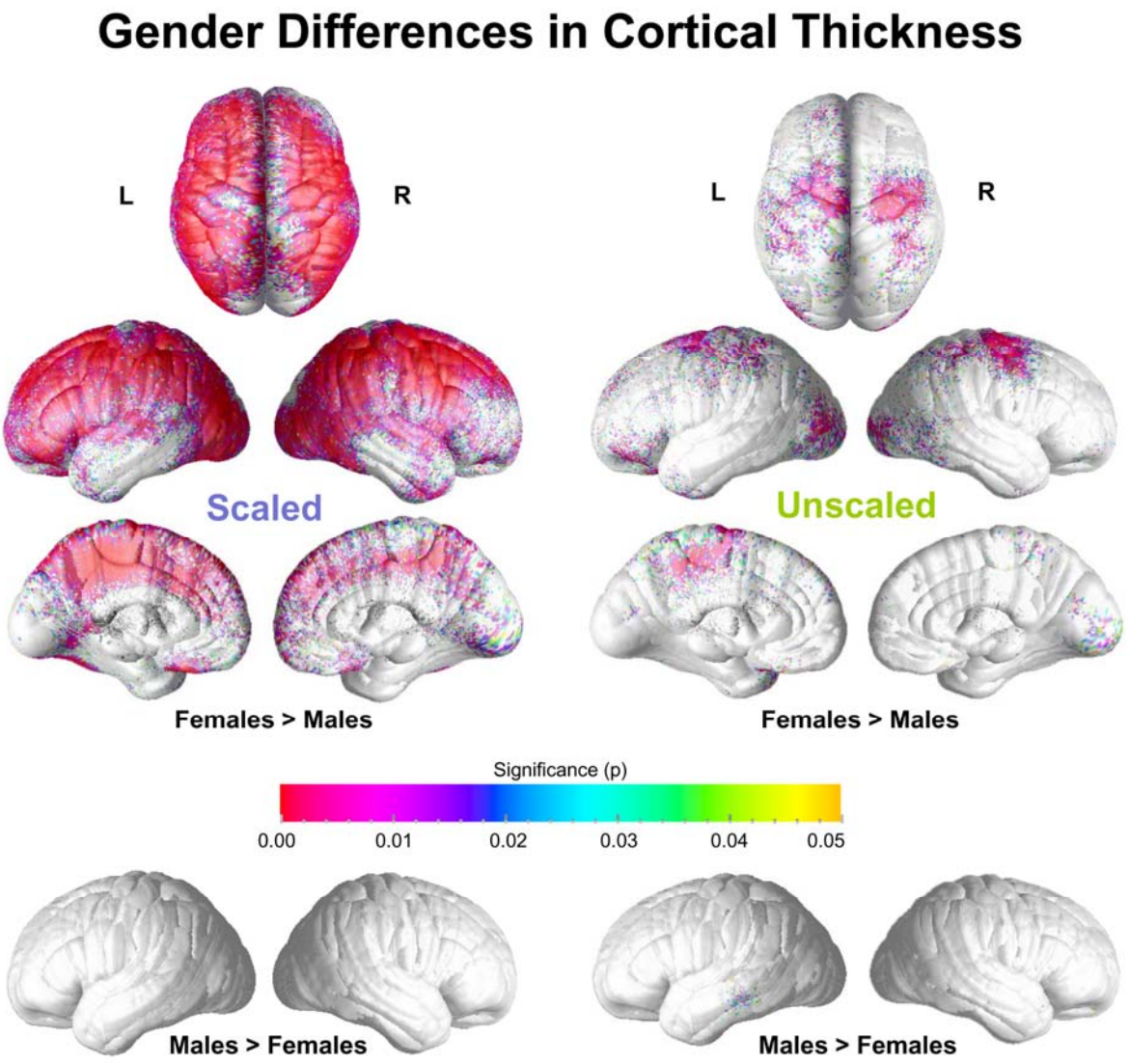

Figure 7. Uncorrected maps of gender differences in regional cortical thickness
Gender differences in cortical thickness were established in ICBM-305 space after using 12-parameter transformations (left) and after using 6-parameter transformations (right). The color bar encodes the p-value associated with the t-tests of cortical thickness performed at each cortical surface point. All colored cortical regions indicate statistically significant differences. All gray-shaded regions are not significantly different between males and females.

8.4. Discussion

We used an automated method to measure thickness across the cortex to characterize the average profile of cortical thickness distributions and to investigate differences between men and women in a well-matched sample of young and healthy adults. Given that allometric relationships have been demonstrated between brain volume and cerebral substructures (Steinmetz et al., 1996; Jancke et al., 1997; Jancke et al., 1999), our analyses also extend previous findings concerning whether brain size normalizations affect the presence and direction of observed gender differences in cortical thickness.

8.4.1 Average Cortical Thickness

8.4.1.1 Correspondence with Previous Findings

Results from this study indicate a heterogeneous distribution of cortical thickness, with different cortical regions exhibiting different thickness values ranging from 1.5 to 3.4 mm. These findings agree with previous reports of average thickness of 1.5-2.8 mm (Kuperberg et al., 2003), 2.0-3.3 mm (Conel, 1967), 1.0-4.5 mm (Fischl and Dale, 2000), 2.0-4.5 mm (Narr et al., 2005), 1.5-5.5 mm (Sowell et al., 2004), and 2.13-2.26 mm (Salat et al., 2004). Of note, several previous analyses revealed thicker cortex in the temporal poles than in more posterior temporal regions (Sowell et al., 2004; Narr et al., 2005). Our data do not confirm those previous reports where the cortex on the temporal poles is clearly thinner. One reason for this discrepancy in findings could be that areas of the cortex that are close to the sinuses (such as the temporal poles etc.) are prone to susceptibility artifacts, which can lead to a loss of contrast due to noise in the temporal poles. Other brain regions are in

line, in terms of minimum and maximum thickness, with others in the literature. For example, our findings of lowest thickness in primary visual regions agree with results by von Economo (1929), Fischl and Dale (2000), Kruggel et al. (2003), Sowell et al. (2004), Narr et al. (2005), and Memoli et al. (2004). Similarly, our findings of lowest thickness in somatosensory regions correspond with reports by Kabani et al.(2001), Fischl and Dale (2000), Kruggel et al. (2003), Sowell et al. (2004), Narr et al. (2005), and Memoli et al. (2004). Moreover, the present study revealed highest thickness in medial frontal regions that also agree with results by Fischl and Dale (2000) and Kuperberg et al. (2003). With regard to the validation of the method, thickness analyses using independent samples in our lab (Sowell et al., 2004; Narr et al., 2005) have revealed spatial distributions of cortical thickness that agree with those based on *post mortem* analyses (von Economo, 1929). Furthermore, thickness maps generated through the same approach as in the present study have been shown to be stable over time in validation studies using short-interval repeat scanning of multiple subjects (Sowell et al., 2004).

8.4.1.2 The Effect of Scaling

Our findings of lower average thickness values in *unscaled* data in the whole study group supports the assumption that cortical thickness is slightly increased through the normalization procedure using 12-parameter registrations. That is, if we scale our male and female brains to the ICBM-152 template – an average of 152 individual brains with blurred edges that therefore possess larger template dimensions than any individual brain – we increase the number of voxels that will be later classified as GM. Since scaling is a uniform

procedure, the numbers of GM voxels along the cortical surface and the thickness of the cortex are both increased. Thus, scaling affects both the thickness of male and female cortices but to a higher extent the latter group because of their typically smaller brain dimensions. In fact, extracting the scaling factor (SF) from our transformation files supports this postulation; brain size was increased on average by 27 % during affine normalization, where female brains were scaled more than male brains (female SF: 1.358; male SF: 1.178).

8.4.2 Effects of Gender on Cortical Thickness

After inter-individual differences in brain size had been removed by applying linear 12-parameter transformations, numerous cortical regions showed increased cortical thickness in females compared to males, while we did not detect any region showing significantly increased thickness in males. Most interestingly, when the actual brain sizes of men and women were preserved (using only 6-parameter transformations into ICBM-305 space), we revealed the same pattern and direction of gender differences in cortical thickness, albeit effects were much less pronounced and a small region in the temporal lobe showed significantly increased thickness in male brains.

8.4.2.1 Scaled versus unscaled data

Linear or non-linear transformations of the data (required to fit the dimensions of a template) alter gender differences in cortical GM density and thickness. Understanding the effects of regional anatomic normalization on these differences has always been a

challenging issue. Here, we show that scaling of the data modulates the structural outcomes to some extent without significantly changing the overall direction of the gender effect. Given that one implicit function of scaling data is to correct for individual brain sizes, and given that female brains are, on average, smaller than male brains, we expected the measured cortical thickness to increase by more in females than in males by correcting for the females' smaller brain volumes. Our observations of stronger regional effects of increased thickness in females in *scaled* data confirmed this assumption.

Exaggerated female thickness in *scaled* imaging data may also be attributable to allometric power laws with disproportionate increases occurring in cortical thickness as compared to brain volume, as demonstrated for several brain structures (Steinmetz et al., 1996; Jancke et al., 1997; Jancke et al., 1999). That is, normalizing data using affine transformations might lead to disproportionate increases of cortical thickness relative to the increase that would be expected for a brain of a larger volume. Surprisingly, although several studies have examined normalized (*scaled*) data to control for different brain sizes between subjects, the issue of how spatial normalizations alter group differences in morphological features has been largely neglected. VBM and some former sulcal pattern matching approaches have typically employed *scaled* data (without systematically evaluating the effect of scaling). However, if the true relation between cortical thickness (or GM) and brain volume is sub-linear or super-linear (i.e. increases more slowly or quickly than linearly with brain volume), then a linear stereotaxic correction (scaling) will leave differences in the data that in principle might be related to brain scale. As a result, morphometric differences that were detected and reported based on *scaled* data do not

necessarily reflect true differences between groups after "taking individual brain volumes into account." Clearly, future studies are needed to better model the possibly nonlinear relation between cortical thickness and brain volume, making it easier to identify the residual effects of gender.

A related issue is that some methodological approaches, such as studies using VBM, evaluate group differences by filtering out the influence of scaling on GM measurements subsequent to the normalization procedure. That is, the intensity values in the normalized segmented images are modulated by the Jacobian determinants (Ashburner and Friston, 2000; Good et al., 2001a; Good et al., 2001b), to test for differences in absolute GM volumes (in contrast to relative GM volumes without the volume preserving step). Interestingly, Good et al. (2001a) detected higher *relative* GM volumes in females only, while both females and males showed regions of higher *absolute* GM volume (as a consequence of the volume preserving step). Thus, analyzing thickness in *scaled* data (like in VBM without the volume preserving step) and *unscaled* data, thickness findings may parallel GM findings. Nevertheless, we detected a similar pattern and direction of gender effects with females showing greater cortical thickness in several brain regions regardless of whether the data were *scaled* or *unscaled* (albeit gender differences were less pronounced, and one small cortical region in the lateral temporal lobes showed greater thickness in males in *unscaled* data). Although cortical thickness and GM constitute different biological measures, they are related (Narr et al., 2005). Thus, VBM results of larger *relative* GM volume in females, and larger *absolute* GM volume in both genders (as opposed to larger thickness in females in *scaled* and *unscaled* data) might be attributable to

the fact that the volume preserving step in VBM does not adjust for the possibility of a power law (which can cause artifactual differences). Consequently, comparing VBM results with findings of other computational image analysis approaches may also be the focus of future studies.

8.4.2.2 Correspondence with Previous Findings

Both measures of GM density/concentration and cortical thickness might reveal features that are associated with the underlying cytoarchitecture. Notwithstanding, in contrast to the analysis of signal-based GM density, the measurement of cortical thickness provides us with an additional dimension of the morphology of the cortex not directly captured by point or sphere measures of signal intensity changes. Consequently, findings from previous GM studies and our present thickness results are only partially comparable. Interestingly, a study by Wiegand et al. (2004) showed significant relationships between GM volumes and cortical thickness measured exclusively in the frontal cortex, while Narr et al. (2005) showed highly significant relationships between GM density and thickness over the majority of the cortical mantle.

Our findings of regionally increased cortical thickness in females correspond to some earlier reports of increased GM volume (bilateral superior temporal lobe, central sulci, inferior frontal gyri, right inferior parietal and cingulate gyri) and GM concentration (bilateral frontal and parietal cortical mantle, banks of the cingulate) in a voxel-based analysis (Good et al., 2001a). Our results also concur with some reports of regionally increased GM and/or cortical volumes in females in the dorsolateral prefrontal cortex

(Schlaepfer et al., 1995), pre-central gyrus, fronto-orbital and superior frontal cortex (Goldstein et al., 2001), inferior frontal cortex (Harasty et al., 1997), superior temporal gyrus (Schlaepfer et al., 1995; Harasty et al., 1997), parietal lobe (Nopoulos et al., 2000), and cingulate sulcus (Paus et al., 1996) as revealed through ROI-analyses of cerebral lobes, parcellated units of the cortex or selected brain slices. There are numerous methodological differences between prior studies (e.g., using *post mortem* versus imaging data and measuring GM volume versus concentration or thickness), so our gender-specific thickness findings are not fully comparable with previous reports. Nevertheless, we think it is of great interest that other automated whole-brain approaches (Good et al., 2001a) did not reveal any cortical region of increased GM concentration in men compared to women, corroborating the present results with respect to cortical thickness in *scaled* data. Furthermore, there is agreement between our findings of regionally increased cortical thickness in females and earlier reports of larger overall cortical volumes relative to cerebrum size in women compared to men (Goldstein et al., 2001), and overall higher GM percentages or proportions in the female brain (Gur et al., 1999; Luders et al., 2002).

Comparing our findings of cortical thickness (Study B) and cortical GM concentration (Study A), analyzing the same set of data, reveals the highest correspondence bilaterally in pre- and post-central regions, the occipital lobe and the left inferior frontal lobe with increased values in females. However, these observations are purely descriptive, given that study-specific peculiarities of the cortical mesh structure did not allow for conducting statistical analyses (e.g., point-wise correlations). Future analyses may help establish the statistical significance of those observations.

8.4.2.3 Potential Confounds

A finer gyrification pattern in the female brain might result in increased partial volume effects, which could appear as thicker cortex in MRI. However, the thickness mapping approach is somewhat immune to partial volume effects for two reasons. First, the partial volume classifier used for GM segmentation in the present study (Shattuck et al., 2001) is one of several classifiers in which the tissue class probabilities are estimated using a Gaussian mixture model. Specific densities are fitted for the mixed GM/WM and GM/CSF tissue classes which could be present in more voxels in brains with a finer fissurization pattern. Notwithstanding, the total amount of GM should be estimated accurately as the partial volume class is modeled explicitly from the intensity histogram of each dataset. Second, the supersampling of the data, before the thickness is measured, allows the fitting of the intensities at the GM/WM interface at slightly finer resolution so that each voxel can be classified more accurately. Finally, it is also possible that thickness and complexity are correlated for biological reasons rather than those due to image rasterization. In a separate sample of 40 normal subjects, who were controls for a study of Williams syndrome, we noted that individual differences in cortical complexity were correlated with cortical thickness in a broad right hemisphere region, including limbic, primary sensorimotor, visual, and perisylvian cortices (Thompson et al., 2005). Thickness and complexity were not correlated in the left hemisphere in normal subjects or in either hemisphere for Williams syndrome subjects. Surprisingly, although Williams syndrome subjects had overall greater complexity, they had less GM and thinner cortices overall. There is,

therefore, no known simple relationship between thickness and complexity, and careful study of these measures in larger samples is warranted.

Contrasting with our present findings of larger thickness in females, some previous analyses revealed a trend toward larger thickness in males (Pakkenberg and Gundersen, 1997; Salat et al., 2004). Others, in turn, suggested that cortical thickness is similar in men and women (Rabinowicz et al., 1999; Nopoulos et al., 2000). Thus, it is possible that thickness differences in males and females, as observed in the present study, might be due to different maturation rates or differences in cortical thinning at that particular age range sampled. Several studies have revealed significant sex by age interactions with males having more prominent age-related brain atrophies than females (Murphy et al., 1996; De Bellis et al., 2001; Good et al., 2001b). Nevertheless some of these findings are conducted on samples with age ranges not applicable to the present study (e.g., 7 to 17 years), or based on morphometric measurements different from cortical thickness (e.g., CSF, GM). In addition, there exist conflicting results with respect to the region of decline (Cowell et al., 1994b; Murphy et al., 1996; Xu et al., 2000; Good et al., 2001b). A study designed to investigate age and gender effects on cortical thickness in particular detected no significant age by gender interactions, and men and women showed a similar degree of global thinning (Salat et al., 2004). Moreover, as observed in the latter thickness study, cortical thinning was not apparent before the third decade, while gender effects in the present study were detected on subjects in their mid-twenties, where the male and female groups were closely age matched and standard deviations were small. However, since another study revealed stronger associations of age and GM in males than in females in the dorsolateral

prefrontal cortex starting in young adulthood (Gur et al., 2002b), further studies remain to be conducted to empirically establish the impact of age on gender-specific thickness results. At this point, it seems rather unlikely that different stages of cortical thinning in male and female brains of subjects in their mid-twenties are responsible for the observed gender effects.

9. Study C: Cortical Convolution – Part I: Lobar Approach

9.1. Background

It is well documented in the normative literature that men have larger brains than women. Mathematical, spatial, and verbal performances are widely reported as sexually disparate, but the differences in brain size observed between sexes seem to occur without equivalent gender effects on general IQ (Halpern, 1992; Mackintosh, 1996; Deary, 1998; Kimura, 1999). Some scientists propose compensation mechanisms in smaller (female) brains. Observations of more neuropil (Jacobs et al., 1993; Rabinowicz et al., 1999), regionally increased neuronal densities (Witelson et al., 1995), and higher regional and global GM percentages in females (Schlaepfer et al., 1995; Gur et al., 1999; Nopoulos et al., 2000; Good et al., 2001a) support the model of brain size-related neuronal compensation. Others challenge this hypothesis arguing, for example, that women still have less absolute GM than men (Good et al., 2001a; Luders et al., 2002; Allen et al., 2003). Furthermore, *post mortem* data revealed 13-16 percent more neocortical neurons and an increased average neuronal density in men (Pakkenberg and Gundersen, 1997; Rabinowicz et al., 1999). Notwithstanding, it is possible that women's smaller brains accommodate more cortical surface area if the folding complexity is greater than in male brains. In that case, histological estimations, which are based on a limited number of cortical loci, might underestimate neuronal numbers in the female cortex.

Increased cortical folding complexities, as a consequence or epiphenomenon of smaller female brains, might result from limited intracranial space causing a constrained brain expansion in females when the brain is still growing. A study by Blanton et al. (2001)

detected a significant gender by age interaction in children and adolescents for some frontal brain regions with cortical complexity only increasing in females with age. However, gender-related differences in sulcal/gyral convolutions were not observed in *post mortem* data based on a two-dimensional (2D) gyrification index, i.e. the ratio between the total (deep) and superficial cortex in coronal brain slices (Zilles et al., 1988). Similarly, no gender differences were found in an *in vivo* study (Nopoulos et al., 2000) defining whole brain surface complexity as the ratio of the total cortical surface area to the overall brain volume, raised to the 2/3 power. A further analysis (Yucel et al., 2001) used surface-to-volume ratios to calculate a fissurization index for the hemispheres and cingulate cortices. This revealed a hemisphere by gender interaction reflecting increased asymmetries of fissurization in male brains. Nonetheless, empirical data on cortical complexity in men and women is sparse and previous investigations have assessed folding complexity in only one dimension, and/or from *post mortem* brains. We therefore examined the degree of cortical convolution in young adults, applying sophisticated 3D parametric mesh-based techniques to high-resolution MRI scans. Rather than assessing gyrification in the whole brain, hemisphere, or in a single brain region, we compared the cortical folding complexity between men and women in five functionally relevant cortical regions in each hemisphere.

9.2. Methods

9.2.1 Image Preprocessing

T1-weighted anatomical image volumes passed through a number of preprocessing steps described in the Appendix and visualized in figure 14: Normalization of anatomical images

into ICBM-305 space using 12 parameter (Module II); RF corrections in anatomical images (Module III); 3D cortical surface extraction based on normalized RF corrected anatomical images (Module IV); Manual delineation of sulcal anatomy in extracted 3D cortical surfaces (Module VII); cortical pattern matching (Module VIII).

9.2.2 Lobar Analysis of Cortical Convolution

In addition to the basis for the cortical pattern matching procedure, the manually delineated sulcal landmarks were used to divide each 3D cortical surface model into five distinct cortical regions within each hemisphere. These regions included: (1) superior-frontal, (2) inferior-frontal, (3) temporal, (4) parietal, and (5) occipital cortices (Figure 8). Both frontal regions were defined as the cortex located anterior to the central sulcus, while superior and inferior frontal regions were distinguished using a line transecting the most inferior aspect of the inferior frontal sulcus. The temporal lobe was delineated by following the Sylvian fissure main body to the most posterior tip. A line was then used to connect this landmark with the most posterior aspects of the inferior temporal, occipital-temporal and collateral sulcus, which served as the lateral and inferior boundary of temporal cortices. The parieto-occipital region included cortex posterior to the central sulcus and superior to the temporal lobe region. A line connecting the most posterior tip of the Sylvian fissure main body and the transverse occipital sulcus served as the separator between the parietal (above) and occipital region (below). The degree of gyrification was obtained in those defined regions.

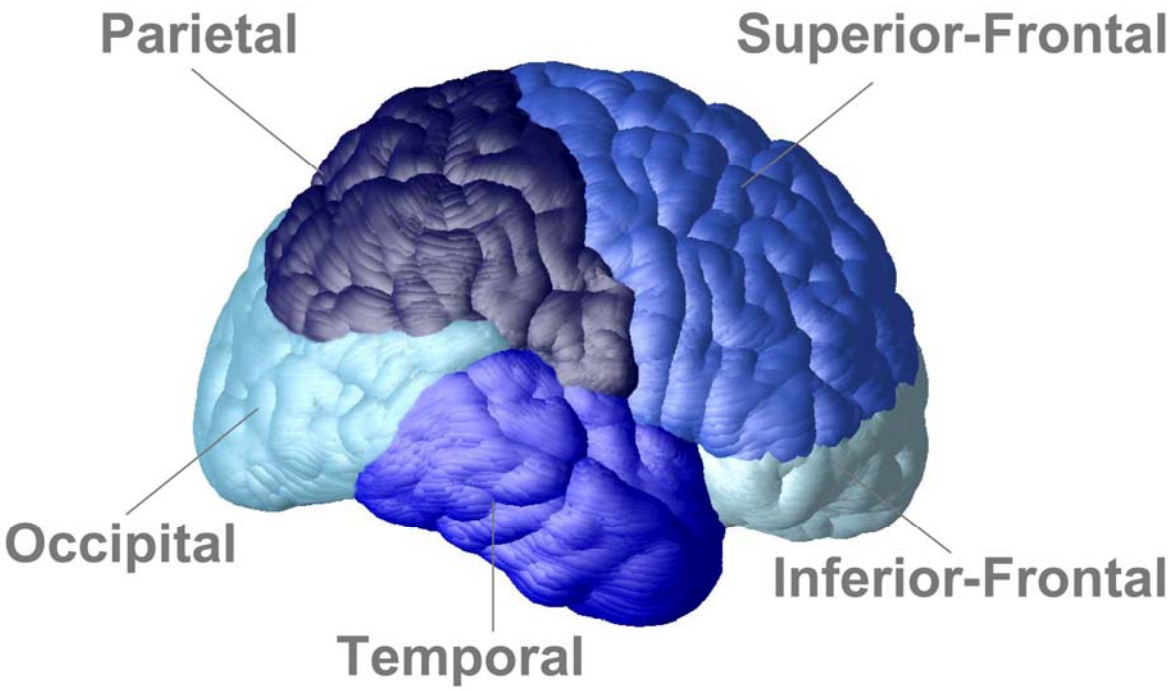

Figure 8. Lobar regions of interest

Since, the cortical surfaces in the present study are represented as parametric meshes, varying the spatial resolution of these meshes may result in modified estimates of surface area. The dependence of the area measurement on the spatial resolution of the parametric grid provides us a measurement of surface complexity. This measure, often termed the *fractal dimension*, reflects the rate at which the measured surface area increases as the spatial detail in the surface representation is increased (Thompson et al., 1996a; Thompson et al., 1996b). For example, the area measured for a flat (planar, non-complex) surface would always be the same at different spatial frequencies, while the area of a convoluted (complex) surface will increase with increasing spatial resolution.

In our analyses, ordered hierarchies of parametric meshes with variable resolutions were generated. For each lobar region, the logarithmic least squares regression of the

achieved surface area was plotted against the logarithm of the spatial frequency of the mesh. Subsequently, the slope of this regression plot was derived and added to the number 2 resulting into complexity values between 2 (for a planar or flat surface) and 3 (for a surface with immense numbers of convolutions and extensive folding). The estimation of lobar gyrification, hereafter referred to as "cortical complexity" is illustrated in figure 9.

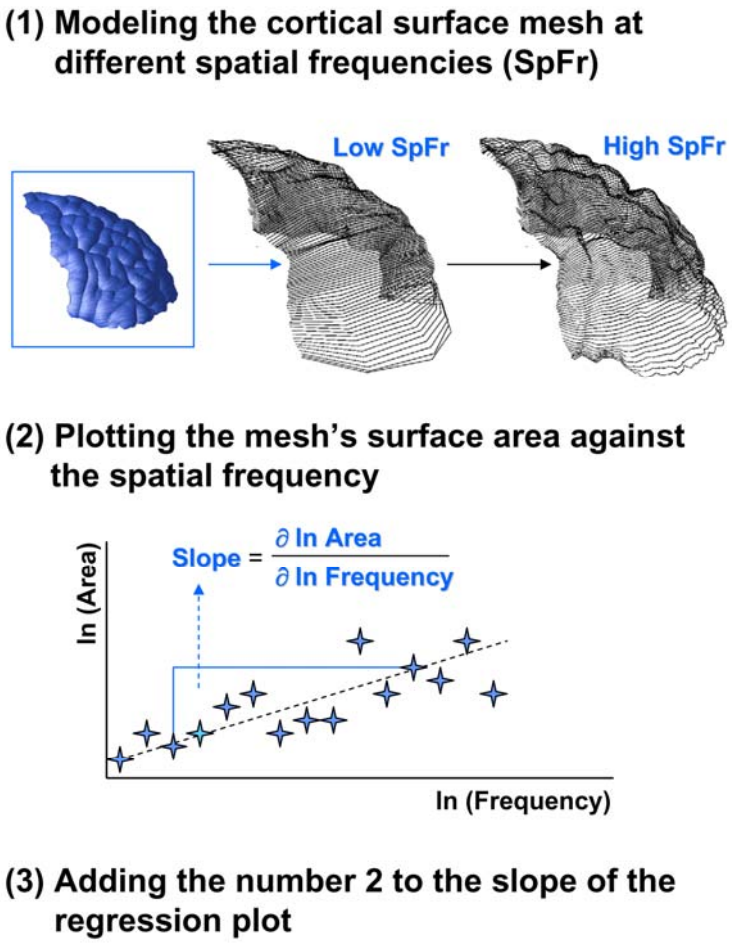

Figure 9. Estimation of cortical complexity
3D surface meshes, obtained from the superior-frontal region, are gridded at different resolutions. The logarithmic least squares regression of the achieved surface area is plotted against the logarithmic spatial frequency of the mesh. The slope of this regression plot is added to the number 2 resulting into complexity values between 2 and 3.

9.2.3 Statistical Analyses

Statistical analyses were performed on a PC workstation using SPSS 10.0 (http://www.spss.com) and SYSTAT (http://www.systat.com/). To compare cortical complexity values between males and females and examine interactions between gender and hemisphere, we used repeated measures ANOVAs including hemisphere as a within-subjects factor. These were followed by univariate analyses only when appropriate (i.e., only in the presence of a significant omnibus effect). Bonferroni correction was employed for the five ANOVAs and a corrected alpha level of $p \leq .01$ was employed as the new criterion for significance.

Finally, Pearson's correlation coefficients were used to assess relationships between cortical complexity and TBV (as determined in study I). Prior to all analyses, the Kolmogorov-Smirnov test was applied to inspect the distribution of the dependent variables.

9.3. Results

9.3.1 Effects of Gender on Cortical Complexity

Descriptively, the lowest cortical complexity in males and females was found in the left inferior-frontal lobes. In contrast, we detected the highest cortical complexity in females in the right superior-frontal lobe, while males exhibited highest complexity in the left occipital lobe. Representative examples of low and high cortical complexity are provided in figure 10.

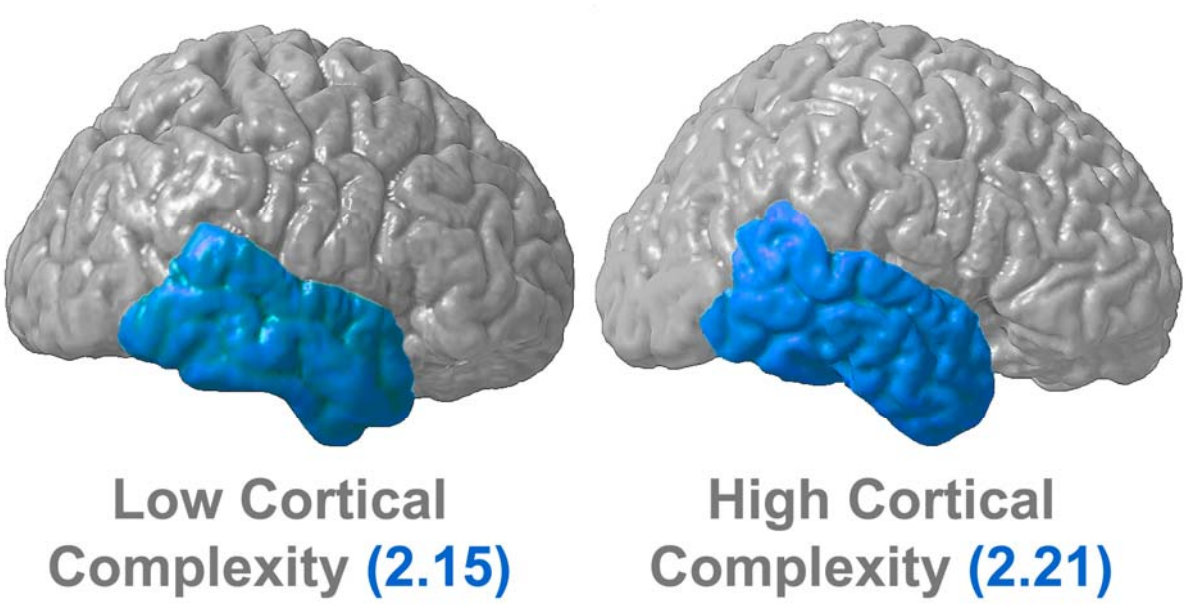

Figure 10. Lower and higher cortical complexity
Examples showing low (2.15) and high (2.21) cortical complexity indices as measured from the temporal lobe region of two different individuals.

Statistical comparisons of cortical complexity values revealed significantly increased cortical complexity in women compared to men in the superior-frontal ($F(1,58)=8.71$, $p<0.005$) and parietal lobes ($F(1,58)=10.38$, $p<0.002$). A trend for hemisphere-by-sex interaction was present for the inferior-frontal lobe ($F=4.25$, $p\leq0.044$), with follow-up analyses revealing significantly increased complexities in the right hemisphere in females compared to males ($F(1,58)=14.87$, $p\leq0.001$). No lobar region in men showed significantly increased cortical complexity compared to women (Table 2). The proportion of variance accounted for by gender differences was medium or large for four out of the five significant results reported, with power ranging up to .97.

Table 2. Statistical descriptors for cortical complexity values

Lobar Region	Males mean (SEM)	Females mean (SEM)	Cohen's d	Power
Inferior Frontal:				
Right	2.16188 (0.00107)	2.16817 (0.00123)*	0.996+	0.940
Left	2.15706 (0.00329)	2.15517 (0.00192)	n.s.	n.s.
Superior Frontal:				
Right	2.16801 (0.00126)	2.17340 (0.00187)*	0.615+	0.609
Left	2.16580 (0.00131)	2.17329 (0.00236)*	0.717+	0.760
Temporal:				
Right	2.15921 (0.00062)	2.16080 (0.00100)	n.s.	n.s.
Left	2.15783 (0.00076)	2.16116 (0.00200)	n.s.	n.s.
Parietal:				
Right	2.16202 (0.00082)	2.16726 (0.00116)*	0.952+	0.967
Left	2.16585 (0.00076)	2.16840 (0.00111)*	0.487+	0.327
Occipital:				
Right	2.16557 (0.00081)	2.16850 (0.00121)	n.s.	n.s.
Left	2.16888 (0.00141)	2.17024 (0.00118)	n.s.	n.s.

n.s. differences not significant between males and females
* indicates the significantly larger volume.
\+ according to Cohen (1988) an effect size of d=0.8 constitutes a large effect, d=0.5 a medium effect, and d=0.2 a small effect (pg 25-27).
SEM Standard Error of Mean

9.3.2 Relationship between Cortical Complexity and Brain Volume

Statistical tests assessing the relationships between TBV and complexity measures revealed negative correlations between TBV and the complexity of the right inferior-frontal (Pearson's $r = -0.364$; $p \leq 0.004$), parietal ($r = -0.307$; $p \leq 0.017$), and occipital lobe ($r = -0.331$; $p \leq 0.010$), as well as left superior-frontal lobe ($r = -0.324$; $p \leq 0.011$).

9.4. Discussion

In this study, we compared regional differences in cortical complexity between young and healthy men and women. Amidst a background of earlier attempts to elucidate why smaller female brains do not coincide with cognitive disadvantages, we hypothesized gender differences in the frequency of sulcal/gyral convolutions.

9.4.1 Correspondence with Previous Findings

Our comparisons of cortical complexity values revealed pronounced gender effect. These findings, however, conflict with previous examinations that failed to detect significant gender differences in gyrification or fissurization indices (Zilles et al., 1988; Nopoulos et al., 2000; Yucel et al., 2001). Methodological differences, however, may account for discrepancies in findings. For example, from the few studies previously examining sex differences, cortical complexity was assessed in *post mortem* brains and/or in a single dimension from non-contiguous brain slices only. Furthermore, prior studies analyzed cortical complexity only for the whole brain or hemispheres, although Yucel et al.(2001) also specifically measured fissurization in anterior cingulate cortices. In our study, we examined cortical complexity *in vivo* using a 3D parametric mesh-based analytic technique. Moreover, we compared sex-related gyral complexity indices from five functionally relevant lobar regions covering the lateral hemispheric surfaces.

9.4.2 Gender Effects and the Relation between Area Size and Convolution

Our results showed greater cortical complexities in bilateral superior-frontal and parietal regions and in the right inferior-frontal cortex in females compared to males. No lobar region showed significantly increased complexity in males. On the one hand, it is possible that the sex differences in cortical convolutions are associated with functional outcomes, where different gyrification patterns may account for gender-specific abilities and/or behavioural differences between men and women (Halpern, 1992; Kimura, 1999). On the other hand, increased folding complexities in female brains may manifest to compensate for their smaller brain volumes (for an exhaustive discussion, please see section 12.2). The idea that increased complexities may compensate for smaller regions by accommodating more cortical tissue, is corroborated by prior findings of larger overall volumes in the right hemisphere and increased fissurization in the left hemisphere (Yucel et al., 2001). Moreover, the present analysis detected only *negative* correlations between complexity measures and TBV which approached significance for the right inferior-frontal, parietal, and occipital lobe, as well as left superior-frontal lobe. Altogether, these findings support the hypothesis that decreased volumes are associated with increased folding complexities, which is also reflected in our gender-related finding of larger complexity in smaller female brains.

10. Study D: Cortical Convolution – Part II: Voxel-wise Approach

10.1. Background

Traditional *post mortem* and *in vivo* morphometric studies have used several unique approaches to examine cortical convolution and to establish the presence and direction of gender differences. Measuring cortical folding in *post mortem* data with a 2D gyrification index (i.e. the ratio between deep and superficial cortex in coronal sections) revealed no differences between men and women (Zilles et al., 1988). Similarly, no gender differences were identified in an *in vivo* study defining whole brain surface complexity as the ratio of total cortical surface area to overall brain volume, raised to the 2/3 power (Nopoulos et al., 2000). However, another MRI investigation used surface-to-volume ratios to calculate a fissurization index for the hemispheres and cingulate cortices. This study detected a hemisphere by gender interaction, reflecting increased asymmetries of fissurization in male brains (Yucel et al., 2001). Moreover, using a sophisticated 3D parametric mesh-based approach (Thompson et al., 1996a; Thompson et al., 1996b) applied to five functionally relevant cortical regions, our group demonstrated that females exhibit greater cortical complexity than males in frontal and parietal regions (Study C) .

Overall, empirical data concerning sex-related differences in cortical convolution is sparse and findings lack consistency, where discrepancies may stem from differences in measurement methods (e.g., *post mortem* versus *in vivo*, 2D versus 3D). Available data, however, suggests that the ability to detect gender-specific differences in gyrification increases by shifting focus from global (e.g., whole brain) to more region-specific examinations (e.g., frontal lobe). ROI-analyses appears to be the most spatially detailed

method used to date. However, since ROI-approaches are accompanied by a number of methodical disadvantages, as outlined in section 3.2.1, we applied a refined and automated whole-brain approach for estimating regional differences in cortical surface convolution. Specifically, we computed the degree of convolution across the entire lateral cortex at thousands of surface points in order to provide color-coded maps indexing the local gyrification. We hypothesized that gender-specific differences in gyrification would exist in numerous cortical regions that would complement and extend existing knowledge from studies using less spatially detailed methods. In order to confirm correspondences with results achieved through a lower resolution parametric mesh-based approach (Thompson et al., 1996a; Thompson et al., 1996b), we examined regional gyrification in the same sample as analyzed in Study C.

10.2. Methods

10.2.1 Image Preprocessing

T1-weighted anatomical image volumes passed through a number of preprocessing steps described in the Appendix and visualized in figure 14: Normalization of anatomical images into ICBM-305 space using 12 parameters (Module II); RF corrections in anatomical images (Module III); 3D cortical surface extraction based on normalized RF corrected anatomical images (Module IV).

10.2.2 Local Analysis of Cortical Convolution

The degree of gyrification is revealed through estimations of "smoothed absolute mean curvature," based on averaging curvature values from each vertex of the spherical surface mesh within a distance of 3 mm, followed by calculating the absolute value of the resulting number within this region and smoothing over 25 mm. A detailed explanation is given in the following paragraphs and figure 11.

The meshes model the cortical surface of the brain consisting of gyri and sulci. We used these meshes to calculate the mean curvature (do Carmo, 1976) at thousands of points across the cortical surface. Mean curvature is an extrinsic surface measure and gives information about the change in normal direction along the surface (normals are vectors pointing outward perpendicular to the surface). Mean curvature at a given point is defined as

$$T_{curvature} = \sum_{v=1}^{n_v} \left(\frac{(\bar{x}_v - \tilde{x}_v) \bullet \tilde{N}_v}{B_v} \right)^2$$

where $\tilde{x}_v$ is the centroid of its neighbors of vertex v, B_v is the average distance from the centroid of each of the neighbors, and $\bullet$ is the vector product operator (MacDonald: A Method for Identifying Geometrically Simple Surfaces from Three Dimensional Images. PhD Thesis McGill University, Montreal). The resulting values of the mean curvature measurement can be expressed either in radians or degrees ranging from -180 to 180 (we will use degrees throughout this paper). Large negative values correspond to sulci and large positive values to gyri. To increase the signal to noise ratio for the curvature measure at a given vertex, we averaged the curvature values within a distance of 3 mm on the

cortical surface and calculated the absolute value of the resulting number within this region. The absolute values of mean curvature (hereafter referred to as absolute mean curvature) are always above zero for both gyri and sulci, and express the local amount of gyrification. Finally, absolute mean curvature values were smoothed using a surface-based heat kernel smoothing filter (Chung et al., 2005) of full width at half maximum (FWHM) of 25 mm, where the width of the smoothing filter was chosen according to the matched filter theorem. That is, the spatial frequency of the sulcus-gyrus pattern suggests a filter that optimally enhances features in the range of the distance between sulci and gyri, which is about 20-30 mm.

Furthermore, we calculated the total surface area and the total absolute mean curvature of the mesh models in ICBM-305 space (after spatial normalization). In order to approximate the impact of spatial normalization on our curvature-based measurements, we calculated absolute mean curvature and smoothed absolute mean curvature of one brain in its native dimension (unscaled image) and after spatial normalization (scaled image). For this purpose, we simulated the scaling of the brain by using a scaling factor of 1.25 along the x-, y-, and z-dimensions, which resulted in a change of volume of almost 200 %, and a change in surface area of about 150 %.

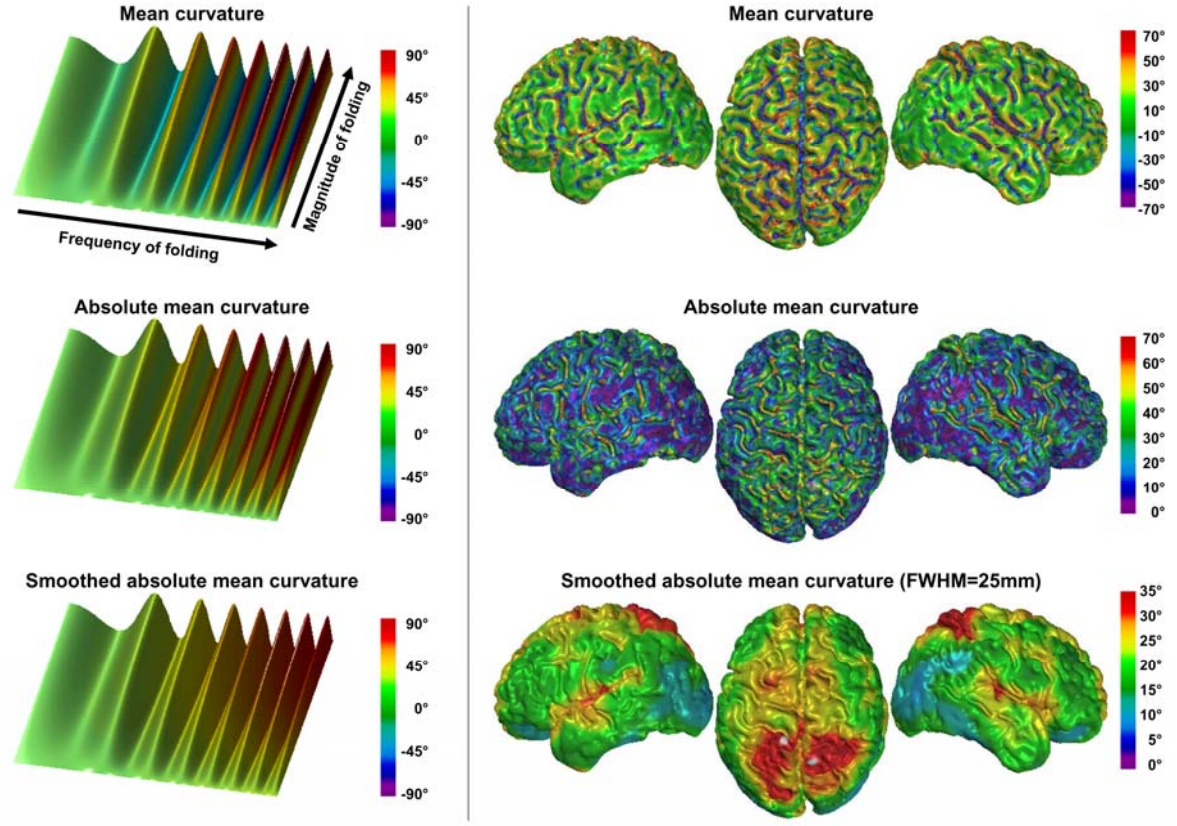

Figure 11. Estimation of mean curvature

The left column demonstrates the computation of gyrification using a simulated folded surface, where the magnitude of the folding increases from proximal to distal, and the wavelength from left to right. The calculation of the mean curvature results in large positive values for local maxima (corresponding to gyri), and large negative values for local minima (corresponding to sulci), where curvature values are expressed in degrees. By calculating the absolute mean curvature, all values are converted into positive values. Finally, curvature values are smoothed using a surface-based heat kernel filter with FWHM = 25 mm. As demonstrated, increases in the amplitude and frequency of the simulated folding are reflected in increased values of smoothed absolute mean curvature.

The right column illustrates the process of estimating gyrification on a single subject brain selected from the sample analyzed in this study. In the first step, the mean curvature is calculated using the 3D mesh of the cortical surface. Sulci can be identified through large negative values (displayed in dark green, blue, and purple), while gyri are characterized by large positive values (displayed in light green, yellow, and red). After calculating the absolute mean curvature, all values are transformed into positive values regardless of whether they represent gyri or sulci. Final surface smoothing with a heat kernel (FWHM = 25mm) reveals higher values for areas with pronounced gyrification.

10.2.3 Statistical Analysis

We linearly averaged the curvature values from each surface mesh point in the male and female group, followed by computing the mean difference between males and females. Statistical differences of local curvature values between male and female group were obtained using a general linear model applied to each corresponding mesh point of the cortical surface. The resulting t-values were thresholded at a p-value of $p<0.05$ and corrected for multiple comparisons using False Discovery Rate [FDR] (Benjamini and Hochberg, 1995). In addition, we compared the total surface area of the cortex in ICBM-305 space between females and males using a one-tailed two-sample t-test. Finally we computed the Spearman correlation coefficient between total surface area and total absolute mean curvature.

10.3. Results

Figure 12 shows the average distributions of cortical convolution in ICBM-305 stereotaxic space for males (left) and females (right). The highest degree of gyrification, in both men and women, appears to be located in the left and right parietal lobes between midline and intra-parietal sulcus, as well as in the left superior frontal cortex and bilaterally along the pre-central sulcus in women, and to a lesser degree also in men. Another small region exhibiting extremely high gyrification was detected at the inferior part of the central sulcus (in both hemispheres and sexes). The lowest gyrification in the left and right hemispheres appears surrounding the occipital poles and expanding into the inferior temporal gyrus, with lower mean gyrification values in males than in females.

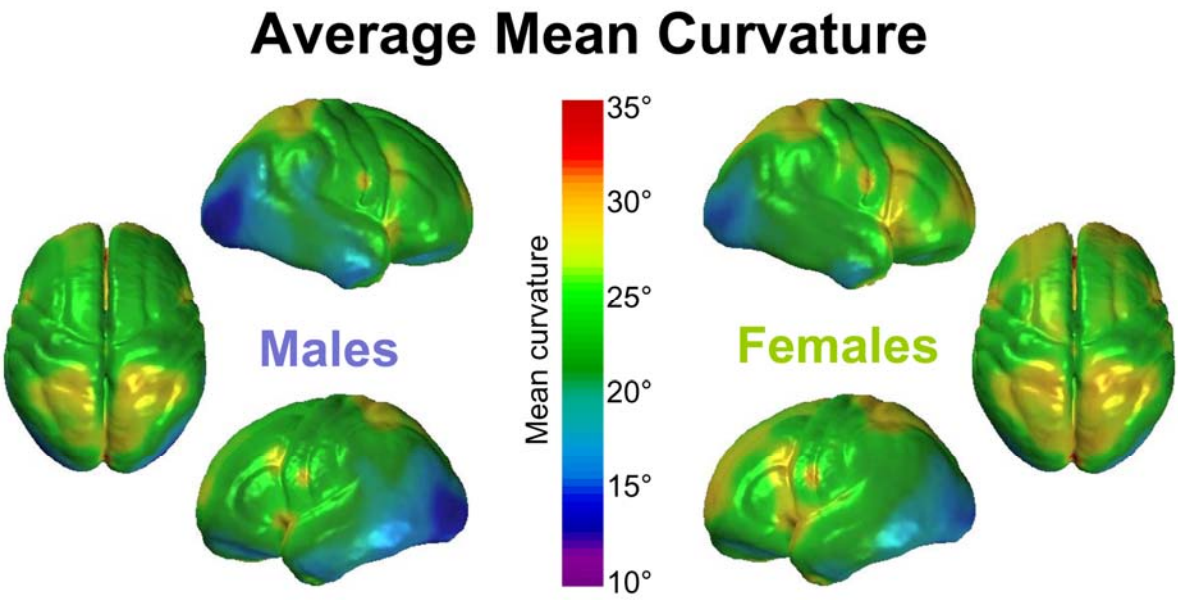

Figure 12. Average maps of mean curvature
The left panel demonstrates the average distribution of mean curvature in males, while the right panel indicates average mean curvature in females. Curvature values are expressed in degrees.

As further illustrated in figure 13, the largest differences between males and females are found in anterior regions of the frontal lobe, with more pronounced gender effects in the left hemisphere than in the right. Large clusters showing significantly increased gyrification in females were also detected in anterior and posterior parts of the left and right temporal lobes, as well as in the occipital lobes (appearing slightly more pronounced in the right hemisphere than in the left). In addition, two regions in the parietal lobes (covering inferior parts of the right post-central sulcus and superior parts of the left and right post-central gyrus) appeared more convoluted in females compared to males. We did not detect any cortical region showing significantly increased gyrification in men compared to women.

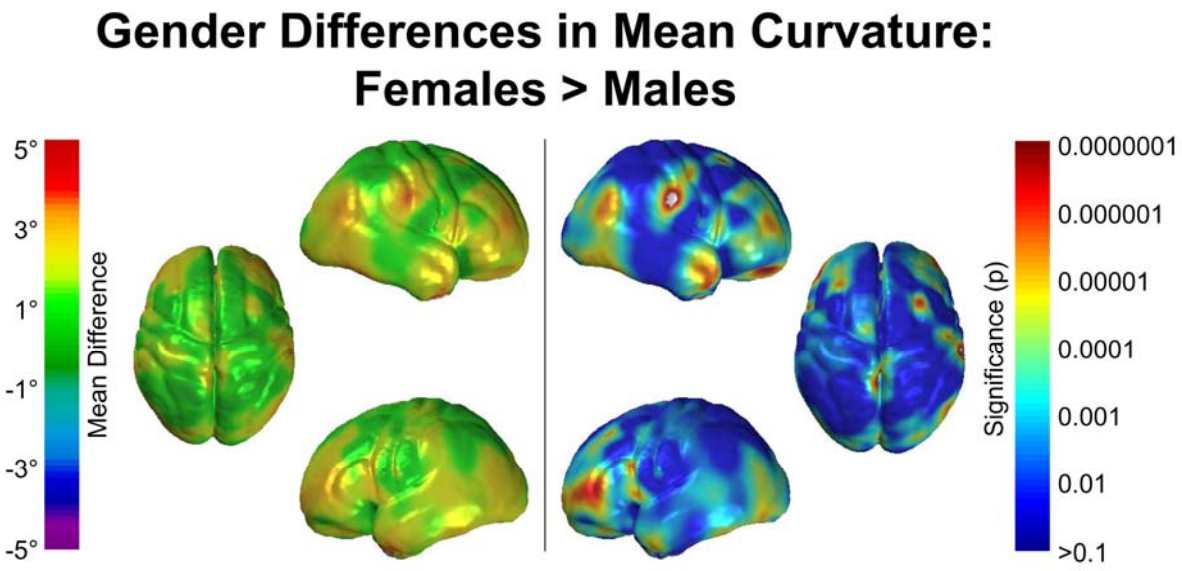

Figure 13. Maps of gender differences in mean curvature
The left panel reveals the mean differences between males and females. Areas with higher gyrification in females than males appear in yellow and red, whereas blue and purple would indicate lower gyrification in females. The right panel illustrates regions of significantly increased gyrification in females compared to males ($p<0.05$), corrected for multiple comparisons using FDR.

The total surface area of the cortex was significantly larger in females compared to males ($p<0.007$, females: 1051.41 ± 42.75 cm^2, males: 1026.07 ± 34.24 cm^2) after transforming images into standard ICBM-305 space by applying 12-parameter transformations. The Spearman correlation coefficient between total surface area and absolute mean curvature for the whole sample was 0.917 ($p<0.001$). The simulated scaling of one brain resulted in a change of absolute mean curvature by a factor of 0.812, while smoothed absolute mean curvature changed by a factor of 0.895. That is, a volume increase of almost 200 % would be accompanied by an 11 % decrease in curvature.

10.4. Discussion

In this study, we present a new method for estimating a local gyrification index. Our approach is related to formerly described calculations of curvature indices (CI) (Magnotta et al., 1999; Nopoulos et al., 2000). However, in contrast to measuring whole-brain sulcal and gyral CIs as implemented previously, we computed the degree of convolution across the entire cortex at thousands of surface points. Our approach further complements traditional methods that produce global measures of gyrification (Zilles et al., 1988; Yucel et al., 2001) and our previously reported approach that provide lobar measures of cortical complexity (Thompson et al., 1996a; Thompson et al., 1996b).

10.4.1 Relationship to Other Approaches

Usually, the classic whole-brain gyrification index is estimated by calculating the ratio between the lengths of the inner and outer contour of the cortex in coronal slices (Zilles et al., 1988; Nopoulos et al., 2000; Yucel et al., 2001). The inner contour exactly follows the peaks and troughs of the sulci and gyri, while the outer contour connects the tops of the gyri using the convex contour with least enclosed area (without following the sulci). These classical approaches require manual tracing that is highly time-consuming, and the gyrification measurement is affected by the orientation of brain slices selected for tracing the contours. In contrast, our newly proposed method works almost fully automatically without introducing any bias from the rater or slice orientation. In addition, our method greatly improves the spatial resolution of gyrification estimates.

The relation of our approach to the classical version of the whole-brain gyrification index can be described as follows: Analogous to the inner and outer contours establishing the classic gyrification index, our cortical mesh models comprise inner and outer surfaces. More specifically, the inner surface is approximated by the total surface area of our cortical meshes, while the outer surface is assumed to be relatively constant over all subjects after spatial normalization. Consequently, the total surface area (the inner surface of the cortex) is suggested to be proportional to the 3D extension of the gyrification index (the ratio between the inner and outer contour of the cortex). Such a relationship between total surface area and gyrification index not only exists on a global level of the whole cortex, but also on a local level at each point of the cortical surface. Given that the present analysis revealed a strong correlation between total surface area and total absolute mean curvature, absolute mean curvature appears to be a suitable means to estimate gyrification on a global and local level.

Because of the excellent spatial resolution, our new method furnishes extremely local measures of convolution that clearly distinguish males from female subjects in a young and healthy group. Moreover, as demonstrated in figure 11, there is a good correspondence between mean curvature and cortical folding: increases in the amplitude and frequency of the folding are reflected in increased values of smoothed absolute mean curvature. Our approach may also serve to identify regional changes in gyrification that occur during neurodevelopment (Blanton et al., 2001) or that manifest as the result of disease (Narr et al., 2005). In addition, gyrification measures may be associated with other measures made point-wise throughout the cortex, such as GM distribution or cortical

thickness (Good et al., 2001a; Sowell et al., 2004; Narr et al., 2005), that may further elucidate sex differences in brain morphology or neuro-pathological processes in individuals with neuro-degenerative or neuro-psychiatric disorders. In fact, a recent study revealed a positive correlation between cortical thickness and whole brain cortical complexity in normal subjects (Thompson et al., 2005).

10.4.2 Correspondence with Previous Findings

In the present study, by comparing local differences in gyrification between men and women, we found pronounced gender differences. Although these findings conflict with some previous examinations that failed to detect significant gender differences in gyrification or fissurization indices (Zilles et al., 1988; Nopoulos et al., 2000; Yucel et al., 2001), our findings corroborate our prior results demonstrating increased complexity in females. The earlier studies that detected no gender differences only assessed cortical convolution or complexity by investigating the whole brain or the hemispheres individually. But pronounced gender effects in the magnitude of complexity and gyrification appear detectable in later studies where more regional analyses are performed at a lobar or voxel level spanning the whole cortical surface. In our prior lobar analysis, we detected an increased complexity in females in the frontal and parietal lobes. These gender differences were also evident in the current study. However, our statistical maps demonstrating sex-related differences in gyrification (Figure 13) showed improved regional specificity for gyrification differences surrounding the frontal pole and inferior/superior frontal sulci. Similarly, larger clusters of significantly increased

gyrification were observed in the parietal lobe that appear restricted to inferior parts of the right post-central sulcus and superior parts of the left and right post-central gyrus. Interestingly, the present study also revealed a higher female gyrification in cortical regions that did not reach significance in our previous study examining complexity collapsed over lobar regions (temporal and occipital lobes). However, in the current analysis, increased gyrification was predominantly observed in anterior and posterior parts of the left and right temporal lobes, which constitute only a portion of the whole temporal lobe. Thus, since gyrification appears similar between males and females for a substantial portion of the temporal cortex, it is likely that global changes in gyrification were not detected previously. Results, therefore, suggest that the current approach is a more powerful means to characterize highly localized differences in gyrification. Our findings complement and refine previously reported gender effects using whole-brain, hemisphere or lobar level analyses where localized gender effects may have remained undetected.

Conversely, it is surprising that the present analysis showed increased gyrification in large parts of the occipital lobe in female compared to male brains, while previously no sex differences were observed in this lobar region overall. Methodological differences may account for these discrepancies. While our earlier approach, described in detail elsewhere (Thompson et al., 1996a; Thompson et al., 1996b), reflects the fractal nature of gyral folding and sulcal fissurization, the current approach appears to be more sensitive to the magnitude of convolution (depths of sulci and heights of gyri). Nevertheless, both approaches confirm that numerous regions in female brains show an increased gyrification, while males show no regional increases compared to females.

10.4.3 Potential Confounds

The current approach analyzes gyrification based on scaled spherical meshes of the cortical surface in ICBM-305 space. We provide evidence that spatial transformations into ICBM-305 space, using 12 parameters, alter the volume and surface area of the brains, but not significantly the degree of gyrification. Notably, volume increases as large as almost 200 % would be accompanied by curvature decreases of only 11 %. Thus, our findings indicate that mean curvature is relatively invariant to affine transforms, and differences between groups would be similar in native space and dimensions.

Another difficulty was pointed out by Magnotta et al. (1999) and is known as the 'problem of buried cortex.' Although volume rendering programs provide visually accurate images of the surface of the brain, they are sometimes inadequate for accurately depicting the presence of sulci. That is, future research has to focus on the development of more sophisticated surface-rendering algorithms in order to detect group-specific differences when deep infolding occurs or when sulcal invaginations are filled with CSF.

III. GENERAL DISCUSSION

The present work revealed clear indicators for a sexual dimorphism in the brains of young and healthy adults. We detected greater gyrification, larger global GM volumes, as well as greater regional GM concentration and cortical thickness in females compared to males, after correcting for individual brain sizes. In contrast, when individual brain volumes were not taken into account, we detected larger global tissue volumes (GM, WM, CSF) in males corroborating our findings of larger brain volumes in men. Interestingly, regional thickness of the cortex was larger in females than in males, even when brains were analyzed in their native dimensions.

The following general discussion is designed to shed light on factors that possibly determine such profound differences in the brains of men and women. Furthermore, I will provide a detailed discussion addressing the potential significance of our gender-specific structural findings for behavioral outcomes, emphasizing obvious gaps of knowledge that clearly indicate the need for further research.

11. Determining Factors of Sexual Dimorphism in the Brain

Clearly, sex differences that arise before birth must be a consequence of prenatal gender-specific hormonal action and genetic determination rather than a result of differential social stimulation. In contrast, morphological sex difference first arising after birth could be the result of either prenatal or postnatal influences (Breedlove, 1994). However, except for the larger total brain weight in men compared to women (Dekaban, 1978), we do not know conclusively whether any of the sexual dimorphisms in the human brain are present at birth or not. Thus, the determining factors for the observed sexual dimorphisms in the brain

remain to be established in future work, where interplay between hormonal exposure, genetic determination, and subsequent differential social stimulation is very likely. The following paragraphs will provide an overview of potential mechanisms and factors that might cause, sustain, accentuate, or attenuate the sexual dimorphism in the brain.

11.1 Environmental Determinants

Over the past centuries, the demands for traditional gender roles have significantly changed with environmental and social influences being more and more similar for men and women. Nevertheless, differences in various fields still exist, with gender-specific environments being established as early as in infancy (e.g., through toys, social interactions, behavioral expectations, etc.).

11.1.1 GM Concentration and Cortical Thickness

Animal studies indicate that experience-related changes in mammalian brain structures are likely (Trachtenberg et al., 2002; Kempermann et al., 2002). An excellent summary with regard to responses of the brain to enrichment throughout life is provided by Diamond (2001). Moreover, recent studies on humans revealed that stimulus dependent influences, like short or long-term training in specific cognitive or motor skills, can modulate regional GM volumes (Maguire et al., 2000; Gaser and Schlaug, 2003; Draganski et al., 2004). In addition, experience-dependent plasticity in humans was demonstrated on a microscopic level, where dendritic lengths and branching altered in dependence of school education (Jacobs et al., 1993).

Moreover, even if men and women are exposed to the same settings, gender-specific effects of environments inducing the alteration of cerebral micro-structures have been reported. Male rats, for example, had more dendritic material per neuron than females in isolated environments while females had a larger dendritic tree than males in complex environments (Juraska et al., 1985). Furthermore, the female neocortex in rats was observed to respond differently than the male neocortex exposed to the same type of enrichment conditions. That is, while male brains showed significant changes in cortical thickness in the occipital cortex, but no significant changes in the somatosensory cortex, the thickness of the occipital and somatosensory cortices increased significantly in females, albeit not as much as in the male brains with respect to the occipital cortex (Diamond, 1988 according to Diamond, 2001). These observations highlight the possibility that gender-specific experiences or differential effects on the brain anatomy are potential contributors to gender differences in cortical thickness and GM, as revealed in the present analyses.

11.1.2 Convolution of the Cortical Surface

Similarly, sexually-dimorphic cortical complexities might develop as a consequence of exposures to different environments and social interactions, mediated by alterations of the underlying cytoarchitecture and neural connectivity of the cortex (Caviness, Jr., 1975; Richman et al., 1975; Goldman-Rakic, 1981; Rakic, 1988; Rademacher et al., 1993; Watson et al., 1993; Roland and Zilles, 1994; Rilling and Insel, 1999a). This hypothesis challenges the assumption that most cortical folding is principally defined in the late second and third trimesters of fetal life (Richman et al., 1975; Chi et al., 1977; Armstrong

et al., 1995), where the degree of gyrification was reported to reach adult levels already around birth (Zilles et al., 1997). However, conflicting reports of age-related increases of cortical complexity in frontal brain regions exist (Blanton et al., 2001). At this point, further research appears necessary in order to establish the true impact of environmental factors on the pattern and degree of cortical folding.

11.2 Non-environmental Determinants

In addition to or in conjunction with differential environmental and social influences, steroid hormones have been proposed to influence the brain during the lifespan.[6] Although gonadal steroids do not appear to play a significant role in regulating neural genesis and neural migration (Davis et al., 1996), steroid-induced alterations in gene expression can stimulate the neuron to make new synapses upon its target cells, to discard old synapses from other neurons, to die while other neurons live, or to remain alive while other neurons die (Breedlove, 1994). Beside such growth-promoting, organizational, and neuro-protective effects (Davis et al., 1996; Wise et al., 2001; Wise, 2002), androgens and estrogens are proposed to have activational effects and modulate brain activity through excitatory or inhibitory mechanisms (Veliskova, 2004).

[6]Animal studies have confirmed the existence of critical periods at early developmental stages, implying a lack of capacity in the adult brain to respond to steroids. Nevertheless, contrasting reports also exist, indicating that hormonal effects constitute lifelong influences on aspects of brain architecture and function (Arnold and Gorski, 1984; Forget and Cohen, 1994). For example, there is evidence for cycle-dependent neurotransmission and synaptogenesis in rodents (Woolley et al., 1990; Segal and Murphy, 2001; Yankova et al., 2001). Moreover, studies on humans revealed a hormone-dependent cortical plasticity affecting both functional lateralization and level of activation (Hausmann and Gunturkun, 2000; Fernandez et al., 2003).

Gender-specific cerebral structures could be a consequence of neuronal events that are initiated by steroid hormones (Breedlove, 1994). Steroid hormones affect cells (e.g., neurons) that have particular steroid receptors specific for androgens and estrogens (Arnold and Gorski, 1984). If, for example, estrogen binds to the estrogen receptor in a neuron, the resulting steroid-receptor complex moves to the nucleus, where it interacts with the neuron's DNA. Such steroid-induced alterations in gene expression can drastically alter the target cell and, consequently, brain structure in men and women (Breedlove, 1994).

11.2.1 GM Concentration and Cortical Thickness

There exists an intriguing correspondence between our revealed regionally increased thickness in female brains and regions with high densities of sex steroid receptors as identified in studies on animals (Goldstein et al., 2001). As visualized by Goldstein and colleagues, higher densities of estrogen receptors have been detected predominantly in superior frontal and fronto-orbital regions, surrounding the pre-, post- and central sulci, the inferior parietal lobe, the occipital pole (lateral surface) and covering the cingulate, para-central and medial frontal gyrus (medial surface). In contrast, the temporal lobes are the most extended regions with developmentally low densities of estrogen receptors, which might be related to the apparent lack of sexual dimorphism in large regions of the temporal lobe in the present study. The striking correspondence between our thickness findings and hormonal receptor densities in animals might serve to generate hypotheses about the spatial organization of hormonal receptors in the postnatal human brain and its association with micro and macro structure in the adult brain.

Nevertheless, other findings from animal studies appear to indicate growth-inhibiting effects of estrogen on the cerebral cortex. In rodents, for example, it was observed that regions with lower estrogen receptor concentrations have a higher cortical thicknesses, as well as numbers of neurons and glia per unit area (Sandhu et al., 1986; Diamond, 1987; Diamond, 1991), clearly contradicting our conclusions based on findings of the present study in humans. Moreover, apoptosis-inhibitory effects of testosterone were suggested based on findings in animals (Davis et al., 1996), but seem to contradict our findings of reduced GM and thickness in males in humans. It remains to be established, whether the observed gender effects are caused by an enhanced neuronal production and/or apoptosis in one gender group compared to the other. Further work is needed to reliably translate conclusions based on animal studies to human brains (Goldstein et al., 2001).

Aside from hormonal influences, genetic effects altering the time frame for neurogenesis might have also contributed to the present findings of gender-specific cortical GM and thickness. For example, as summarized in Rakic (1998), before neurogenesis, two main phases of cellular division can be distinguished, with the first one generating two daughter cells (symmetric cell division), and the second one generating one permanent post-mitotic neuron (asymmetric cell division). Since the latter phase produces neuronal precursors of the cortical micro-columns, the duration of this phase determines the number of neurons in each column and, hence, cortical thickness (Rakic, 1998). Thus, a gender-specific regional thickness of the cortex might be attributable to a genetically determined longer duration of phase 2 in females. Future studies are needed to verify this theory.

11.2.2 Convolution of the Cortical Surface

Similarly, the extent to which changes in sulcal and gyral shape occur during adult life and to which they are genetically programmed versus environmentally influenced is at present unknown (Magnotta et al., 1999). With regard to the morphogenesis of the regional degree of folding, several theories implicate factors intrinsic to the cortex in the primary mechanism of folding. For example, it was proposed that greater expansion of outer versus inner cortical layers causes gyrification (Richman et al., 1975; Rakic, 1988). According to White et al. (2003), a tension-based theory is currently perhaps the most widely accepted mechanism of gyrification of the cortex. It is proposed that regions with greater connectivity provide tension that draw them closer together (Van Essen 1997), inducing the warping of the cerebral cortex from the lissencephalic fetal brain to the highly gyrified adult brain. Gender-specific rates of brain maturation (Geschwind and Galaburda, 1985) may partly account for present findings of sexual dimorphism in gyrification, although the details of this relationship require further examination. Genetic determination and/or the differential effects of gonadal hormones during brain growth are likely to affect the gender-specific degree of gyrification, similarly as with regard to cortical thickness or GM. However, given that brain growth is partly confined by the size of the intracranial cavity (Hofman, 1989; Van Essen, 1997; Courchesne et al., 2000), increased gyrification in female brains might alternatively (or additionally) be caused by a greater constraint of brain expansion due to smaller skull sizes in women.

12. Association with Gender-specific Behavior and Abilities

12.1 GM Concentration and Cortical Thickness

The MRI signal strength is related to cellular characteristics such as cell packing density, myelination, cell size and number of cortical neurons (Kruggel et al., 2003; Eickhoff et al., 2004). However, at this point, it is unclear how exactly the cortical cellular and fiber structure translates into intensity profiles as revealed by high-resolution MRI (a critical outline is provided in section 3.2.3.2). If increased thickness and/or GM concentration reflect a regionally increased number of cortical neurons, it may have functional significance, such as contributing to advantages in performing particular cognitive actions. That is, our anatomical findings may account for gender-specific cognitive abilities. However, the thickness of the cortex, for example, is a composite measure of axonal, dendritic, synaptic, and glial numbers and sizes, and not just simply "neurons" (Landing et al., 2002). Furthermore, it appears rather questionable that there is a simple relationship between cerebral structure and its implications for cognitive functioning, such as "the more the better," which will be further discussed in the following paragraphs. Various arguments are provided challenging the assumption of a one-dimensional link between cortical structure and functional outcomes.

12.1.1 More Neurons – Enhanced Performance

If, in some cortical regions, a larger thickness or GM concentration indeed reflects more numerous neurons, such tissue enlargements might be advantageous by facilitating an efficient processing of ingoing and outgoing information, which in turn, might be

beneficial for cognitive performances. For example, histo-pathological data has shown regionally increased neuronal densities in the posterior temporal cortex in females (Witelson et al., 1995), which seems to agree with our findings of increased GM concentration in the left posterior superior temporal gyrus. Importantly, the superior temporal gyrus constitutes part of the Wernicke area, which is a language-associated cortical region. It is possible that the observed gender effect in this region might be related to the better language skills previously reported in females (Halpern, 1992; Kimura, 1999). Further support for this association comes from other studies that revealed a direct link between correlations between GM and IQ, as well as spatial and verbal performances (Gur et al., 1999; Thompson et al., 2001a; Haier et al., 2004). However, in view of the apparent lack of increased thickness or GM in any region of male brains, it appears to be rather insufficient to assume a simple positive correlation between neuronal number in a particular area and the functional capacity supplied by this region.

12.1.2 More Neurons – Worse Performance?

Another interesting hypothesis mentioned in DeFelipe (2002) suggests that a wider separation of neurons could imply a greater refinement of neuronal connections due to a richer fiber plexus. Similar arguments are provided by de Court (1999), proposing that more extensive cortical neuropil is accompanied by more extensive dendritic arborization and, thus, overall more numerous connections between nerve cells. Interestingly, nerve cells were detected to be farther apart in enriched versus impoverished rat brains, implying that the major component of the brain changes due to enrichment had to do with alterations

in the dendritic branching (Diamond, 2001). Thus, decreased numbers of neurons might increase the opportunity for neuronal interactions and possibly lead to improved, more effective (or just different) functioning.

Indeed, some of our findings actually seem to contradict an intuitive positive relationship between neuronal number and performance (as suggested in section 11.3.1), and seem to support the idea of an inversed relationship between cell number and functional outcome. For example, cognitive tasks that require visuo-spatial abilities are better performed by males than by females (Halpern, 1992; Masters and Sanders, 1993). It was demonstrated that visuo-spatial information is predominantly processed in (left) parietal regions (Keating and Gooley, 1988; Petersen et al., 1989; Alivisatos and Petrides, 1997). We detected less regional GM and thickness in male brains in those regions, which might imply that fewer neurons are not necessarily disadvantageous for cognitive functioning. Similar observations have been reported with respect to GM in parietal regions, where higher percentages and concentrations were observed in females (Nopoulos et al., 2000; Good et al., 2001a). Moreover, thicker cortex, higher neuronal densities, and more neurons in the left temporal sites involved with language functions were observed in males contrasting with reports of better language performances in females (Rabinowicz et al., 1999; de Court, 1999), albeit also contradicting our observations. Consequently, it is possible that positive and negative relationships might exist between the neuronal number in a particular cortical region and functional performance mediated by this region.

12.1.3 More Neurons – Same Performance and Behavior?

From a different point of view, it is also likely that neuronal compensation through similar or approximately equal numbers of cortical neurons in larger male and smaller female brains is the only functional correlate to increased regional thickness or GM concentrations. Gur and colleagues (1999), for example, argue that the higher relative GM composition of women's brains may compensate for smaller cranial capacity by devoting more of that space to computation rather than information transfer. The assumption of approximately equal numbers of neurons seems to conflict with *post mortem* analysis, where more neurons were found in the cortex of male brains (Pakkenberg and Gundersen, 1997; Rabinowicz et al., 1999). However, given that such histological estimations are based on tissue sections from a restricted number of cortical loci, neuronal numbers in the female cortex may be underestimated if female brains accommodate more cortex due to a higher degree of convolution, as demonstrated in the current thesis. Nonetheless, if increased cortical thickness or GM simply reflects a reallocation of neurons in female brains (because of smaller brain dimensions), then there remains the question why thickness and GM are only increased in certain regions of the female cortex and not evenly distributed (e.g., not in the temporal lobes).

12.1.4 Neuronal Interplay and Organization

Apart from this question, it is still uncertain, whether neuronal quantity alone determines the functional outcome mediated by a particular region. It is more likely that the neuronal interplay within and between functional units, determined by the wiring pattern of neuronal

connections, outranges the impact of the neuronal number (which might be advantageous to some extent). Another possibly significant contributor to functional outcomes may be the relation between neuronal numbers in different layers of the cortex. For example, if a sexual dimorphism would be restricted to certain layers only, there could be a different ratio of input and output components in men and women, which possibly could contribute to gender-specific abilities moderated via different brain organizations, as observed and discussed by Witelson and colleagues (1995). Further modulations of cognitive functioning and behavior could result from the effect of increased neuronal numbers in one particular region on other neurons projecting to and receiving from this neuronal pool [inspired by comments by Arnold and Gorski (1984)]. Gur and colleages (2002a), for example, detected increased orbital volume relative to amygdale volume in females compared to males. Thus, they suggest, women may have more tissue volume available for modulating amygdale input possibly accounting for gender differences in emotional manners. Similar to inter-regional connectivity and layer-specific cell numbers, the inter-dependence in the quantity of thickness/GM between different regions remains to be investigated in future studies.

12.2 Convolution of the Cortical Surface

The measurement of mean curvature and cortical complexity is determined by the magnitude (sulcal depths and gyral heights) and frequency of folding (number of sulci and gyri) in certain cortical regions. Sulcal/gyral formation is influenced by the underlying cytoarchitecture of the cortex (Rademacher et al., 1993; Watson et al., 1993; Roland and Zilles, 1994). Furthermore, gyrification is thought to be influenced by neural connectivity

(Caviness, Jr., 1975; Goldman-Rakic, 1981; Rakic, 1988) and to change as a function of the volumetric ratio between outer and inner cortical layers (Richman et al., 1975). It was additionally proposed that greater folding complexities accompany higher intra-cortical connectivities (originating in outer cortical layers) and smaller descending projections (originating in inner cortical layers) (Rilling and Insel, 1999a). Thus, it is possible that different mean curvatures and cortical complexities in men and women reflect gender-specific underlying cytoarchitecture and neural connectivity of specific brain regions, which could have functional significance. This could account for differences between men's and women's behavior, cognitive strategies and outcomes. Alternatively, cognition and behavior might not be modulated at all based on the observed gender differences if different (but similarly effective) processing mechanisms accompany gender-specific cortical convolutions.

12.2.1 Higher Gyrification – Enhanced Performance?

An increased cortical convolution in female brains may constitute part of the anatomical substrate that supports some of the cognitive skills where women tend to outperform men. For example, increased mean curvature as detected in regions adjacent or including Broca's and Wernicke's areas, might account for better verbal performances, as reported in females (Halpern, 1992; Kimura, 1999). However, if this proposed relationship were true, then we would have to ask once more why there is no cortical region in male brains that shows a higher degree of convolution than its counterpart in female brains. Consequently, we should probably assume that there is much more than a simple one-dimensional link

between structure and function. Alternatively we could infer that gender not only determines brain morphology, but also the special relationship between structure and function. Theories that might be true when applied to females brains might loose their validity when related to the link between structure and function in males brains. A "more" in female brains that modulates a functional outcome in favor of a woman might not necessarily be advantageous to the same extent if in a male brain.

12.2.2 Higher Gyrification – A Global Compensation Mechanism?

Alternatively, it is also likely that increased gyrification in females may constitute a compensation mechanism for their smaller brains, similar as argued for larger regional GM and cortical thickness. This, for example, may help to explain why men and women perform equally, on average, in tests of general intelligence. On the one hand, compensation might result from a gender-specific brain organization that finds its expression in the frequency or amplitude of gyral folding and sulcal fissurization. In the same way, gender differences in structural asymmetries (Jancke et al., 1994; Kulynych et al., 1994; Amunts et al., 2000) or in the size and shape of the CC (DeLacoste-Utamsing and Holloway, 1982; Witelson, 1989; Steinmetz et al., 1992) have been suggested to account for sexual-dimorphic functional lateralities or interhemispheric communications. On the other hand, an increased gyrification in females is likely to accompany increased cortical volumes (Goldstein et al., 2001). Similarly, enlarged cortical surface areas were detected in females when adjusting for brain volume (Nopoulos et al., 2000), although larger cortical surface areas were reported in men without brain size correction

(Pakkenberg and Gundersen, 1997; Nopoulos et al., 2000; Salat et al., 2004). That is, the higher degree of cortical convolutions in females may compensate to some extent for reduced overall brain volumes.

12.2.3 Higher Gyrification – A Regional Compensation Mechanism?

It is also possible that increased gyrification in particular brain regions might be associated with regionally higher neuronal numbers, thus accounting for compensation on a local level. In fact, the present results of increased gyrification in frontal and parietal regions in females might support previous findings of increased GM in those regions (Schlaepfer et al., 1995; Nopoulos et al., 2000; Good et al., 2001a). Furthermore, in concordance with our results of increased gyrification in anterior and posterior parts of the temporal lobe in females, increased GM was detected in females in temporal regions (Good et al., 2001a). Moreover, the number of neurons per unit volume was reported to be significantly increased in the posterior temporal cortex in females (Witelson et al., 1995). Nevertheless, even if the local degree of gyrification and the regional number of neurons would be positively correlated, we still would not know whether more neurons are advantageous or disadvantageous (see discussion in section 12.1). Furthermore, other micro-structural compounds (besides neuronal numbers) are probably determined by the degree of gyrification. That is, compensation on a local level is likely, where the exact nature remains to be addressed in future studies.

13. Where to Go from Here – Implications for Future Studies

The work summarized in this thesis revealed the presence and direction of cerebral gender differences in great details with respect to a variety of morphological measures. The careful planning and thorough conduction of adequate image preprocessing and subsequent analyses provided for a high reliability of the results. Application of state-of-the-art tools allowed for pilot measurements to examine several morphological characteristics for the first time in young and healthy controls. Moreover, this work supplies significant insight into how image preprocessing and analysis can influence results and thereby alter the detected sexual dimorphism. Nevertheless, the studies also have some limitations which provide an important source to stimulate future research and which can be reviewed in the final chapter.

13.1 Cross-Correlations between Measurements

Clearly, we can neither determine the cell or molecular biology of our observed structural gender differences, nor can we draw valid conclusions with respect to functional consequences. Subsequent studies correlating structural and functional parameters in the same sample of subjects will be challenging endeavors to unscramble the relationships between cerebral micro- and macrostructure as well as cognitive functioning. Those will be necessary steps before we can relate our macro-structural findings to specific cellular differences, gender-specific abilities, or particular behavioral differences between men and women. Those investigations will also help to determine whether gender only determines

brain morphology or if it is also a moderator with respect to the link between brain anatomy, function and outcome.

Against this background, it will also be desirable to develop sophisticated methods that allow to directly correlate point-wise regional morphometric measurements with each other. First steps were accomplished by examining the same variables of interest (e.g., cortical convolution expressed as lobar fractal dimension as well as local mean curvature) in the same sample of subjects. Future analyses, however, remain to be conducted to establish cross-correlation at the same co-ordinates. This way, for example, we could investigate how the measured convolution of the cortex is related to observed differences in GM and thickness.

13.2 Controlling for Potential Confounds

Another concern are potential confounds, such as the influences of age, hormones, intelligence, handedness, and ethnicity of the examined subjects. Of note, these confounds constitute a different set of contributors to the observed findings, apart from the methodological influences already discussed at length in the respective Discussion sections of the sub-studies.

13.2.1 Hormones and Intelligence

Brain structure might be sensitive to hormonal fluctuations across the estrous cycle (or even seasonal and daily fluctuations of testosterone), which may lead to alterations in structural differences between male and female brains depending on when subjects

undergo the brain scanning procedure. Consequently, future studies could try to control for those factors by collecting samples of blood and/or saliva in order to diminish intra-group variability by carefully matching subjects or including hormonal states as covariate in statistical models.

In addition, data on intelligence, or at least some valid indicators for cognitive abilities, should be collected in future analyses in order to better match samples or statistically control for those variables. At this point we cannot rule out the possibility that the observed gender differences may have been due to different levels of intelligence in the male and female subjects examined despite the fact that they were all university students.

13.2.2 Handedness and Ethnicity

Since we exclusively analyzed right handed Caucasian subjects, extrapolations of our findings to other samples in the population, ranging outside the criteria that apply to the present sample, are problematic. Since handedness (Steinmetz et al., 1991; Witelson and Kigar, 1992; Jancke et al., 1994; Zilles et al., 1996; Amunts et al., 2000) and ethnicity (Zilles et al., 2001; Kochunov et al., 2003) have been suggested as clear determinants for brain structure, additional analyses remain to be conducted in order to establish the presence and nature of gender differences in mixed- or left-handers and non Caucasian populations (e.g., Asians, Hispanics, Blacks).

13.2.3 Age and Brain Maturation

Similarly, in order to establish the presence and nature of gender differences in subjects below or above the examined age range (e.g., pediatric or geriatric populations), additional analyses remain to be conducted. Moreover, although we analyzed brains of young adults with a relatively narrow age range so as to minimize the influences of age and possible interactions of age with gender on morphological measurements (Courchesne et al., 2000; De Bellis et al., 2001; Jernigan et al., 2001; Good et al., 2001b; Sowell et al., 2003), we can not determine whether the detected gender differences are due to different maturation rates in men and women or differences in maturational states at that particular age range sampled. Longitudinal studies (with one imaging session when subjects are in their mid-twenties) remain to be conducted to establish empirically the impact of age on our gender-specific findings.

Appendix

The Appendix provides details and references for the image analysis methods used in the studies presented throughout this thesis. Volume data sets of each subject passed through a number of preprocessing steps using several interactive or manual **(M)** as well as automated **(A)** procedures implemented in the LONI Pipeline Processing Environment[7] (Rex et al., 2003). For summary, illustration, and orientation regarding imaging preprocessing throughout this thesis please also refer to figure 14.

[7] The Pipeline Processing Environment was developed by the Laboratory of Neuro Imaging (LONI) at the University of California, Los Angeles (UCLA). It provides a visual programming interface that allows researchers to link many independently developed analysis programs into a processing "pipeline" (Rex et al., 2003).

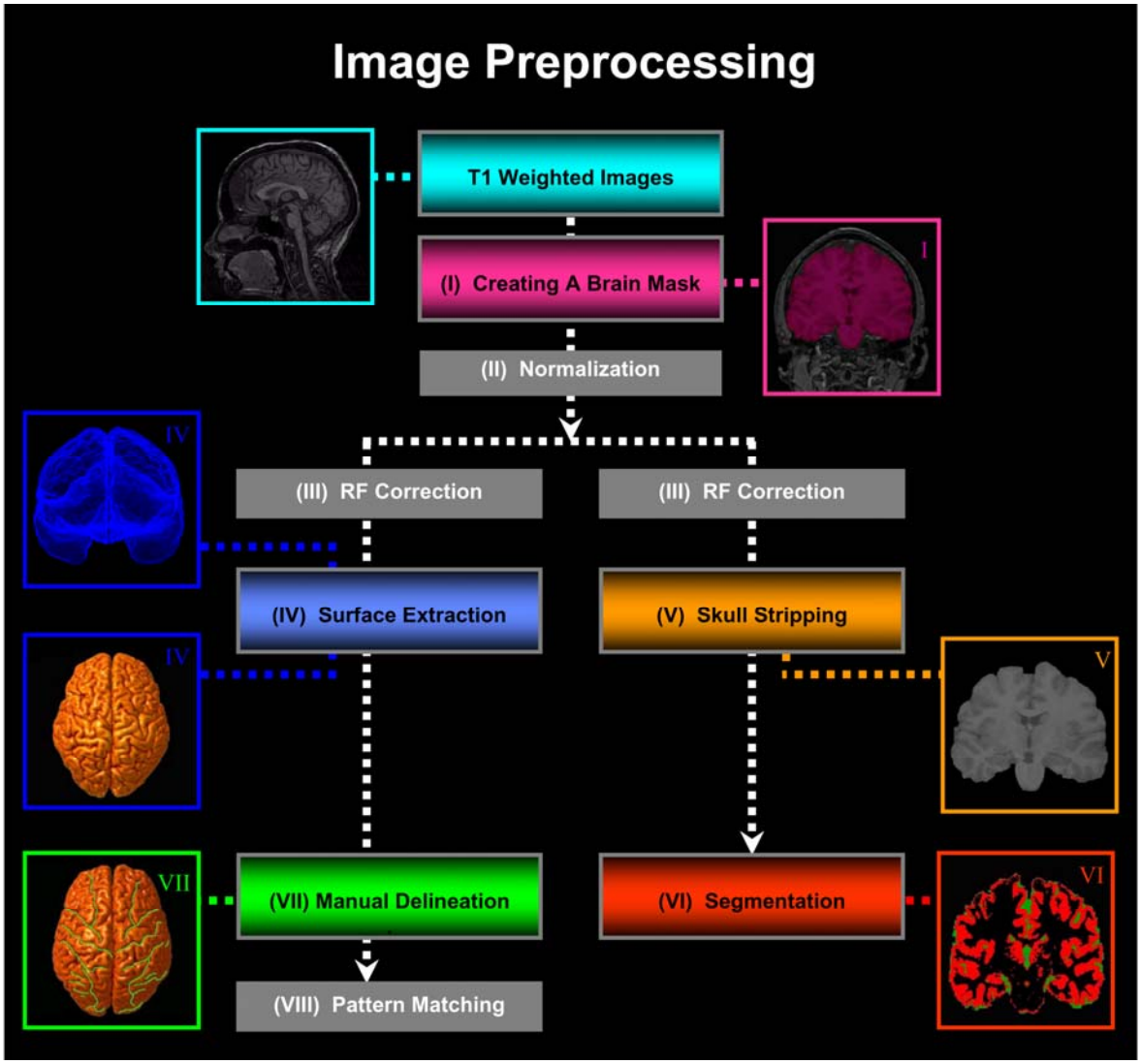

Figure 14. Summary of image preprocessing steps

Creating a Brain Mask (Module $I^{A,M}$): First, we automatically created an intracranial mask of the brain using a brain surface extraction algorithm tool (BSE) (Shattuck and Leahy, 2002). In each subject, we inspected the automatically generated brains masks (raw masks), slice by slice, and manually fixed any inaccuracies to isolate intracranial regions from surrounding extra-cranial tissue and extra-cortical CSF (modified masks), as

demonstrated in figure 15. These modified brain masks will guide the segmentation procedures (Module VI), since especially veins and meninges are hard to discriminate based on intensity criteria, and thus could spuriously contribute to the segmented grey matter compartment (Kruggel, 2000).

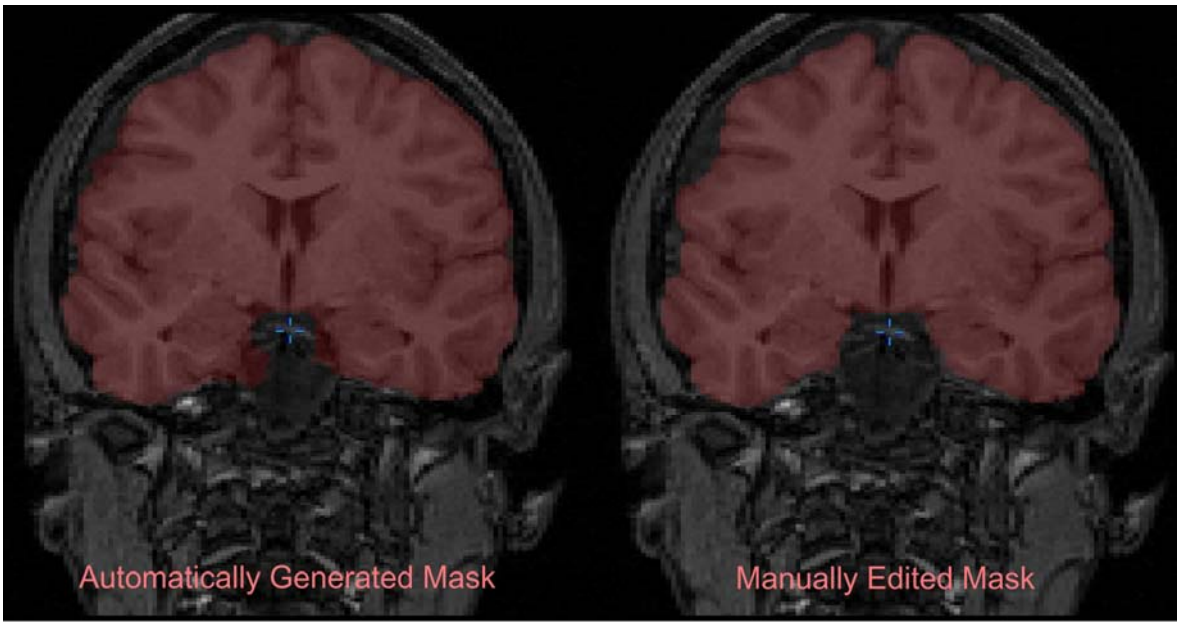

Figure 15. Raw and modified brain masks

In each subject, we inspected the automatically generated brains masks (left), followed by manually correcting any inaccuracies revealing modified masks (right).

Normalization (Module II^{A}): Brain masks and anatomical images were corrected for head position and individual differences in brain size by using an automatic 12-parameter linear registration which includes a translation, rotation, scaling, and shearing in x-, y-, and z-dimension (Woods et al., 1998). We transformed each brain volume into the ICBM-305 stereotaxic space by adapting them to the ICBM-152 template created by the ICBM, as described in section 3.2.2.1. (Mazziotta et al., 1995)

RF Correction (Module III^{A}): To eliminate intensity drifts due to magnetic field inhomogeneities in the anatomical brain images, we applied RF bias field corrections. As opposed to using the same RF approach prior to the surface extractions and in tissue classifications, previous analyses in our lab revealed more accurate results applying RF corrections based on different parameters. Of note, the RF correction used prior to the cortex extraction was developed by the same group of researchers who developed the tool for cortex extraction (Sled et al., 1998). Likewise, the RF correction used in the data processing stream resulting in classified tissues was developed by the same group of researchers who developed the tool for classifying tissue (Shattuck et al., 2001). This approach insures that the data is in the proper state for the best possible results.

3D Cortical Surface Extraction (Module IV^{A}):

We created 3D cortical surface models for each hemisphere based on automatically generated mesh surfaces that were continuously deformed to fit a threshold intensity value that best differentiates extra-cortical CSF from underlying cortical GM (MacDonald et al., 1994). The idea of this deformation process is to use a starting mesh (automatically provided based on a template in ICBM-305 space) which is deformed until its borders fit to a given intensity threshold of the respective individual images. In each subject, we inspected the automatically generated surface models. If the automated surface extraction revealed surfaces that were too "under-extracted" (smooth) or "over-extracted" (Figure 16), the discriminating intensity value was chosen interactively based on an automatically generated intensity histogram until the created surface models met the requirements.

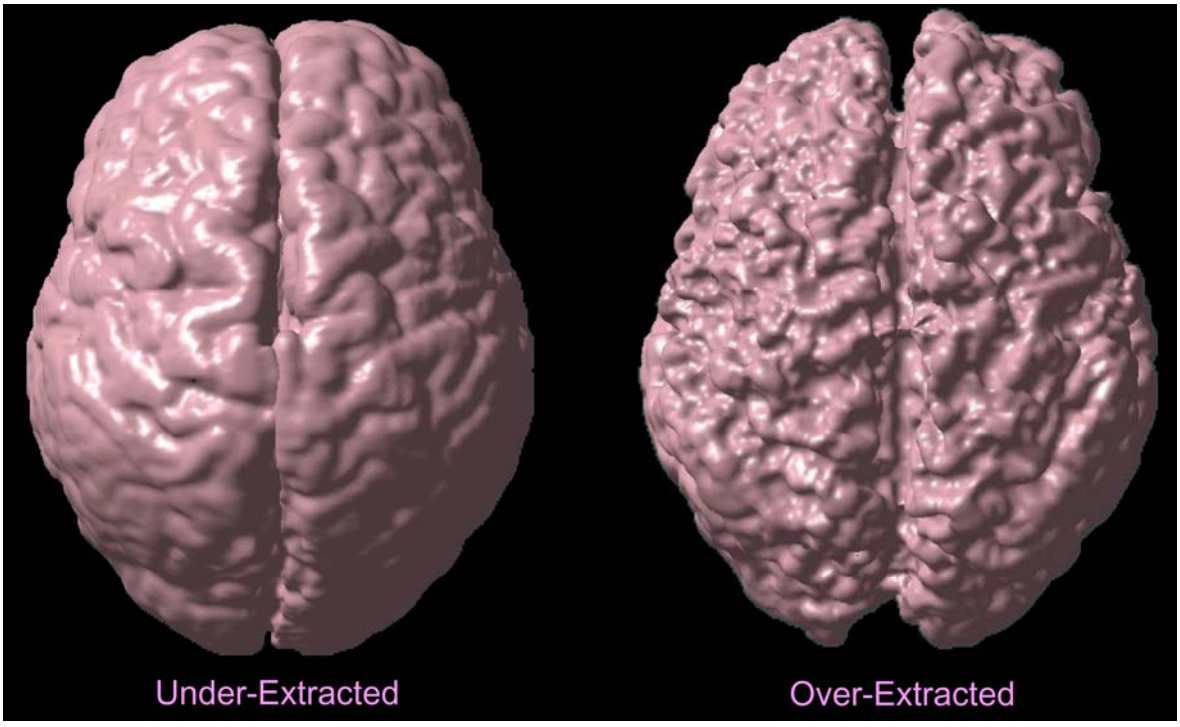

Figure 16. Examples of inadequate cortical surface models
In each subject, we inspected the automatically generated surface models, followed by repeating the surface extraction procedure interactively, if surfaces were "under-extracted" (left) or "over-extracted" (right).

Skull Stripping and Segmentation (Module V-VI^{A}): Using the manually modified brain masks, all extra-cerebral tissues (including extra-cranial CSF) were automatically removed from the image volumes. Each image volume was then segmented into different tissue types by classifying voxels based on signal intensities. More precisely, the measurement model takes into consideration both tissue class means and noise variance values computed from the global image, as well as the probability of each tissue type within the neighbourhood. Tissue class probabilities are estimated using a Gaussian mixture model, where mixed GM/WM and GM/CSF tissue classes (partial volume classes) are also modelled (Shattuck et al., 2001). The tissue classification result are then converted into a

three-class (CSF, GM, WM) labelling, where each voxel is assigned by setting its label to the pure tissue having the greatest fraction.

Delineation of Sulcal Anatomy (Module VII^{M}): The 3D cortical surface models from each individual (created in Module IV) were used to identify and manually outline 16 sulci in each lateral hemisphere as well as 12 sulci in each medial hemisphere, where the rater was blind to group status. In addition to contouring the major sulci, a set of six midline landmark curves bordering the longitudinal fissure were outlined in each hemisphere to establish hemispheric limits in order to facilitate the process of sulcal pattern matching by setting the boundaries of the hemispheres.

The outlined lateral sulci included the Sylvian fissure, central, pre- and post-central sulcus, inferior and superior temporal sulcus (main body and ascending branch), inferior and middle frontal sulcus, intra-parietal sulcus, transverse occipital sulcus, occipital-temporal sulcus, olfactory and collateral sulcus, as well as primary and secondary intermediate sulcus, which constitute the posterior borders of the supramarginal and angular gyrus, respectively. The set of medial sulci included the callosal sulcus and inferior callosal outline segment, superior and inferior rostral sulcus, para-central sulcus, anterior and posterior segments of the cingulate sulcus, outer segment of a double parallel cingulate sulcus (when present), parieto-occipital sulcus, anterior and posterior segments of the calcarine sulcus, as well as the sub-parietal sulcus.

Sulcal lines were drawn on the 3D cortical surface, but spatially registered gray-scale image volumes in coronal, axial, and sagittal planes were available simultaneously to

help disambiguate brain anatomy. As a rule of thumb, the shortest direct route between the origin and termination points was used to delineate each sulcus. Points of origin were defined as the point on the surface model where contrast was darkest. Origin and termination points for each sulcus are summarized in table 3. More detailed anatomic guidelines for tracing the patterns of cortical surface sulci are available online at http://www.loni.ucla.edu/~esowell/edevel/MedialLinesProtocol.htm and have been previously validated (Narr et al., 2001; Blanton et al., 2001; Sowell et al., 2002). Since it is not possible to compute intra-class correlations for 3D curves (as these are not simple scalar measures), inter-rater reliability of manual outlining was measured by mapping the 3D root mean square (r.m.s.) difference in millimeters between 100 equidistant points from each sulcal landmark in six test brains that were traced by the rater and compared to a standard arrived at by a consensus of raters. Intra-rater reliability was also computed by comparing the 3D r.m.s. distance between equidistant surface points from each sulcal landmark traced 6 times in one test brain by the same rater. 3D r.m.s. distance was < 2mm, and on average < 1mm, for all landmarks within the rater and relative to the standard.

Table 3. Anatomical boundaries for sulcal anatomy

	SULCUS	ORIGIN	TERMINATION
		Lateral Sulcal Lines	
1.	*Sylvian Fissure*	- Temporal and frontal lobe separation	- Inside the supramarginal gyrus
2.	*Central Sulcus*	- Near midline	- Superior to Sylvian fissure
3.	*Post-central Sulcus*	- Near midline	- Superior to Sylvian fissure

4.	*Pre-central Sulcus*	- Near midline	- At or near Sylvian fissure
5.	*Superior Temporal Sulcus - Main Body*	- Temporal pole furthest anterior high-contrast point	- Temporal-occipital notch, or the anterior occipital sulcus
6.	*Superior Temporal Sulcus - Ascending Branch*	- Superior temporal sulcus main body bifurcation	- Inside the angular gyrus
7.	*Inferior Temporal Sulcus*	- Temporal pole furthest anterior high-contrast point	- Temporal-occipital notch or insular gyrus
8.	*Intra-parietal Sulcus*	- Post-central sulcus	- Transverse-occipital sulcus
9.	*Primary Intermediate Sulcus*	- Apex of supramarginal gyrus at the intra-parietal or post-central sulcus	- End of the sulcus to contain the supramarginal gyrus
10.	*Secondary Intermediate Sulcus*	- Intra-parietal sulcus	- End of sulcus
11.	*Transverse Occipital Sulcus*	- Nearest midline on medial surface of hemisphere	- Branches that extend to insular type sulcus
12.	*Inferior Frontal Sulcus*	- Most posterior segment of the lateral orbital sulcus	- Pre-central sulcus
13.	*Middle Frontal Sulcus*	- Point closest to midline of the most inferior frontal marginal gyrus	- On or near the pre-central sulcus
14.	*Olfactory Sulcus*	- Most anterior extent of sulcus, near the frontal pole	- Curve of the sulcus away from midline
15.	*Occipital-Temporal Sulcus*	- Most anterior high-contrast point before the temporal pole	- In occipital pole; highest contrast point near midline
16.	*Collateral Sulcus*	- Level with the pons at its widest lateral extent	- On midline

Medial Sulcal Lines

1.	*Callosal Sulcus*	- Rostrum of the CC	- Splenium of the CC
2.	*Inferior Callosal Segment*	- Rostrum of the CC	- Splenium of the CC
3.	*Superior Rostral Sulcus*	- Inferior to Genu of the CC	- Close to boundary of the dorso-lateral surface
4.	*Inferior Rostral Sulcus*	- Inferior to Genu of the CC	- Close to the boundary of the dorso-lateral surface
5.	*Para-central Sulcus*	- Anterior portion of pre-central gyrus	- Ending point of the anterior segment of the cingulate sulcus
6.	*Cingulate Sulcus - Anterior Segment*	- Anterior to the genus of CC	- Intersecting at the inferior extent of the para-central sulcus
7.	*Cingulate Sulcus - Posterior Segment*	- Inferior to the para-central sulcus or posterior to the ending point of the anterior segment of the cingulate sulcus	- Near the dorso-lateral surface
8.	*Outer Segment of a Double Parallel Anterior Cingulate Sulcus*	- Anterior to the genu of the CC, the outer of two double anterior cingulate sulci	- Adjacent or near the para-central sulcus
9.	*Parieto-Occipital Sulcus*	- Close to the boundary of the dorso-lateral surface	- Superior to calcarine sulcus
10.	*Calcarine Sulcus - Anterior Segment*	- Parieto-occipital sulcus	- Inferior to the splenium

11. *Calcarine Sulcus - Posterior Segment*	- Near dorso-lateral surface in the occipital pole	- Parieto-occipital sulcus
12. *Sub-parietal Sulcus*	- Posterior segment of the cingulate sulcus	- At the Y intersection between the anterior / posterior segment of the calcarine sulcus and parieto-occipital sulcus

Cortical Pattern Matching (Module VIII^{A}): As a result of the linear transformation procedure (Module II), cortical surface models correspond globally in size, orientation, and parameter space coordinates. However, in order to compare the brain anatomy within and between subject groups, it is also essential to maximize the correspondence of anatomical regions across brains.

For this purpose, the cortical surface is inflated to a spherical shape. By inverting this inflation mapping, a spherical coordinate system can be projected back onto the 3D model,[8] or the 3D surface may be flattened to a 2D plane (Figure 17). An average set of flattened sulci is created for the study group after making sulcal outlines spatially uniform and matching homologous sulcal surface points between subjects (Thompson et al., 1996a). An elastic warp is then applied to each individual's flat map that drives individual landmarks onto this average set of curves (Thompson et al., 2003). That is, the sulcal landmarks are used as anchors to drive the surrounding cortical surface anatomy of each individual into correspondence. During the surface-warping procedures, the algorithm

[8] Each point on the cortical surface is color-coded in RGB color format with every color value accurately indexing the specific location on a map or sphere.

computes a 3D deformation field that records the amount of x-, y-, and z-coordinate shift (or deformation) associating the same cortical surface locations in each subject with reference to the average anatomical pattern of the entire study group (Thompson et al., 2000b; Thompson et al., 2001b).

Based on the deformation fields, cortical data (e.g., GM concentration or thickness values), are re-assigned to a particular point in 3D space (Figure 17). As a result, cortical GM and thickness represent measurements obtained from the same sulcal/gyral anatomy across data from all subjects. Averaging and comparing individual maps after re-assigning GM or thickness values to a particular spatial co-ordinate allows for the comparisons in corresponding regions across different brains. Consequently, cortical pattern matching methods can substantially improve the statistical power and ability to localize group-specific effects. If gyral pattern are not matched from one subject to another, cortical differences among subjects will be severely underestimated due to variations in gyral patterning (Thompson et al., 2003).

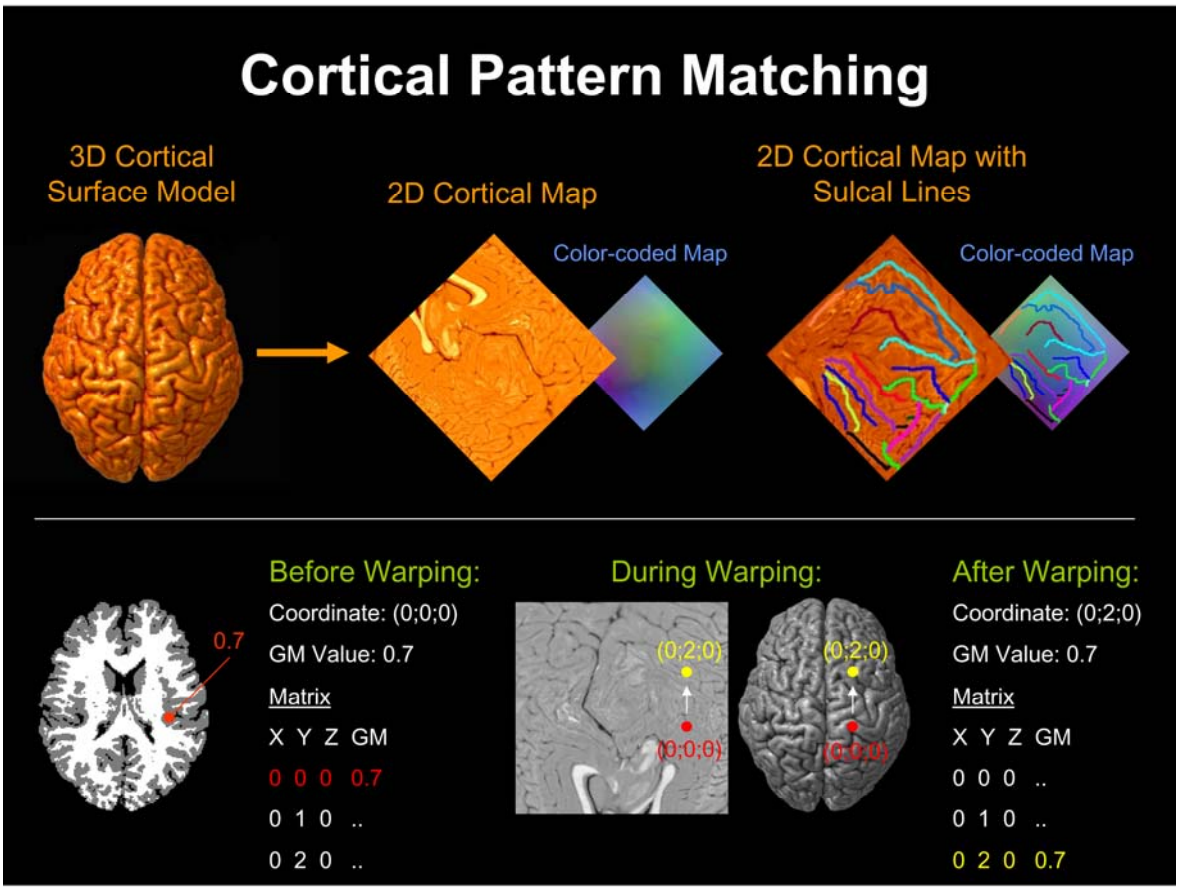

Figure 17. Cortical pattern matching
Initially the cortical surface is inflated to a spherical shape or a 2D plane. Together with the surfaces, sulcal lines are flattened (top), followed by creating an average set of flattened sulci. By using the sulcal landmarks as anchors, the surrounding cortical surface anatomy of each individual is driven into correspondence with this average set. During the surface-warping procedures, the algorithm computes a 3D deformation field that records the amount of x-, y-, and z-coordinate shift. Based on those deformation fields, cortical data (e.g., GM concentration), are re-assigned to a particular point in 3D space (bottom).

References

Aboitiz, F., Scheibel, A.B., Fisher, R.S., Zaidel, E. (1992). Fiber composition of the human corpus callosum. Brain Res. 598, 143-153.

Alivisatos, B., Petrides, M. (1997). Functional activation of the human brain during mental rotation. Neuropsychologia 35, 111-118.

Allen, L.S., Hines, M., Shryne, J.E., Gorski, R.A. (1989). Two sexually dimorphic cell groups in the human brain. J.Neurosci. 9, 497-506.

Allen, L.S., Gorski, R.A. (1991). Sexual dimorphism of the anterior commissure and massa intermedia of the human brain. J.Comp Neurol. 312, 97-104.

Allen, L.S., Richey, M.F., Chai, Y.M., Gorski, R.A. (1991). Sex differences in the corpus callosum of the living human being. J.Neurosci. 11, 933-942.

Allen, J.S., Damasio, H., Grabowski, T.J., Bruss, J., Zhang, W. (2003). Sexual dimorphism and asymmetries in the gray-white composition of the human cerebrum. Neuroimage. 18, 880-894.

Altman, J. (1969). Autoradiographic and histological studies of postnatal neurogenesis. IV. Cell proliferation and migration in the anterior forebrain, with special reference to persisting neurogenesis in the olfactory bulb. J.Comp Neurol. 137, 433-457.

Amunts, K., Jancke, L., Mohlberg, H., Steinmetz, H., Zilles, K. (2000). Interhemispheric asymmetry of the human motor cortex related to handedness and gender. Neuropsychologia 38, 304-312.

Anderson, S.A., Eisenstat, D.D., Shi, L., Rubenstein, J.L. (1997). Interneuron migration from basal forebrain to neocortex: dependence on Dlx genes. Science 278, 474-476.

Andreason, P.J., Zametkin, A.J., Guo, A.C., Baldwin, P., Cohen, R.M. (1994). Gender-related differences in regional cerebral glucose metabolism in normal volunteers. Psychiatry Res. 51, 175-183.

Ankney, C.D. (1992). The brain size/IQ debate. Nature 360, 292.

Armstrong, E., Schleicher, A., Omran, H., Curtis, M., Zilles, K. (1995). The ontogeny of human gyrification. Cereb.Cortex 5, 56-63.

Arnold, A.P., Gorski, R.A. (1984). Gonadal steroid induction of structural sex differences in the central nervous system. Annu.Rev.Neurosci. 7, 413-442.

Ashburner, J., Friston, K.J. (2000). Voxel-based morphometry - The methods. Neuroimage 11, 805-821.

Ashburner, J., Csernansky, J.G., Davatzikos, C., Fox, N.C., Frisoni, G.B., Thompson, P.M. (2003). Computer-assisted imaging to assess brain structure in healthy and diseased brains. Lancet Neurol. 2, 79-88.

Azari, N.P., Pettigrew, K.D., Pietrini, P., Murphy, D.G., Horwitz, B., Schapiro, M.B. (1995). Sex differences in patterns of hemispheric cerebral metabolism: a multiple regression/discriminant analysis of positron emission tomographic data. Int.J.Neurosci. 81, 1-20.

Barton, R.A. (1996). Neocortex size and behavioural ecology in primates. Proc.R.Soc.Lond B Biol.Sci. 263, 173-177.

Bear, D., Schiff, D., Saver, J., Greenberg, M., Freeman, R. (1986). Quantitative analysis of cerebral asymmetries. Fronto-occipital correlation, sexual dimorphism and association with handedness. Arch.Neurol. 43, 598-603.

Benjamini,Y., Hochberg, Y. (1995). Controlling the False Discovery Rate: a Practical and Powerful Approach to Multiple Testing. Journal of the Royal Statistical Society 57, 289-300.

Bishop, K.M., Wahlsten, D. (1997). Sex differences in the human corpus callosum: myth or reality? Neurosci.Biobehav.Rev. 21, 581-601.

Blanton, R.E., Levitt, J.G., Thompson, P.M., Narr, K.L., Capetillo-Cunliffe, L., Nobel, A., Singerman, J.D., McCracken, J.T., Toga, A.W. (2001). Mapping cortical asymmetry and complexity patterns in normal children. Psychiatry Res. 107, 29-43.

Blatter, D.D., Bigler, E.D., Gale, S.D., Johnson, S.C., Anderson, C.V., Burnett, B.M., Parker, N., Kurth, S., Horn, S.D. (1995). Quantitative volumetric analysis of brain MR: normative database spanning 5 decades of life. AJNR Am.J.Neuroradiol. 16, 241-251.

Breedlove, S.M. (1994). Sexual differentiation of the human nervous system. Annu.Rev.Psychol. 45, 389-418.

Castellano Smith, A.D. (1999). The Folding of the Human Brain: From Shape to Function. PhD Thesis. University of London. London.

Caviness, V.S., Jr. (1975). Mechanical model of brain convolutional development. Science 189, 18-21.

Chance, S.A., Tzotzoli, P.M., Vitelli, A., Esiri, M.M., Crow, T.J. (2004). The cytoarchitecture of sulcal folding in Heschl's sulcus and the temporal cortex in the normal brain and schizophrenia: lamina thickness and cell density. Neurosci.Lett. 367, 384-388.

Chi, J.G., Dooling, E.C., Gilles, F.H. (1977). Gyral development of the human brain. Ann.Neurol. 1, 86-93.

Chung, M.K., Robbins, S.M., Dalton, K.M., Davidson, R.J., Alexander, A.L., Evans, A.C. (2005). Cortical thickness analysis in autism with heat kernel smoothing. Neuroimage. 25, 1256-1265.

Clarke, S., Kraftsik, R., Van der, L.H., Innocenti, G.M. (1989). Forms and measures of adult and developing human corpus callosum: is there sexual dimorphism? J.Comp Neurol. 280, 213-230.

Clarke, J.M., Zaidel, E. (1994). Anatomical-behavioral relationships: corpus callosum morphometry and hemispheric specialization. Behav.Brain Res. 64, 185-202.

Cohen, J. (1988). Statistical power analysis for the behavioral sciences. New York: Academic Press.

Courchesne, E., Chisum, H.J., Townsend, J., Cowles, A., Covington, J., Egaas, B., Harwood, M., Hinds, S., Press, G.A. (2000). Normal brain development and aging: quantitative analysis at in vivo MR imaging in healthy volunteers. Radiology 216, 672-682.

Cowell, P.E., Allen, L.S., Kertesz, A., Zalatimo, N.S., Denenberg, V.H. (1994a). Human corpus callosum: a stable mathematical model of regional neuroanatomy. Brain Cogn 25, 52-66.

Cowell, P.E., Turetsky, B.I., Gur, R.C., Grossman, R.I., Shtasel, D.L., Gur, R.E. (1994b). Sex differences in aging of the human frontal and temporal lobes. J.Neurosci. 14, 4748-4755.

Davatzikos, C., Resnick, S.M. (1998). Sex differences in anatomic measures of interhemispheric connectivity: correlations with cognition in women but not men. Cereb.Cortex 8, 635-640.

Davis, E.C., Popper, P., Gorski, R.A. (1996). The role of apoptosis in sexual differentiation of the rat sexually dimorphic nucleus of the preoptic area. Brain Res. 734, 10-18.

De Bellis, M.D., Keshavan, M.S., Beers, S.R., Hall, J., Frustaci, K., Masalehdan, A., Noll, J., Boring, A.M. (2001). Sex differences in brain maturation during childhood and adolescence. Cerebral Cortex 11, 552-557.

de Court (1999). The human cerebral cortex: gender differences in structure and function. J.Neuropathol.Exp.Neurol. 58, 217-226.

de Lacoste, M.C., Holloway, R.L., Woodward, D.J. (1986). Sex differences in the fetal human corpus callosum. Hum.Neurobiol. 5, 93-96.

Deary, I.J. (1998). Differences in mental abilities. BMJ 317, 1701-1703.

DeFelipe, J., onso-Nanclares, L., Arellano, J.I. (2002). Microstructure of the neocortex: comparative aspects. J.Neurocytol. 31, 299-316.

Dekaban, A.S. (1978). Changes in brain weights during the span of human life: relation of brain weights to body heights and body weights. Ann.Neurol. 4, 345-356.

DeLacoste-Utamsing, C., Holloway, R.L. (1982). Sexual dimorphism in the human corpus callosum. Science 216, 1431-1432.

Denenberg, V.H., Berrebi, A.S., Fitch, R.H. (1989). A factor analysis of the rat's corpus callosum. Brain Res. 497, 271-279.

Denenberg, V.H., Kertesz, A., Cowell, P.E. (1991). A factor analysis of the human's corpus callosum. Brain Res. 548, 126-132.

Diamond, M.C. (1987). Sex differences in the rat forebrain. Brain Res. 434, 235-240.

Diamond, M.C. (1988). Enriching heredity. NewYork: The Free Press.

Diamond, M.C. (1991). Hormonal effects on the development or cerebral lateralization. Psychoneuroendocrinology 16, 121-129.

Diamond, M.C. (2001). Response of the brain to enrichment. An.Acad.Bras.Cienc. 73, 211-220.

do Carmo, M.P. (1976). Differential Geometry of Curves and Surfaces. New Jersey: Prentice-Hall, Inc.

Draganski, B., Gaser, C., Busch, V., Schuierer, G., Bogdahn, U., May, A. (2004). Neuroplasticity: changes in grey matter induced by training. Nature 427, 311-312.

Duvernoy, H.M. (1999). The human brain: Surface, three-dimensional sectional anatomy with MRI, and blood supply. New York: Springer-Wien.

Eickhoff, S., Walters, N.B., Schleicher, A., Kril, J., Egan, G.F., Zilles, K., Watson, J.D., Amunts, K. (2004). High-resolution MRI reflects myeloarchitecture and cytoarchitecture of human cerebral cortex. Hum.Brain Mapp. 24, 206-215.

Elias, H., Schwartz, D. (1971). Cerebro-cortical surface areas, volumes, lengths of gyri and their interdependence in mammals, including man. Z. f. Saugetierkunde 36, 147–163.

Eriksson, P.S., Perfilieva, E., Bjork-Eriksson, T., Alborn, A.M., Nordborg, C., Peterson, D.A., Gage, F.H. (1998). Neurogenesis in the adult human hippocampus. Nat.Med. 4, 1313-1317.

Eriksson, P.S. (2003). Neurogenesis and its implications for regeneration in the adult brain. J.Rehabil.Med. 17-19.

Esposito, G., Van Horn, J.D., Weinberger, D.R., Berman, K.F. (1996). Gender differences in cerebral blood flow as a function of cognitive state with PET. J.Nucl.Med. 37, 559-564.

Fernandez, G., Weis, S., Stoffel-Wagner, B., Tendolkar, I., Reuber, M., Beyenburg, S., Klaver, P., Fell, J., de, G.A., Ruhlmann, J., Reul, J., Elger, C.E. (2003). Menstrual cycle-dependent neural plasticity in the adult human brain is hormone, task, and region specific. J.Neurosci. 23, 3790-3795.

Fernandez-Guasti, A., Kruijver, F.P., Fodor, M., Swaab, D.F. (2000). Sex differences in the distribution of androgen receptors in the human hypothalamus. J.Comp Neurol. 425, 422-435.

Filipek, P.A., Richelme, C., Kennedy, D.N., Caviness, V.S., Jr. (1994). The young adult human brain: an MRI-based morphometric analysis. Cereb.Cortex 4, 344-360.

Fischl, B., Dale, A.M. (2000). Measuring the thickness of the human cerebral cortex from magnetic resonance images. Proc.Natl.Acad.Sci.U.S.A 97, 11050-11055.

Forget, H., Cohen, H. (1994). Life after birth: the influence of steroid hormones on cerebral structure and function is not fixed prenatally. Brain Cogn 26, 243-248.

Foundas, A.L., Faulhaber, J.R., Kulynych, J.J., Browning, C.A., Weinberger, D.R. (1999). Hemispheric and sex-linked differences in Sylvian fissure morphology: a quantitative approach using volumetric magnetic resonance imaging. Neuropsychiatry Neuropsychol.Behav.Neurol. 12, 1-10.

Frahm, H.D., Stephan, H., Stephan, M. (1982). Comparison of brain structure volumes in Insectivora and Primates. I. Neocortex. J.Hirnforsch. 23, 375-389.

Frederikse, M.E., Lu, A., Aylward, E., Barta, P., Pearlson, G. (1999). Sex differences in the inferior parietal lobule. Cereb.Cortex 9, 896-901.

Ganeshwaran, H., Mochida, G.H., Walsh, C.A. (2004). Genetic Basis of Developmental Malformations of the Cerebral Cortex. Arch Neurol 61, 637-640.

Gaser, C., Schlaug, G. (2003). Brain structures differ between musicians and non-musicians. J Neurosci. 23, 9240-9245.

Geschwind, N., Galaburda, A.M. (1985). Cerebral lateralization. Biological mechanisms, associations, and pathology: II. A hypothesis and a program for research. Arch.Neurol. 42, 521-552.

Geyer, S., Schleicher, A., Schormann, T., Mohlberg, H., Bodegard, A., Roland, P.E., Zilles, K. (2001). Integration of microstructural and functional aspects of human somatosensory areas 3a, 3b, and 1 on the basis of a computerized brain atlas. Anat.Embryol.(Berl) 204, 351-366.

Giedd, J.N., Snell, J.W., Lange, N., Rajapakse, J.C., Casey, B.J., Kozuch, P.L., Vaituzis, A.C., Vauss, Y.C., Hamburger, S.D., Kaysen, D., Rapoport, J.L. (1996). Quantitative magnetic resonance imaging of human brain development: ages 4-18. Cereb.Cortex 6, 551-560.

Gittins, R., Harrison, P.J. (2004). A quantitative morphometric study of the human anterior cingulate cortex. Brain Res. 1013, 212-222.

Goldman-Rakic, P.S. (1981). Prenatal formation of cortical input and development of cytoarchitectonic compartments in the neostriatum of the rhesus monkey. J.Neurosci. 1, 721-735.

Goldstein, J.M., Seidman, L.J., Horton, N.J., Makris, N., Kennedy, D.N., Caviness, V.S., Jr., Faraone, S.V., Tsuang, M.T. (2001). Normal Sexual Dimorphism of the Adult Human Brain Assessed by In Vivo Magnetic Resonance Imaging. Cereb.Cortex 11, 490-497.

Good, C.D., Johnsrude, I., Ashburner, J., Henson, R.N., Friston, K.J., Frackowiak, R.S. (2001a). Cerebral asymmetry and the effects of sex and handedness on brain structure: a voxel-based morphometric analysis of 465 normal adult human brains. Neuroimage. 14, 685-700.

Good, C.D., Johnsrude, I.S., Ashburner, J., Henson, R.N.A., Friston, K.J., Frackowiak, R.S.J. (2001b). A voxel-based morphometric study of ageing in 465 normal adult human brains. Neuroimage 14, 21-36.

Gould, E., Reeves, A.J., Graziano, M.S., Gross, C.G. (1999). Neurogenesis in the neocortex of adult primates. Science 286, 548-552.

Gross, C.G. (2000). Neurogenesis in the adult brain: death of a dogma. Nat.Rev.Neurosci. 1, 67-73.

Gur, R.C., Mozley, L.H., Mozley, P.D., Resnick, S.M., Karp, J.S., Alavi, A., Arnold, S.E., Gur, R.E. (1995). Sex differences in regional cerebral glucose metabolism during a resting state. Science 267, 528-531.

Gur, R.C., Turetsky, B.I., Matsui, M., Yan, M., Bilker, W., Hughett, P., Gur, R.E. (1999). Sex differences in brain gray and white matter in healthy young adults: correlations with cognitive performance. J.Neurosci. 19, 4065-4072.

Gur, R.C., Alsop, D., Glahn, D., Petty, R., Swanson, C.L., Maldjian, J.A., Turetsky, B.I., Detre, J.A., Gee, J., Gur, R.E. (2000). An fMRI study of sex differences in regional activation to a verbal and a spatial task. Brain Lang 74, 157-170.

Gur, R.C., Gunning-Dixon, F., Bilker, W.B., Gur, R.E. (2002a). Sex differences in temporo-limbic and frontal brain volumes of healthy adults. Cereb.Cortex 12, 998-1003.

Gur, R.C., Gunning-Dixon, F.M., Turetsky, B.I., Bilker, W.B., Gur, R.E. (2002b). Brain region and sex differences in age association with brain volume: a quantitative MRI study of healthy young adults. Am.J.Geriatr.Psychiatry 10, 72-80.

Haier, R.J., Jung, R.E., Yeo, R.A., Head, K., Alkire, M.T. (2004). Structural brain variation and general intelligence. Neuroimage. 23, 425-433.

Halpern, D.F. (1992). Sex differences in cognitive abilities (2nd ed.). New York: Erlbaum.

Harasty, J., Double, K.L., Halliday, G.M., Kril, J.J., McRitchie, D.A. (1997). Language-associated cortical regions are proportionally larger in the female brain. Arch.Neurol. 54, 171-176.

Hastings, N.B., Tanapat, P., Gould, E. (2000). Comparative Views of Adult Neurogenesis. The Neuroscientist 6, 315-325.

Haug, H. (1987). Brain sizes, surfaces, and neuronal sizes of the cortex cerebri: a stereological investigation of man and his variability and a comparison with some

mammals (primates, whales, marsupials, insectivores, and one elephant). Am.J.Anat. 180, 126-142.

Hausmann, M., Gunturkun, O. (2000). Steroid fluctuations modify functional cerebral asymmetries: the hypothesis of progesterone-mediated interhemispheric decoupling. Neuropsychologia 38, 1362-1374.

Highley, J.R., Esiri, M.M., McDonald, B., Roberts, H.C., Walker, M.A., Crow, T.J. (1999). The size and fiber composition of the anterior commissure with respect to gender and schizophrenia. Biol.Psychiatry 45, 1120-1127.

Hiscock, M., Inch, R., Jacek, C., Hiscock-Kalil, C., Kalil, K.M. (1994). Is there a sex difference in human laterality? I. An exhaustive survey of auditory laterality studies from six neuropsychology journals. J.Clin.Exp.Neuropsychol. 16, 423-435.

Hiscock, M., Israelian, M., Inch, R., Jacek, C., Hiscock-Kalil, C. (1995). Is there a sex difference in human laterality? II. An exhaustive survey of visual laterality studies from six neuropsychology journals. J.Clin.Exp.Neuropsychol. 17, 590-610.

Hiscock, M., Inch, R., Hawryluk, J., Lyon, P.J., Perachio, N. (1999). Is there a sex difference in human laterality? III. An exhaustive survey of tactile laterality studies from six neuropsychology journals. J.Clin.Exp.Neuropsychol. 21, 17-28.

Hiscock, M., Perachio, N., Inch, R. (2001). Is there a sex difference in human laterality? IV. An exhaustive survey of dual-task interference studies from six neuropsychology journals. J.Clin.Exp.Neuropsychol. 23, 137-148.

Hofman, M.A. (1989). On the evolution and geometry of the brain in mammals. Prog.Neurobiol. 32, 137-158.

Holloway, R.L., de Lacoste, M.C. (1986). Sexual dimorphism in the human corpus callosum: an extension and replication study. Hum.Neurobiol. 5, 87-91.

Hopkins, W.D., Pilcher, D.L., MacGregor, L. (2000). Sylvian fissure asymmetries in nonhuman primates revisited: a comparative mri study. Brain Behav.Evol. 56, 293-299.

Hopkins, W.D., Rilling, J.K. (2000). A comparative MRI study of the relationship between neuroanatomical asymmetry and interhemispheric connectivity in primates: implication for the evolution of functional asymmetries. Behav.Neurosci. 114, 739-748.

Hubel, D. H., Wiesel, T. N. (1962). Receptive fields, binocular architecture and functional architecture in the cat's visual cortex. J. Physiol. 160, 106-154.

Ide, A., Rodriguez, E., Zaidel, E., Aboitiz, F. (1996). Bifurcation patterns in the human sylvian fissure: hemispheric and sex differences. Cereb.Cortex 6, 717-725.

Jacobs, B., Schall, M., Scheibel, A.B. (1993). A quantitative dendritic analysis of Wernicke's area in humans. II. Gender, hemispheric, and environmental factors. J.Comp Neurol. 327, 97-111.

Jancke, L., Schlaug, G., Huang, Y., Steinmetz, H. (1994). Asymmetry of the planum parietale. Neuroreport 5, 1161-1163.

Jancke, L., Staiger, J.F., Schlaug, G., Huang, Y., Steinmetz, H. (1997). The relationship between corpus callosum size and forebrain volume. Cereb.Cortex 7, 48-56.

Jancke, L., Preis, S., Steinmetz, H. (1999). The relation between forebrain volume and midsagittal size of the corpus callosum in children. Neuroreport 10, 2981-2985.

Jancke, L. (2003). Current methods for cognitive neuroanatomy. In: Hugdahl, K. [Ed.], Experimental methods in neuropsychology. Boston: Kluwer Academic Press, 197-222.

Jerison, H. J. (1982). Allometry, brain size, cortical surface, and convolutedness. In: Armstrong, E., Falk, D [Eds] Primate Brain Evolution. New York: Plenum Press, 77–84.

Jernigan, T.L., Archibald, S.L., Fennema-Notestine, C., Gamst, A.C., Stout, J.C., Bonner, J., Hesselink, J.R. (2001). Effects of age on tissues and regions of the cerebrum and cerebellum. Neurobiology of Aging 22, 581-594.

Johnson, S.C., Farnworth, T., Pinkston, J.B., Bigler, E.D., Blatter, D.D. (1994). Corpus callosum surface area across the human adult life span: effect of age and gender. Brain Res.Bull. 35, 373-377.

Jones, E.G. (2000). Microcolumns in the cerebral cortex. Proc.Natl.Acad.Sci.U.S.A 97, 5019-5021.

Jones, S.E., Buchbinder, B.R., Aharon, I. (2000). Three-dimensional mapping of cortical thickness using Laplace's equation. Hum.Brain Mapp. 11, 12-32.

Jordan, K., Wustenberg, T., Heinze, H.J., Peters, M., Jancke, L. (2002). Women and men exhibit different cortical activation patterns during mental rotation tasks. Neuropsychologia 40, 2397-2408.

Juraska, J.M., Fitch, J.M., Henderson, C., Rivers, N. (1985). Sex differences in the dendritic branching of dentate granule cells following differential experience. Brain Res. 333, 73-80.

Kabani, N., Le, G.G., MacDonald, D., Evans, A.C. (2001). Measurement of cortical thickness using an automated 3-D algorithm: a validation study. Neuroimage. 13, 375-380.

Kansaku, K., Yamaura, A., Kitazawa, S. (2000). Sex differences in lateralization revealed in the posterior language areas. Cereb.Cortex 10, 866-872.

Kaplan, M.S. (2001). Environment complexity stimulates visual cortex neurogenesis: death of a dogma and a research career. Trends Neurosci. 24, 617-20.

Keating, E.G., Gooley, S.G. (1988). Disconnection of parietal and occipital access to the saccadic oculomotor system. Exp.Brain Res. 70, 385-398.

Kempermann, G., Gast, D., Gage, F.H. (2002). Neuroplasticity in old age: sustained fivefold induction of hippocampal neurogenesis by long-term environmental enrichment. Ann.Neurol. 52, 135-143.

Kertesz, A., Polk, M., Howell, J., Black, S.E. (1987). Cerebral dominance, sex, and callosal size in MRI. Neurology 37, 1385-1388.

Kimura, D. (1999). Sex and Cognition. Cambridge, Mass: MIT Press.

Kochunov, P., Fox, P., Lancaster, J., Tan, L.H., Amunts, K., Zilles, K., Mazziotta, J., Gao, J.H. (2003). Localized morphological brain differences between English-speaking Caucasians and Chinese-speaking Asians: new evidence of anatomical plasticity. Neuroreport 14, 961-964.

Konradi, C., Kornhuber, J., Sofic, E., Heckers, S., Riederer, P., Beckmann, H. (1992). Variations of monoamines and their metabolites in the human brain putamen. Brain Res. 579, 285-290.

Kruggel, F., von Cramon, D.Y. (2000). Measuring the cortical thickness. In: Workshop on Mathematical Methods in Biomedical Image Analysis. Los Alamitos: IEEE Computer Society Press, 154–161.

Kruggel, F., Bruckner, M.K., Arendt, T., Wiggins, C.J., von Cramon, D.Y. (2003). Analyzing the neocortical fine-structure. Med.Image Anal. 7, 251-264.

Kulynych, J.J., Vladar, K., Jones, D.W., Weinberger, D.R. (1994). Gender differences in the normal lateralization of the supratemporal cortex: MRI surface-rendering morphometry of Heschl's gyrus and the planum temporale. Cereb.Cortex 4, 107-118.

Kuperberg, G.R., Broome, M.R., McGuire, P.K., David, A.S., Eddy, M., Ozawa, F., Goff, D., West, W.C., Williams, S.C., van der Kouwe, A.J., Salat, D.H., Dale, A.M., Fischl, B. (2003). Regionally localized thinning of the cerebral cortex in schizophrenia. Arch.Gen.Psychiatry 60, 878-888.

Landing, B.H., Shankle, W.R., Hara, J., Brannock, J., Fallon, J.H. (2002). The development of structure and function in the postnatal human cerebral cortex from birth to 72 months: changes in thickness of layers II and III co-relate to the onset of new age-specific behaviors. Pediatr.Pathol.Mol.Med. 21, 321-342.

Lerch, J.P., Evans, A.C. (2005). Cortical thickness analysis examined through power analysis and a population simulation. Neuroimage. 24, 163-173.

Lohmann, G., Preul, C., Hund-Georgiadis, M. (2003). Morphology-based cortical thickness estimation. Inf.Process Med.Imaging 18, 89-100.

Luders, E., Steinmetz, H., Jancke, L. (2002). Brain size and grey matter volume in the healthy human brain. Neuroreport 13, 2371-2374.

Luders, E., Rex, D.E., Narr, K.L., Woods, R.P., Jancke, L., Thompson, P.M., Mazziotta, J.C., Toga, A.W. (2003). Relationships between sulcal asymmetries and corpus callosum size: gender and handedness effects. Cereb.Cortex 13, 1084-1093.

Luders, E., Gaser, C., Jancke, L., Schlaug, G. (2004). A voxel-based approach to gray matter asymmetries. Neuroimage. 22, 656-664.

Luders, E., Narr, K.L., Zaidel, E., Thompson, P.M., Jancke, L., Toga, A.W. (2005). Parasagittal Asymmetries of the Corpus Callosum. Cereb.Cortex .

MacDonald, D., Avis, D., Evans, A. (1994). Multiple surface identification and matching in magnetic resonance imaging. Proc SPIE 2359, 160-169.

MacDonald, D. (1997). A Method for Identifying Geometrically Simple Surfaces from Three Dimensional Images. PhD Thesis, McGill University, Montreal.

Mackintosh, N.J. (1996). Sex differences and IQ. Journal of Biosocial Science 28, 559-571.

Mackowiak, M., Chocyk, A., Markowicz-Kula, K., Wedzony, K. (2004). Neurogenesis in the adult. Pol.J.Pharmacol. 56, 673-687.

Magnotta, V.A., Andreasen, N.C., Schultz, S.K., Harris, G., Cizadlo, T., Heckel, D., Nopoulos, P., Flaum, M. (1999). Quantitative in vivo measurement of gyrification in the human brain: changes associated with aging. Cereb.Cortex 9, 151-160.

Maguire, E.A., Gadian, D.G., Johnsrude, I.S., Good, C.D., Ashburner, J., Frackowiak, R.S., Frith, C.D. (2000). Navigation-related structural change in the hippocampi of taxi drivers. Proc.Natl.Acad.Sci.U.S.A 97, 4398-4403.

Mansfield, P., P. G. Morris. (1982). NMR Imaging in Biomedicine. Advances in Magnetic Resonance. New York: Academic Press.

Marino, L. (2004). Cetacean Brain Evolution: Multiplication Generates Complexity. International Journal of Comparative Psychology 17, 1-16.

Marin-Padilla, M. (1990). Origin, formation, and prenatal maturation of the human cerebral cortex: an overview. J.Craniofac.Genet.Dev.Biol. 10, 137-146.

Masters, M.S., Sanders, B. (1993). Is the gender difference in mental rotation disappearing? Behav.Genet. 23, 337-341.

Mazziotta, J.C., Toga, A.W., Evans, A., Fox, P., Lancaster, J. (1995). A probabilistic atlas of the human brain: theory and rationale for its development. The International Consortium for Brain Mapping (ICBM). Neuroimage. 2, 89-101.

Medland, S.E., Geffen, G., McFarland, K. (2002). Lateralization of speech production using verbal/manual dual tasks: meta-analysis of sex differences and practice effects. Neuropsychologia 40, 1233-1239.

Memoli, F., Sapiro, G., Thompson, P. (2004). Implicit brain imaging. Neuroimage. 23 Suppl 1, S179-S188.

Miller, M.I., Massie, A.B., Ratnanather, J.T., Botteron, K.N., Csernansky, J.G. (2000). Bayesian construction of geometrically based cortical thickness metrics. Neuroimage. 12, 676-687.

Mountcastle, V.B. (1957). Modality and topographic properties of single neurons of cat's somatic sensory cortex. J.Neurophysiol. 20, 408-434.

Murphy, D.G., DeCarli, C., McIntosh, A.R., Daly, E., Mentis, M.J., Pietrini, P., Szczepanik, J., Schapiro, M.B., Grady, C.L., Horwitz, B., Rapoport, S.I. (1996). Sex differences in human brain morphometry and metabolism: an in vivo quantitative magnetic resonance imaging and positron emission tomography study on the effect of aging. Arch.Gen.Psychiatry 53, 585-594.

Narr, K., Thompson, P., Sharma, T., Moussai, J., Zoumalan, C., Rayman, J., Toga, A. (2001). Three-dimensional mapping of gyral shape and cortical surface asymmetries in schizophrenia: gender effects. Am.J.Psychiatry 158, 244-255.

Narr, K.L., Bilder, R.M., Toga, A.W., Woods, R.P., Rex, D.E., Szeszko, P.R., Robinson, D., Sevy, S., Gunduz-Bruce, H., Wang, Y.P., DeLuca, H., Thompson, P.M. (2005). Mapping cortical thickness and gray matter concentration in first episode schizophrenia. Cereb.Cortex 15, 708-719.

Nopoulos, P., Flaum, M., O'Leary, D., Andreasen, N.C. (2000). Sexual dimorphism in the human brain: evaluation of tissue volume, tissue composition and surface anatomy using magnetic resonance imaging. Psychiatry Res. 98, 1-13.

Oka, S., Miyamoto, O., Janjua, N.A., Honjo-Fujiwara, N., Ohkawa, M., Nagao, S., Kondo, H., Minami, T., Toyoshima, T., Itano, T. (1999). Re-evaluation of sexual dimorphism in human corpus callosum. Neuroreport 10, 937-940.

Ono, M., Kubik, S., Abernathey, C.D. (1991). Atlas of the cerebral sulci. Stuttgart: Georg Thieme Verlag.

Pakkenberg, B., Gundersen, H.J. (1997). Neocortical neuron number in humans: effect of sex and age. J.Comp Neurol. 384, 312-320.

Passe, T.J., Rajagopalan, P., Tupler, L.A., Byrum, C.E., MacFall, J.R., Krishnan, K.R. (1997). Age and sex effects on brain morphology. Prog.Neuropsychopharmacol.Biol.Psychiatry 21, 1231-1237.

Paus, T., Otaky, N., Caramanos, Z., MacDonald, D., Zijdenbos, A., D'Avirro, D., Gutmans, D., Holmes, C., Tomaiuolo, F., Evans, A.C. (1996). In vivo morphometry of the intrasulcal gray matter in the human cingulate, paracingulate, and superior-rostral sulci: hemispheric asymmetries, gender differences and probability maps. J.Comp Neurol. 376, 664-673.

Peters, M. (1991). Sex differences in human brain size and the general meaning of differences in brain size. Can.J.Psychol. 45, 507-522.

Peters, M., Oeltze, S., Seminowicz, D., Steinmetz, H., Koeneke, S., Jancke, L. (2002). Division of the corpus callosum into subregions. Brain Cogn 50, 62-72.

Petersen, S.E., Robinson, D.L., Currie, J.N. (1989). Influences of lesions of parietal cortex on visual spatial attention in humans. Exp.Brain Res. 76, 267-280.

Pinel, J. P. J. (2002). Biopsychology. Boston: Allyn and Bacon

Pitcher, J.B., Ogston, K.M., Miles, T.S. (2003). Age and sex differences in human motor cortex input-output characteristics. J.Physiol 546, 605-613.

Pravitha, R., Sreenivasan, R., Nampoori, V.P. (2005). Complexity analysis of dense array EEG signal reveals sex difference. Int.J.Neurosci. 115, 445-460.

Rabinowicz, T., de Court, Petetot, J.M., Xi, G., de los, R.E. (1996). Human cortex development: estimates of neuronal numbers indicate major loss late during gestation. J.Neuropathol.Exp.Neurol. 55, 320-328.

Rabinowicz, T., Dean, D.E., Petetot, J.M., de Court (1999). Gender differences in the human cerebral cortex: more neurons in males; more processes in females. J.Child Neurol. 14, 98-107.

Rabinowicz, T., Petetot, J.M., Gartside, P.S., Sheyn, D., Sheyn, T., de, C.M. (2002). Structure of the cerebral cortex in men and women. J.Neuropathol.Exp.Neurol. 61, 46-57.

Rademacher, J., Caviness, V.S., Jr., Steinmetz, H., Galaburda, A.M. (1993). Topographical variation of the human primary cortices: implications for neuroimaging, brain mapping, and neurobiology. Cereb.Cortex 3, 313-329.

Radinsky, L. (1975). Primate brain evolution. Am.Sci. 63, 656-663.

Ragland, J.D., Coleman, A.R., Gur, R.C., Glahn, D.C., Gur, R.E. (2000). Sex differences in brain-behavior relationships between verbal episodic memory and resting regional cerebral blood flow. Neuropsychologia 38, 451-461.

Rakic, P. (1972). Mode of cell migration to the superficial layers of fetal monkey neocortex. J.Comp Neurol. 145, 61-83.

Rakic, P. (1988). Specification of cerebral cortical areas. Science 241, 170-176.

Rakic, P. (1998). Images in neuroscience. Brain development, VI: radial migration and cortical evolution. Am.J.Psychiatry 155, 1150-1151.

Ratnanather, J.T., Botteron, K.N., Nishino, T., Massie, A.B., Lal, R.M., Patel, S.G., Peddi, S., Todd, R.D., Miller, M.I. (2001). Validating cortical surface analysis of medial prefrontal cortex. Neuroimage. 14, 1058-1069.

Rex, D.E., Ma, J.Q., Toga, A.W. (2003). The LONI Pipeline Processing Environment. Neuroimage 19, 1033-1048.

Richman, D.P., Stewart, R.M., Hutchinson, J.W., Caviness, V.S. (1975). Mechanical Model of Brain Convolutional Development. Science 189, 18-21.

Rilling, J.K., Insel, T.R. (1998). Evolution of the cerebellum in primates: differences in relative volume among monkeys, apes and humans. Brain Behav.Evol. 52, 308-314.

Rilling, J.K., Insel, T.R. (1999a). The primate neocortex in comparative perspective using magnetic resonance imaging. J.Hum.Evol. 37, 191-223.

Rilling, J.K., Insel, T.R. (1999b). Differential expansion of neural projection systems in primate brain evolution. Neuroreport 10, 1453-1459.

Ringo, J.L., Doty, R.W., Demeter, S., Simard, P.Y. (1994). Time is of the essence: a conjecture that hemispheric specialization arises from interhemispheric conduction delay. Cereb.Cortex 4, 331-343.

Roland, P.E., Zilles, K. (1994). Brain atlases--a new research tool. Trends Neurosci. 17, 458-467.

Sadato, N., Ibanez, V., Deiber, M.P., Hallett, M. (2000). Gender difference in premotor activity during active tactile discrimination. Neuroimage. 11, 532-540.

Salat, D.H., Buckner, R.L., Snyder, A.Z., Greve, D.N., Desikan, R.S., Busa, E., Morris, J.C., Dale, A.M., Fischl, B. (2004). Thinning of the cerebral cortex in aging. Cereb.Cortex 14, 721-730.

Sandhu, S., Cook, P., Diamond, M.C. (1986). Rat cerebral cortical estrogen receptors: male-female, right-left. Exp.Neurol. 92, 186-196.

Schlaepfer, T.E., Harris, G.J., Tien, A.Y., Peng, L., Lee, S., Pearlson, G.D. (1995). Structural differences in the cerebral cortex of healthy female and male subjects: a magnetic resonance imaging study. Psychiatry Res. 61, 129-135.

Segal, M., Murphy, D. (2001). Estradiol induces formation of dendritic spines in hippocampal neurons: functional correlates. Horm.Behav. 40, 156-159.

Shattuck, D.W., Sandor-Leahy, S.R., Schaper, K.A., Rottenberg, D.A., Leahy, R.M. (2001). Magnetic resonance image tissue classification using a partial volume model. Neuroimage 13, 856-876.

Shattuck, D.W., Leahy, R.M. (2002). BrainSuite: an automated cortical surface identification tool. Med.Image Anal. 6, 129-142.

Shaywitz, B.A., Shaywitz, S.E., Pugh, K.R., Constable, R.T., Skudlarski, P., Fulbright, R.K., Bronen, R.A., Fletcher, J.M., Shankweiler, D.P., Katz, L., . (1995). Sex differences in the functional organization of the brain for language. Nature 373, 607-609.

Sherwood, C.C., Lee, P.W., Rivara, C.B., Holloway, R.L., Gilissen, E.P., Simmons, R.M., Hakeem, A., Allman, J.M., Erwin, J.M., Hof, P.R. (2003). Evolution of specialized pyramidal neurons in primate visual and motor cortex. Brain Behav.Evol. 61, 28-44.

Sherwood, C.C., Hof, P.R., Holloway, R.L., Semendeferi, K., Gannon, P.J., Frahm, H.D., Zilles, K. (2005). Evolution of the brainstem orofacial motor system in primates: a comparative study of trigeminal, facial, and hypoglossal nuclei. J.Hum.Evol. 48, 45-84.

Sidman, R.L., Rakic, P. (1973). Neuronal migration, with special reference to developing human brain: a review. Brain Res. 62, 1-35.

Sidman, R.L., Rakic, P. (1982). Development of the human central nervous system. In: Haymaker, W., Adams, R. [Eds.] Histology and Histopathology of the Nervous System. SpringfieldIL: Thomas, 3–145.

Sled, J.G., Zijdenbos, A.P., Evans, A.C. (1998). A nonparametric method for automatic correction of intensity nonuniformity in MRI data. IEEE Trans.Med.Imaging 17, 87-97.

Sowell, E.R., Thompson, P.M., Rex, D., Kornsand, D., Tessner, K.D., Jernigan, T.L., Toga, A.W. (2002). Mapping sulcal pattern asymmetry and local cortical surface gray matter distribution in vivo: maturation in perisylvian cortices. Cereb.Cortex 12, 17-26.

Sowell, E.R., Peterson, B.S., Thompson, P.M., Welcome, S.E., Henkenius, A.L., Toga, A.W. (2003). Mapping cortical change across the human life span. Nature Neuroscience 6, 309-315.

Sowell, E.R., Thompson, P.M., Leonard, C.M., Welcome, S.E., Kan, E., Toga, A.W. (2004). Longitudinal mapping of cortical thickness and brain growth in normal children. J.Neurosci. 24, 8223-8231.

Steinmetz, H., Volkmann, J., Jancke, L., Freund, H.J. (1991). Anatomical left-right asymmetry of language-related temporal cortex is different in left- and right-handers. Ann.Neurol. 29, 315-319.

Steinmetz, H., Jancke, L., Kleinschmidt, A., Schlaug, G., Volkmann, J., Huang, Y. (1992). Sex but no hand difference in the isthmus of the corpus callosum. Neurology 42, 749-752.

Steinmetz, H., Staiger, J.F., Schlaug, G., Huang, Y., Jancke, L. (1995). Corpus callosum and brain volume in women and men. Neuroreport 6, 1002-1004.

Steinmetz, H., Staiger, J.F., Schlaug, S.G., Huang, Y., Jancke, L. (1996). Inverse relationship between brain size and callosal connectivity. Naturwissenschaften 83, 221.

Swaab, D.F., Fliers, E. (1985). A sexually dimorphic nucleus in the human brain. Science 228, 1112-1115.

Swaab, D.F., Fliers, E., Partiman, T.S. (1985). The suprachiasmatic nucleus of the human brain in relation to sex, age and senile dementia. Brain Res. 342, 37-44.

Talairach J., Tournoux P. (1988). Co-planar Stereotaxic Atlas of the Human Brain. New York: Thieme.

Thompson, P.M., Schwartz, C., Lin, R.T., Khan, A.A., Toga, A.W. (1996a). Three-dimensional statistical analysis of sulcal variability in the human brain. J.Neurosci. 16, 4261-4274.

Thompson, P.M., Schwartz, C., Toga, A.W. (1996b). High-resolution random mesh algorithms for creating a probabilistic 3D surface atlas of the human brain. Neuroimage. 3, 19-34.

Thompson, P.M., Giedd, J.N., Woods, R.P., MacDonald, D., Evans, A.C., Toga, A.W. (2000a). Growth patterns in the developing brain detected by using continuum mechanical tensor maps. Nature 404, 190-193.

Thompson, P.M., Woods, R.P., Mega, M.S., Toga, A.W. (2000b). Mathematical/computational challenges in creating deformable and probabilistic atlases of the human brain. Hum.Brain Mapp. 9, 81-92.

Thompson, P.M., Cannon, T.D., Narr, K.L., van Erp, T., Poutanen, V.P., Huttunen, M., Lonnqvist, J., Standertskjold-Nordenstam, C.G., Kaprio, J., Khaledy, M., Dail, R., Zoumalan, C.I., Toga, A.W. (2001a). Genetic influences on brain structure. Nat.Neurosci. 4, 1253-1258.

Thompson, P.M., Vidal, C., Giedd, J.N., Gochman, P., Blumenthal, J., Nicolson, R., Toga, A.W., Rapoport, J.L. (2001b). Mapping adolescent brain change reveals dynamic wave of accelerated gray matter loss in very early-onset schizophrenia. Proc.Natl.Acad.Sci.U.S.A 98, 11650-11655.

Thompson, P.M., Rapoport, J.L., Cannon, T.D., Toga, A.W. (2003). Automated Analysis of Structural MRI Data, Chapter 5. In: Lawrie, A.L., Johnstone, E.C., Weinberger, D. [Eds.] Brain Imaging in Schizophrenia. Oxford: University Press.

Thompson, P.M., Toga, A.W. (2003). Cerebral cortex diseases & cortical localization. Nature Encyclopedia of the Life Sciences. London: Nature Publishing Group.

Thompson, P.M., Hayashi, K.M., Sowell, E.R., Gogtay, N., Giedd, J.N., Rapoport, J.L., de Zubicaray, G.I., Janke, A.L., Rose, S.E., Semple, J., Doddrell, D.M., Wang, Y., van Erp, T.G., Cannon, T.D., Toga, A.W. (2004). Mapping cortical change in Alzheimer's disease, brain development, and schizophrenia. Neuroimage. 23 Suppl 1, S2-18.

Thompson, P.M., Lee, A.D., Dutton, R.A., Geaga, J.A., Hayashi, K.M., Eckert, M.A., Bellugi, U., Galaburda, A.M., Korenberg, J.R., Mills, D.L., Toga, A.W., Reiss, A.L. (2005). Abnormal cortical complexity and thickness profiles mapped in Williams syndrome. J.Neurosci. 25, 4146-4158.

Tisserand, D.J., Pruessner, J.C., Sanz Arigita, E.J., van Boxtel, M.P., Evans, A.C., Jolles, J., Uylings, H.B. (2002). Regional frontal cortical volumes decrease differentially in aging: an MRI study to compare volumetric approaches and voxel-based morphometry. Neuroimage. 17, 657-669.

Toga, A.W., Mazziotta, J.C. (2000). Brain Mapping: The Systems. San Diego: Academic Press.

Trachtenberg, J.T., Chen, B.E., Knott, G.W., Feng, G., Sanes, J.R., Welker, E., Svoboda, K. (2002). Long-term in vivo imaging of experience-dependent synaptic plasticity in adult cortex. Nature 420, 788-794.

Van Essen, D.C. (1997). A tension-based theory of morphogenesis and compact wiring in the central nervous system. Nature 385, 313-318.

Veliskova, J. (2004). [Effects of sex hormones in the CNS]. Cesk.Fysiol. 53, 66-75.Vogeley, K., Schneider-Axmann, T., Pfeiffer, U., Tepest, R., Bayer, T.A., Bogerts, B., Honer, W.G., Falkai, P. (2000). Disturbed gyrification of the prefrontal region in male schizophrenic patients: A morphometric postmortem study. Am.J.Psychiatry 157, 34-39.

Vogt, C., Vogt, O. (1919). Allgemeinere Ergebnisse unserer Hirnforschung. J Psychol Neurol 25, 279–461.

von Economo, C. (1929). The cytoarchitectonics of the human cerebral cortex. London: Oxford Univ. Press.

Walla, P., Hufnagl, B., Lindinger, G., Deecke, L., Lang, W. (2001). Physiological evidence of gender differences in word recognition: a magnetoencephalographic (MEG) study. Brain Res.Cogn Brain Res. 12, 49-54.

Watkins, K.E., Paus, T., Lerch, J.P., Zijdenbos, A., Collins, D.L., Neelin, P., Taylor, J., Worsley, K.J., Evans, A.C. (2001). Structural asymmetries in the human brain: a voxel-based statistical analysis of 142 MRI scans. Cereb.Cortex 11, 868-877.

Watson, J.D., Myers, R., Frackowiak, R.S., Hajnal, J.V., Woods, R.P., Mazziotta, J.C., Shipp, S., Zeki, S. (1993). Area V5 of the human brain: evidence from a combined study using positron emission tomography and magnetic resonance imaging. Cereb.Cortex 3, 79-94.

Weaver, A.H. (2005). Reciprocal evolution of the cerebellum and neocortex in fossil humans. Proc.Natl.Acad.Sci.U.S.A 102, 3576-3580.

Welker, W. (1990). Why does the cerebral cortex fissure and fold? A review of determinants of gyri and sulci. In: Jones, E.G., Peters, A. [Eds.] Cerebral Cortex. New York: Plenum Press, 3–136.

White, T., Andreasen, N.C., Nopoulos, P., Magnotta, V. (2003). Gyrification abnormalities in childhood- and adolescent-onset schizophrenia. Biol.Psychiatry 54, 418-426.

Wiegand, L.C., Warfield, S.K., Levitt, J.J., Hirayasu, Y., Salisbury, D.F., Heckers, S., Dickey, C.C., Kikinis, R., Jolesz, F.A., McCarley, R.W., Shenton, M.E. (2004). Prefrontal cortical thickness in first-episode psychosis: a magnetic resonance imaging study. Biol.Psychiatry 55, 131-140.

Wise, P.M., Dubal, D.B., Wilson, M.E., Rau, S.W., Bottner, M. (2001). Minireview: neuroprotective effects of estrogen-new insights into mechanisms of action. Endocrinology 142, 969-973.

Wise, P.M. (2002). Estrogens and neuroprotection. Trends Endocrinol.Metab 13, 229-230.

Witelson, S.F. (1989). Hand and sex differences in the isthmus and genu of the human corpus callosum. A postmortem morphological study. Brain 112 (Pt 3), 799-835.

Witelson, S.F., Kigar, D.L. (1992). Sylvian fissure morphology and asymmetry in men and women: bilateral differences in relation to handedness in men. J.Comp Neurol. 323, 326-340.

Witelson, S.F., Glezer, I.I., Kigar, D.L. (1995). Women have greater density of neurons in posterior temporal cortex. J.Neurosci. 15, 3418-3428.

Woods, R.P., Grafton, S.T., Watson, J.D., Sicotte, N.L., Mazziotta, J.C. (1998). Automated image registration: II. Intersubject validation of linear and nonlinear models. J.Comput.Assist.Tomogr. 22, 153-165.

Woolley, C.S., Gould, E., Frankfurt, M., McEwen, B.S. (1990). Naturally occurring fluctuation in dendritic spine density on adult hippocampal pyramidal neurons. J.Neurosci. 10, 4035-4039.

Xu, J., Kobayashi, S., Yamaguchi, S., Iijima, K., Okada, K., Yamashita, K. (2000). Gender effects on age-related changes in brain structure. AJNR Am.J.Neuroradiol. 21, 112-118.

Yankova, M., Hart, S.A., Woolley, C.S. (2001). Estrogen increases synaptic connectivity between single presynaptic inputs and multiple postsynaptic CA1 pyramidal cells: a serial electron-microscopic study. Proc.Natl.Acad.Sci.U.S.A 98, 3525-3530.

Yucel, M., Stuart, G.W., Maruff, P., Velakoulis, D., Crowe, S.F., Savage, G., Pantelis, C. (2001). Hemispheric and Gender-related Differences in the Gross Morphology of the Anterior Cingulate/Paracingulate Cortex in Normal Volunteers: An MRI Morphometric Study. Cereb.Cortex 11, 17-25.

Zhou, J.N., Hofman, M.A., Gooren, L.J., Swaab, D.F. (1995). A sex difference in the human brain and its relation to transsexuality. Nature 378, 68-70.

Zilles, K., Armstrong, E., Schleicher, A., Kretschmann, H.J. (1988). The human pattern of gyrification in the cerebral cortex. Anat.Embryol.(Berl) 179, 173-179.

Zilles, K., Armstrong, E., Moser, K.H., Schleicher, A., Stephan, H. (1989). Gyrification in the cerebral cortex of primates. Brain Behav.Evol. 34, 143-150.

Zilles, K., Dabringhaus, A., Geyer, S., Amunts, K., Qu, M., Schleicher, A., Gilissen, E., Schlaug, G., Steinmetz, H. (1996). Structural asymmetries in the human forebrain and the forebrain of non-human primates and rats. Neurosci.Biobehav.Rev. 20, 593-605.

Zilles, K., Schleicher, A., Langemann, C., Amunts, K., Morosan, P., Palomero-Gallagher, N., Schormann, T., Mohlberg, H., Bürgel, U., Steinmetz, H., Schlaug, G., Roland, P.E. (1997). A quantitative analysis of sulci in the human cerebral cortex: development, regional heterogeneity, gender difference, asymmetry, intersubject variability and cortical architecture. Human Brain Mapping 5, 218-221.

Zilles, K., Kawashima, R., Dabringhaus, A., Fukuda, H., Schormann, T. (2001). Hemispheric shape of European and Japanese brains: 3-D MRI analysis of intersubject variability, ethnical, and gender differences. Neuroimage. 13, 262-271.

Zilles, K., Palomero-Gallagher, N., Schleicher, A. (2004). Transmitter receptors and functional anatomy of the cerebral cortex. J.Anat. 205, 417-432.

CURRICULUM VITAE

PERSONAL DETAILS

Name:	Lueders, Eileen
Date of Birth:	September 09, 1977
Nationality:	German
Work Address:	Laboratory of Neuro Imaging, Department of Neurology, UCLA School of Medicine 635 Charles Young Drive South, Suite 225 Los Angeles, CA 90095-7334 Phone: 310-206-2101 Fax: 310-206-5518

EDUCATION

December 2005	Ph.D. (summa cum laude) at the University of Zurich, Switzerland
October 2004 to December 2005	Ph.D. Candidate at the University of Zurich, Switzerland
August 2001 to September 2004	Ph.D. Candidate at the Otto-von-Guericke-University of Magdeburg, Germany
July 2001	Diplom in Psychology at the Otto-von-Guericke-University of Magdeburg, Germany Outstanding Graduate Student Award (Faculty of Natural Sciences) at the University of Magdeburg, Germany
October 1996 to July 2001	Masters Program of Psychology at the Otto-von-Guericke-University of Magdeburg, Germany

WORK EXPERIENCE

December 2005 to present	***Postdoctoral Scholar*** at the Laboratory of Neuro Imaging, Department of Neurology, UCLA School of Medicine (Los Angeles, CA, USA)
April 2005 to December 2005	***Staff Research Associate II*** at the Laboratory of Neuro Imaging, Department of Neurology, UCLA School of Medicine (Los Angeles, CA, USA)
October 2002 to April 2005	***Staff Research Associate I*** at the Laboratory of Neuro Imaging, Department of Neurology, UCLA School of Medicine (Los Angeles, CA, USA)
July 2002 to September 2002	***Visiting Research Fellow*** at the Department of Neurology, Beth Israel Deaconess Medical Center, Harvard Medical School (Boston, MA, USA).
August 2001 to September 2002	***Scientific Assistant*** at the Department of General Psychology at the Otto-von-Guericke-University of Magdeburg (Magdeburg, Germany)
March 2002 to May 2002	***Visiting Research Fellow*** at the Laboratory of Neuro Imaging, Department of Neurology, UCLA School of Medicine (Los Angeles, CA, USA)
February 2000 to April 2000	***Intern*** at the Department of Neurology, Beth Israel Deaconess Medical Center, Harvard Medical School (Boston, MA, USA)
October 1997 to July 2001	***Research Assistant*** at the Department of General Psychology at the Otto-von-Guericke-University of Magdeburg (Magdeburg, Germany)

PUBLICATIONS

(1) Articles in Peer Reviewed Journals:

Luders E, Narr KL, Thompson PM, Rex DE, Jancke L, and Toga AW. Asymmetry effects on cortical thickness. *Cereb Cortex*. 2005 Nov 2; [Epub ahead of print]

Luders E, Thompson PM, Narr KL, Toga AW, Jancke L, and Gaser C. A curvature-based approach to estimate local gyrification on the cortical surface. *Neuroimage*. 2005 Oct 10; [Epub ahead of print]

Luders E, Narr KL, Thompson PM, Rex DE, Woods RP, DeLuca H, Jancke L, and Toga AW. Gender Effects on Cortical Thickness and the Influence of Scaling. *Human Brain Mapping*. 2005 Aug 25; [Epub ahead of print]

Luders E, Narr KL, Woods RP, Rex DE, Thompson PM, Jancke L, Steinmetz H, and Toga AW. Mapping Cortical Gray Matter in the Young Adult Brain: Effects of Gender. *Neuroimage*. 2005 Jun;26(2):493-501.

Luders E, Narr KL, Zaidel E, Thompson PM, Jancke L, and Toga AW. Parasagittal Asymmetries of the Corpus Callosum. *Cerbral Cortex*. 2005 May 18; [Epub ahead of print]

Rex DE, Shattuck DW, Woods RP, Narr KL, **Luders E**, Rehm K, Stolzner SE, Rottenberg DA, Toga AW. A meta-algorithm for brain extraction in MRI. *Neuroimage*. 2004 Oct;23(2):625-37.

Luders E, Narr KL, Thompson PM, Rex DE, Jancke L, Steinmetz H, Toga AW. Gender differences in cortical complexity. *Nat Neurosc*i. 2004 Aug;7(8):799-800

Boesen K, Rehm K, Schaper K, Stoltzner S, Woods R, **Luders E**, Rottenberg D. Quantitative comparison of four brain extraction algorithms. *Neuroimage*. 2004 Jul;22(3):1255-61.

Luders E, Gaser C, Jancke L, and Schlaug G. A voxel-based approach to gray matter asymmetries. *Neuroimage*. 2004 Jun;22(2):656-64.

Narr KL, Bilder RM, Kim S, Thompson PM, Szeszko P, Robinson D, **Luders E**, Toga AW. Abnormal gyral complexity in first-episode schizophrenia. *Biol Psychiatry*. 2004 Apr 15;55(8):859-67.

Luders E, Rex DE, Narr KL, Woods RP, Jancke L, Thompson PM, Mazziotta JC, Toga AW. Relationships between sulcal asymmetries and corpus callosum size: gender and handedness effects. *Cereb Cortex*. 2003 Oct;13(10):1084-93.

Luders E, Steinmetz H, Jancke L. Brain size and grey matter volume in the healthy human brain. *Neuroreport*. 2002 Dec 3;13(17):2371-4.

Schulze K, **Luders E**, Jancke L. Intermanual transfer in a simple motor task. *Cortex*. 2002 Dec;38(5):805-15.

PUBLICATIONS

(2) Book Chapter:

Luders E. Groessere Gehirne, bessere Leistungen? In: Warum Frauen glauben, sie koennten nicht einparken - und Maenner ihnen Recht geben. Ueber Schwaechen, die gar keine sind. Eine Antwort auf A. & B. Pease. Eds.: Quaiser-Pohl C & Jordan K. Beck Verlag (2004).

(3) Abstracts & Posters:

Ogren JA, Staba RJ, Lin JJ, Salamon N, Dutton RA, **Luders E**, Toga AW, Engel J, Thompson PM, Wilson C. Fast Ripple Oscillations Correlate with Increases in Hippocampal Atrophy in Unilateral Mesial Temporal Lobe Epilepsy. *Poster und Abstract-Presentation.* (AES).Washington, USA, 2005.

Luders E, Narr KL, Thompson PM, Rex DE, Woods RP, DeLuca H, Jancke L, and Toga AW. Gender Effects on Cortical Thickness. *Poster und Abstract-Presentation* (HBM). Toronto, Canada, 2005.

Lin JJ, Salamon N, Lee AD, Dutton RA, Geaga JA, Hayashi KM, **Luders E**, Toga AW, Engel J, Thompson PM. Mapping Reduced Cortical Thickness and Complexity in Mesial Temporal Lobe Epilepsy with Hippocampal Sclerosis. *Poster und Abstract-Presentation* (HBM). Toronto, Canada, 2005.

Luders E, Narr KL, Zaidel E, Thompson PM, Jancke L, Gaser C, and Toga AW. Asymmetries in the corpus callosum and the influence of gender. *Poster und Abstract-Presentation* (SfN). San Diego, USA, 2004.

Gaser C, **Luders E**, Wang H, Toga AW, Thompson PM. Cortical Complexity Measured Via Regional Surface Shape. *Poster und Abstract-Presentation* (SfN). San Diego, USA, 2004.

Luders E, Narr KL, Thompson PM, Rex DE, Jancke L, Steinmetz H, and Toga AW. Gender differences in cortical complexity. *Poster und Abstract-Presentation* (HBM). Budapest, Ungarn, 2004.

Luders E, Gaser C, Jancke L, Schlaug G. Structural asymmetries in the musician's brain: a whole-brain voxel-based approach. *Poster und Abstract-Presentation* (HBM). New York, USA, 2003.

Luders E, Rex DE, Narr KL, Woods RP, Jancke L, Thompson PM, Mazziotta J, Toga AW. Relationships between sulcal asymmetries and corpus callosum morphometry: gender and handedness effects. *Poster und Abstract-Presentation* (HBM). New York, USA, 2003.

Luders E, Steinmetz H, Jäncke L. Brain size and not sex determines proportional grey matter volume in the healthy human brain. *Poster und Abstract-Presentation* (HBM). Sendai, Japan, 2002.